UNIVERSITY OF CALIFORNIA, SAN DIEGO

Insights into the Homeostatic Regulation of I kappa B alpha

A dissertation submitted in partial satisfaction of the requirements for the degree
Doctor of Philosophy

in

Chemistry

by

Erika Mathes Lisabeth

Committee in Charge:

Professor Gourisankar Ghosh, Chair
Professor Alexander Hoffmann
Professor Elizabeth Komives
Professor Andrew Kummel
Professor Kees Murre
Professor Roger Y. Tsien

2009

The Dissertation of Erika Mathes Lisabeth is approved, and is acceptable in quality and form for publication on microfilm and electronically:

_____

_____

_____

_____

_____

_____

Chair

University of California, San Diego

2009

TABLE OF CONTENTS

LIST OF FIGURES

LIST OF TABLES

ACKNOWLEGEMENTS

I would first like to thank my advisor, Dr. Gourisankar Ghosh, for allowing me to join his lab and learn about the interesting transcription factor, NF-κB. I will always remember his enthusiasm for current science and also his appreciation of the history of science. Dr. Alexander Hoffmann, and Dr. Elizabeth Komives in particular have played very important roles in this dissertation, each bringing their own perspectives to understanding of the NF-κB system, from which I have learned a great deal. The other people involved in this project, namely Diego Ferreiro and Stephanie Truhlar in the Komives lab and Ellen O'Dea and Soumen Basak in the Hoffmann lab have each contributed to this project. This truly has been a collaborative effort.

I would also like to thank the wonderful members of the Gourisankar Ghosh lab, both past and present. In particular, Drs. Jacky Ngo, Randall Lukasiewicz, Amanda Fusco and Sutapa Chakrabarti made the Ghosh lab a wonderful and exciting place to join for my Ph.D. Dr. Anu Moorthy had the extreme patience of answering many of my questions, Dr. Olga Savinova taught me about how to become an inquisitive and thoughtful scientist, and Jessica Ho is one of the most supportive graduate students I have ever known. In addition, I would like to thank Lily Wang, an undergraduate who helped me immensely with experiments contributing to the last chapter of this dissertation.

Finally, I would like to thank my husband, Derek, for his support through my graduate school experience.

Chapter III, in part, is a reprint of the material as it appears in
Mathes E, O'Dea EL, Hoffmann A, Ghosh G. "NF-kappaB dictates the degradation pathway of IkappaBalpha." EMBO J. 2008 May 7;27(9):1357-67. Epub 2008 Apr 10.
The dissertation author was the primary investigator and author of this paper.

Chapter IV, in part, is as it appears in Truhlar SM, Mathes E, Cervantes CF, Ghosh G, Komives EA. "Pre-folding IkappaBalpha Alters Control of NF-kappaB Signaling." J Mol Biol. 2008 Jun 27;380(1):67-82. Epub 2008 Mar 4. The dissertation author was a co-author of this paper.

Chapter V, in part, is currently being prepared for submission for publication of the material. Mathes E, Ghosh G. "Hydrophobic residues within flexible regions of IkappaBalpha contribute to ubiquitin-independent degradation" In preparation for EMBO reports.
The dissertation author was the primary investigator and author of this material.

VITA

2003 Bachelor of Science, Michigan State University

2005 Master of Science, University of California, San Diego

2009 Doctor of Philosophy, University of California, San Diego

PUBLICATIONS

Vaezeslami S, **Mathes E**, Vasileiou C, Borhan B, Geiger JH. "The Structure of Apo-wild-type Cellular Retinoic Acid Binding Protein II at 1.4 A and its Relationship to Ligand Binding and Nuclear Translocation."
J Mol Biol. 2006 Oct 27;363(3):687-701. Epub 2006 Aug 26.

Mathes E, O'Dea EL, Hoffmann A, Ghosh G. "NF-kappaB dictates the degradation pathway of IkappaBalpha."
EMBO J. 2008 May 7;27(9):1357-67. Epub 2008 Apr 10.

Truhlar SM, **Mathes E**, Cervantes CF, Ghosh G, Komives EA. "Pre-folding IkappaBalpha Alters Control of NF-kappaB Signaling."
J Mol Biol. 2008 Jun 27;380(1):67-82. Epub 2008 Mar 4.

Mathes E, Ghosh G. "Hydrophobic residues within flexible regions of IkappaBalpha contribute to ubiquitin-independent degradation" In preparation.

ABSTRACT OF THE DISSERTATION

Insights into the Homeostatic Regulation of I kappa B alpha

by

Erika Mathes Lisabeth

Doctor of Philosophy in Chemistry

University of California, 2009

Dr. Gourisankar Ghosh, Chair

The regulation of the transcription factor NF-κB is crucial to proper cell physiology, as misregulation of this transcription factor can lead to many disease states, including chronic inflammation and cancer. NF-κB is inhibited by a class of inhibitor proteins known as IκB; the most effective IκB is IκBα. Signal induced degradation of IκBα leading to NF-κB translocation and activation is well documented and requires post-translational modifications such as phosphorylation and ubiquitination. It has recently been demonstrated that IκBα also undergoes stimulus-independent degradation and this degradation pathway might be important for NF-κB activity regulation. The focus of this study is to investigate the mechanism of stimulus independent degradation of IκBα and its effect on NF-κB activity. Chapter 1 introduces the NF-κB:IκB signaling system, ubiquitin-independent degradation of several substrates, and also various regulatory proteasome complexes. Chapter 3

describes the delineation of the pathways regulating the degradation of IκBα. Results presented here show that the degradation pathway of IκBα is determined by binding to NF-κB subunits. It is further shown that perturbations of ubiquitin-independent degradation pathway alter NF-κB activation. Chapter 4 focuses on the ankyrin repeat sequence of IκBα. Of the six ankyrin repeats present in IκBα, several deviate from the consensus ankyrin repeat sequence. Mutations back to the consensus sequence in several ankyrin repeats demonstrate that the location of thermodynamic stabilization determines the degradation rate of IκBα. Finally, Chapter 5 dissects the degradation requirements of IκBα. Our results show that there are two degrons within IκBα; one located in the 5^{th} ankyrin repeat, and the other within the PEST domain of IκBα. Both degrons are controlled by hydrophobic residues within long stretches of flexible regions.

I. Introduction

A. NF-κB Signaling System

The transcription factor known as NF-κB was discovered as a nuclear factor required for transcription of the immunoglobulin kappa light chain gene in B cells (Sen and Baltimore, 1986; Singh et al., 1986). NF-κB was shown to bind a specific DNA sequence present in the transcriptional regulatory region. It was thought that NF-κB might be a B cell specific factor since NF-κB DNA binding could not be detected in other tested cell types. However, it was soon discovered that NF-κB is present in all cells, but remains in the cytoplasm as an inhibited factor (Baeuerle and Baltimore, 1988; Karin and Ben-Neriah, 2000). In order for the release of NF-κB from the inhibitor to allow for DNA binding and activation of target genes, this inhibitor, known as IκB, must be degraded (Baldwin, 1996; Sen and Baltimore, 1986). Degradation of the IκB occurs when a cell encounters a variety of physiological and pathological extracellular stimuli. These stimuli activate NF-κB, which then regulates the expression of hundreds of genes, which are involved in the innate and adaptive immune response, cell differentiation, cell death pathways, and inflammation (Karin and Ben-Neriah, 2000). IκBα is also a NF-κB target gene, and its synthesis in response to stimulus participates in post-transcriptional repression of NF-κB. Stimulus-dependent periodic degradation and synthesis of IκBα generates an oscillatory activity of NF-κB which has been captured through mathematical modeling (Hoffmann et al., 2002a; Kearns et al., 2006).

Since NF-κB is involved in a myriad of cell processes, it is not surprising that the IκB/NF-κB signaling system is highly evolutionarily conserved (Ghosh et al.,

1998). NF-κB and IκB like proteins are found in species ranging from the phylum *Cnidaria* to humans (Sullivan et al., 2007). They are found in the lower organism sea anemone *Nematostella vectensis*, but not in yeast and *C.elegans*, suggesting that these proteins have been lost during the evolution of those particular species (Sullivan et al., 2007). In *Drosophilia*, three NF-κB proteins *dorsal*, *dif* and *relish* have been described, as well as an IκB-like protein, *cactus.* The NF-κB-like proteins are involved in various functions such as polarity of expression of genes, immune response, and upregulation during infections (Ghosh et al., 1998).

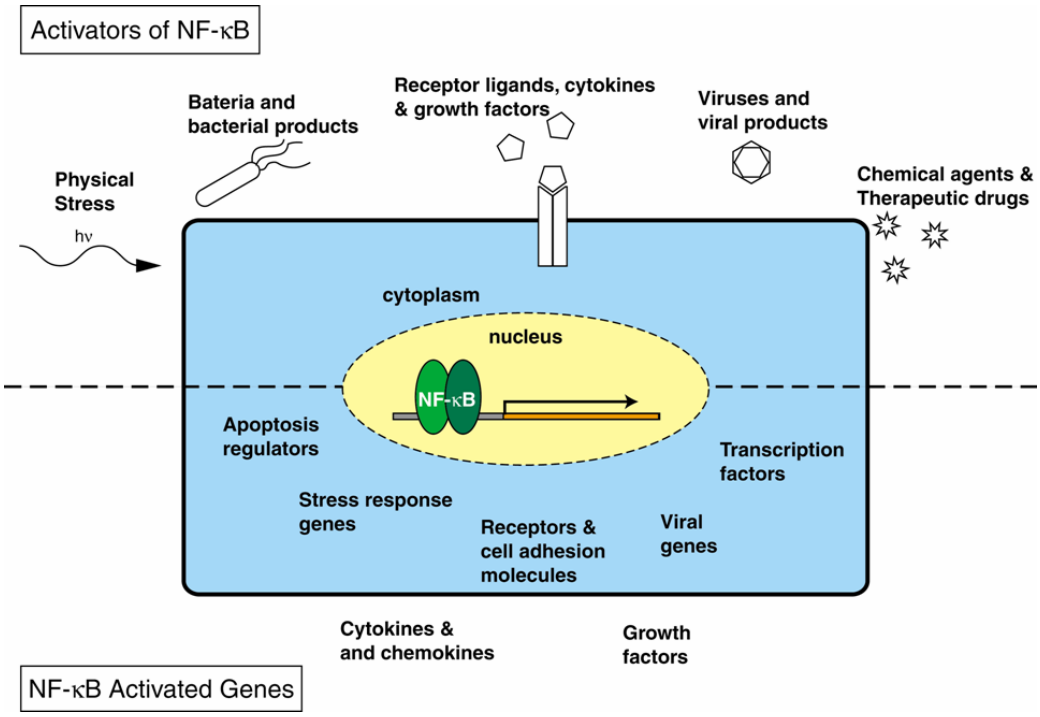

Figure 1-1. A variety of stimuli can activate NF-κB dependent gene transcription NF-κB dependent genes include genes involved in cell death, stress response, receptors, viral genes, inflammation and growth. (courtesy Chris Phelps).

B. NF-κB Activation Pathway

NF-κB activation begins with the interaction of a ligand molecule with its cognate receptor on the cell surface. Although the types of ligands can vary significantly, all converge onto central kinase in NF-κB signaling, I kappa B kinase (IKK) (Ghosh and Karin, 2002) (Figure 1-2). Thus, signals that a cell encounters that activate IKK can signify infection (LPS, viral transactivating proteins, ds RNA), or inflammation (TNF-α, IL-1, IL-6) (Ghosh and Karin, 2002). The IKK complex is comprised of three subunits, two catalytic kinase cores, IKKα and IKKβ and one adaptor molecule, NEMO (NF-κB essential modifier, or IKKγ) (Ghosh and Karin, 2002; Sun and Ley, 2008). In the canonical pathway, IKKβ is the IKK subunit that is responsible for phosphorylation of IκBα (Figure 1-2). However, there are alternative pathways of NF-κB activation which activate a different IKK complex. For instance, stimulation with BAFF or CD40 leads to activation of an IKKα complex and phosphorylation of another IκB like protein, p100. This phosphorylation leads to processing of p100 into the NF-κB subunit p52 (Sun and Ley, 2008). Finally, IKKβ phosphorylation of p105 induces processing of p105 into the NF-κB subunit p50 (Sun and Ley, 2008) (Figure 1-2). Although there are many pathways of NF-κB activation, all converge on the central kinase complex, IKK.

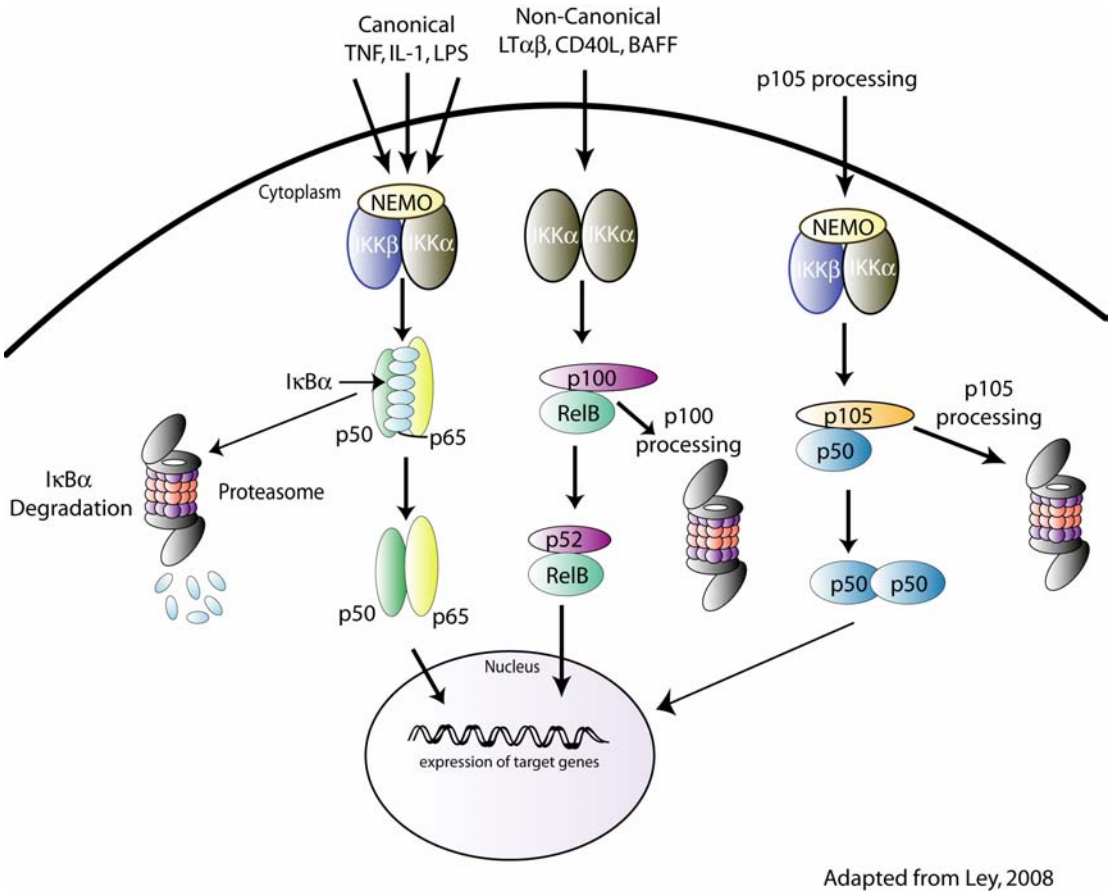

Figure 1-2. Various pathways converge on the IKK kinase complex
The canonical pathway of NF-κB activation includes stimuli such as TNF-α or LPS and activates an IKK complex composed of IKKα, IKKβ and IKKγ (NEMO). This activated complex phosphorylates IκBα and leads to its proteasomal degradation. Released NF-κB subunits (in this case, p50 and p65) are allowed to bind to target DNA and activate target genes. Alternative IKK complexes include an IKKα complex which is responsible for p100 induced processing into p52. p100/p52 preferentially binds to RelB. Finally, p105 can be phosphorylated by IKKβ as well, leading to processing of p105 to 50.

C. NF-κB Family Members

Once NF-κB is released from the inhibitor molecule, IκB, it binds as a dimer to its 10 bp target site with the consensus 5'-GGGRN W YYCC-3' where R=purine, N=any base, W=adenine or thymine and Y=pyrimidine (Hoffmann et al., 2006). The family of NF-κB subunits which can bind to the consensus DNA sequence is comprised of two classes of proteins; those which are processed from precursors, and those which contain a transactivation domain. p50 and p52 (from the gene products nfkb1 and nfkb2) are processed from p105 and p100 respectively, while p65 (RelA), c-Rel and RelB contain TADs (Gilmore, 2006). The Rel Homology Region (RHR), common to all NF-κB family members, is comprised of two Ig-like domains; the amino terminal domain, which is responsible for base specific DNA recognition, and the dimerization domain, which is primarily responsible for dimerization of NF-κBs (Hoffmann et al., 2006). Together these domains provide a platform for IκB binding. Interestingly, RelB differs from all other NF-κB subunits since it contains a Leucine Zipper (LZ) domain, whose presence is required for full RelB dependent transcriptional activation (Dobrzanski et al., 1993). Knockout mice reveal some specificity for each subunit (Table I-I), and although this is not a complete list, it gives some insight into the role each NF-κB family member plays (Gerondakis et al., 2006). NF-κB family members can be functionally redundant, as shown by the lethality of only one family member, p65. However, there is some specificity as shown by defects either in specific cell types or reduced specific gene expression (Table I-I).

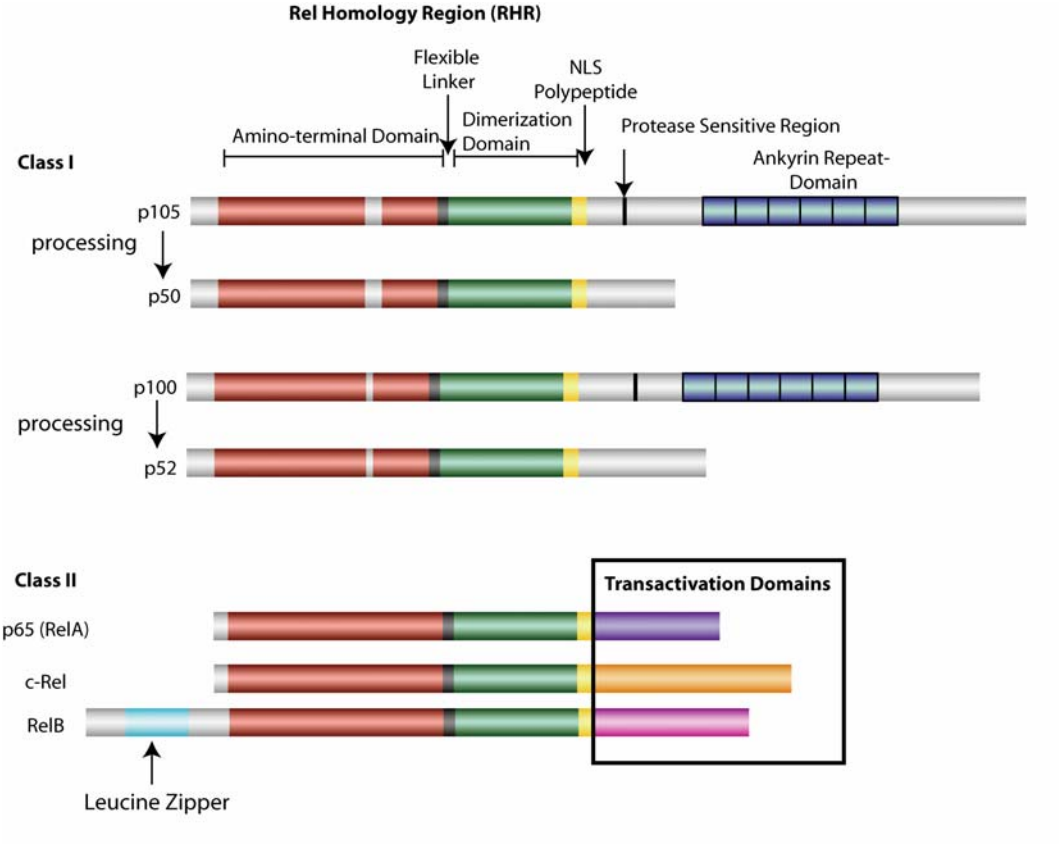

Figure 1-3. NF-κB domain organization and family members
Two classes of NF-κB family members exist which either are processed from precursors with ankyrin repeat domains or those which have transactivation domains.

Table I-I. Knockout Phenotypes for NF-κB Transcription Factors

Genotype /knockout	Lethality	Defect/phenotype
nfkb1$^{-/-}$ (protein product p105)	No	B cells: response to LPS diminished, turnover is rapid in vivo, defective isotype switching, Th2 differentiation is impaired Natural Killer cells (NK): enhanced proliferation and increased IFNy production Macrophages: ERK mitogen-activated protein kinase pathway impaired in response to TLR signals
nfkb2$^{-/-}$ (protein product p100)	No	Defective secondary lymphoid organ development, impaired B-cell development, enchanced dendridic cell function
crel$^{-/-}$	No	B cells: cell-cycle and survivial defects; impaired isotype switching T cells: defects in CD4 and CD8 T-cell responses Reduced number of pDC, impaired IL-12 production Neuronal survival defects
rela$^{-/-}$	Yes (~E15)	TNF-α induced cell death in hepatocytes, macrophages and fibroblasts Impaired secondary lympoid organ development Defects in leukocyte recruitment, T-cell dependent responses, isotype switching to IgG3, spatial learning responses
relb$^{-/-}$	No	Complex inflammatory phenotype and hematopoietic abnormalities Defects in secondary lympoid organ structure and germinal center formation Lack certain DC populations, DC functional defects

*Adapted from (Gerondakis et al., 2006)

D. The IκB Family

Since NF-κB is involved in the regulation of hundreds of genes in a precise fashion (Ghosh et al., 1998) its activity must be highly regulated by the IκB molecules. There are five cytoplasmic IκBs (Figures 1-3 and 1-4), IκBα, IκBβ, IκBε, p100 and p105. Of these, the first three are referred to as classical IκBs whereas the last two are non-classical IκBs, and all bind to and inhibit NF-κB activity. Inhibitory complexes which include p100 and p105 are very large oligomeric complexes (~600 kDa) and can accommodate many NF-κB subunits, while IκB containing complexes are smaller and have equal stochiometric ratios between NF-κB and IκB molecules (Savinova et al., 2009). In addition to the cytoplasmic inhibitors there are other IκB-like proteins which are primarily nuclear, known as IκBζ, Bcl-3 and IκB-NS. These IκB proteins primarily act as co-activators of NF-κB p50 and p52 homodimers (Yamamoto and Takeda, 2008).

Classical IκB molecules contain three domains: A N-terminal signal response domain (SRD), a central ankyrin repeat domain (ARD) and a C-terminal PEST sequence. Contained within the N-terminal signal response region are the conserved serine sites of phosphorylation by IKK. Roughly ten amino acids amino-terminal to this pair of serines reside conserved lysine amino acid sites of poly-ubiquitination. This amino-terminal region of IκBα also contains a functional nuclear export sequence (Huang et al., 2000; Johnson et al., 1999).

All IκBs share a centrally located ankyrin repeat domain (ARD). The ankyrin repeat (AR) is a 33 amino acid consensus amino acid sequence that appears in multiple copies in numerous proteins (Sedgwick and Smerdon, 1999). At their carboxy-terminal ends, the classical IκB proteins contain a short sequence rich in the amino acids proline, glutamic acid, serine, and threonine. This so-called PEST region is common to many proteins that, like IκBα, display rapid turnover in cells (Pando and Verma, 2000; Rogers et al., 1986).

A sequence alignment of the classical IκBs can be found in Figure 1-5. Knockout studies of *ikba*, *ikbe* and *bcl3* show that none are embryonically lethal, and there are specific defects associated with each of the knockouts, with the most severe defects in the *ikba*$^{-/-}$ mouse (Table I-II).

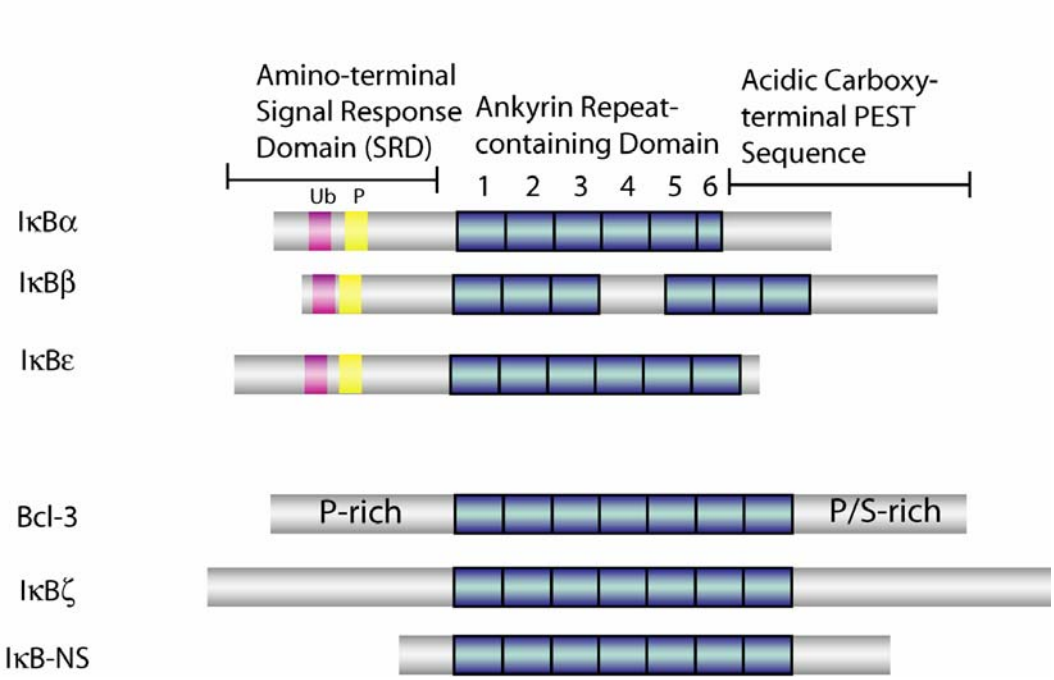

Figure 1-4. Domain organization of IκB proteins
There are 5 independent IκB proteins which can bind to NF-κB subunits. IκBα, β and ε contain a Signal Response Domain (SRD) which contains IKK phosphorylation sites and ubiquitination sites. This domain is followed by the Ankyrin Repeat Domain (ARD) and then followed by the PEST domain. Bcl-3 and IκBζ are both primarily nuclear IκBs.

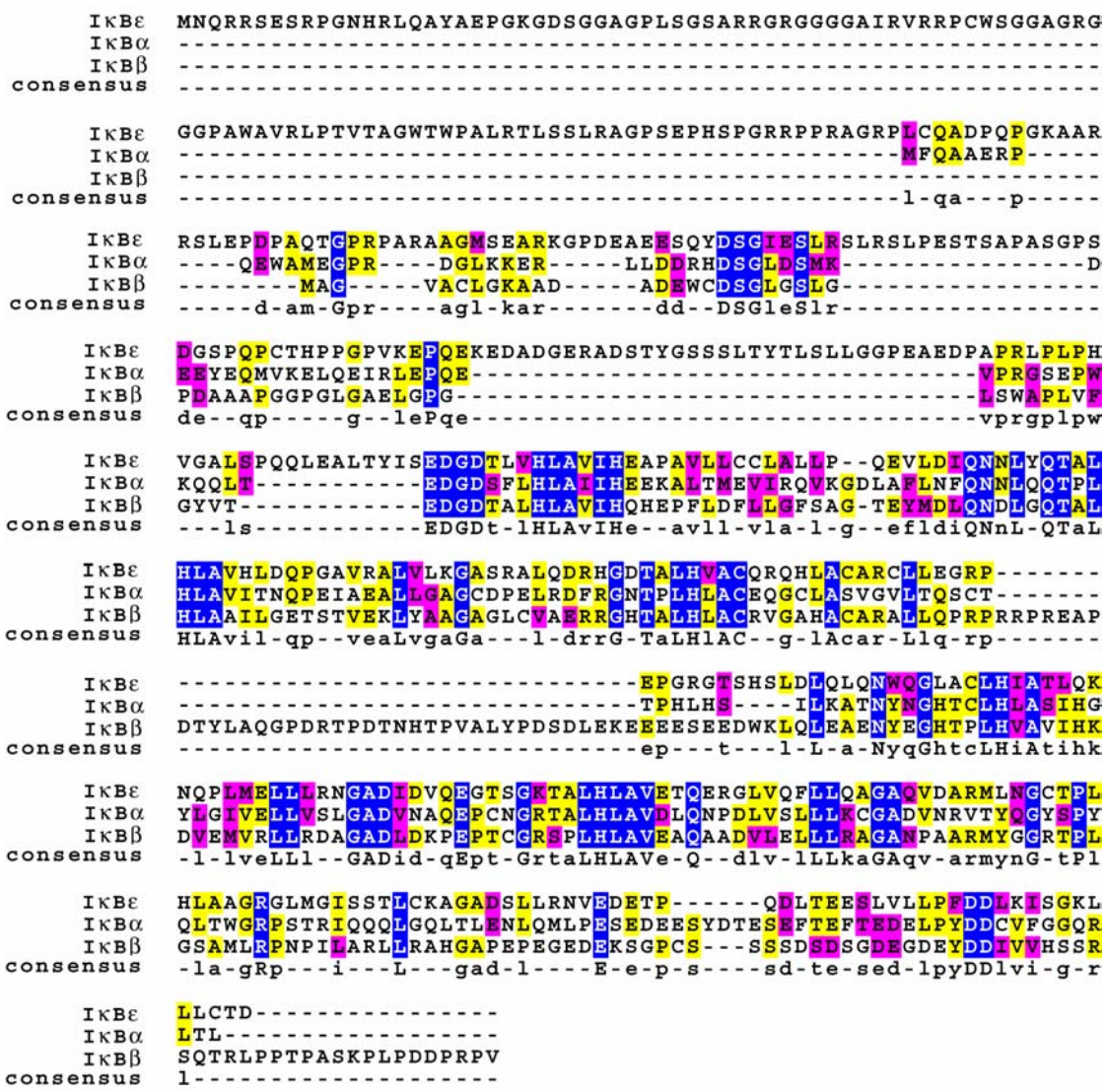

Figure 1-5. Sequence alignment of IκBs Human IκBα, IκBβ and IκBε were aligned using CLUSTALW (Thompson). Yellow shading indicates identical residues across several species, purple indicates similar residues, and blue shading with white text indicates complete conservation

Table I-II. Knockout Phenotypes for IκB proteins

Genotype /knockout	Lethality	Defect/phenotype
ikba$^{-/-}$	7-10 days after birth	Severe inflammatory dermatitis and amplified granulocytic compartment Proliferation of B cells is enhanced and proliferation of T cells is reduced
ikbe$^{-/-}$	No	Increased expression of certain Ig isotypes and cytokines
bcl3$^{-/-}$	No	Splenic architecture disrupted Defective Th1 and Th2 differentiation

*Adapted from (Gerondakis et al., 2006)

E. IκB interactions with NF-κB

The X-ray structure of IκBα in complex with the NF-κB p50:p65 heterodimer was determined independently by two separate laboratories in 1998 (Huxford et al., 1998; Jacobs and Harrison, 1998). Both groups relied on a similar strategy of removing the signal response region of IκBα and the amino-terminal domain of the p50 subunit in order to stabilize the conformationally dynamic complex for co-crystallization (Huxford et al., 1998; Jacobs and Harrison, 1998). The structure reveals how IκBα uses its entire ankyrin repeat-containing domain as well as its carboxy-terminal PEST sequence to mediate an extensive protein-protein interface of roughly 4300 $Å^2$ (Figure 1-6). Ankyrin repeats three through five participate in multiple van der Waals contacts with one surface of the p50:p65 heterodimer dimerization domains. The sixth ankyrin repeat and PEST region of IκBα present a vast acidic patch, which opposes the largely positively charged DNA binding surfaces of the p65 amino-terminal domain. As a consequence of this electrostatic interaction, the p65 amino-terminal domain occupies a position relative to the dimerization domain that is rotated roughly 180° and translated 40 Å when compared with it DNA bound structures. The transition of p65 to the conformation observed in the NF-κB:IκB complex does not disrupt the amino-terminal domain structure and is afforded entirely by the flexible linker region that connects the amino-terminal and dimerization domains. The structure of a similar construct of IκBβ bound to the dimerization domain from the NF-κB p65 homodimer suggests that IκBβ uses a

similar strategy in binding to NF-κB although it relies less on interactions with the p65 amino-terminal domain for complex stability (Malek et al., 2003).

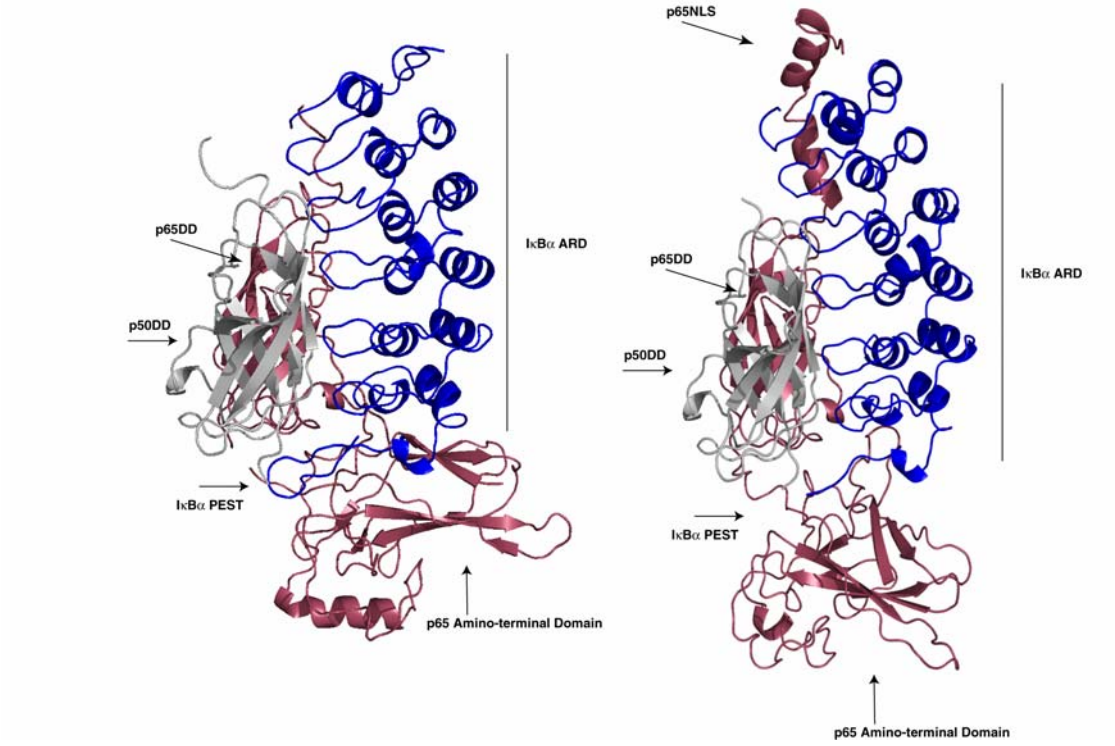

Figure 1-6. The structure of IκBα bound to the NF-κB subunits p50 and p65
Ribbon diagram where IκBα is blue, p65 is magenta, and p50 is silver. The Dimerization Domain (DD) of both p50 and p65 are shown, as well as the Amino-terminal Domain of p65. The Ankyrin Repeat Domain (ARD) and PEST sequence of IκBα are also highlighted. Left panel: Structure determined by T. Huxford (Huxford et al., 1998), Right panel: Structure determined by M.D. Jacobs (Jacobs and Harrison, 1998). The structure in the left panel has extended density for the IκBα PEST domain, while the Jacobs structure has additional contacts shown by the p65 NLS with the first ankyrin repeat of IκBα.

F. Alternate IκBα Degradation Pathways

In addition to the well characterized IKK phosphorylation and ubiquitin dependent degradation of IκBα, there are several reports of alternative pathways of IκBα degradation. For instance, calpain 3 has been implicated in the cleavage of nuclear IκBα in muscle cells (Baghdiguian et al., 1999). μ-calpain has also been shown to cleave IκBα *in vitro* (Shumway et al., 1999). Inhibition of calpains was found to increase the level of IκBα in IgM^+ B cells, as well as degrade it *in vitro* and is dependent on Casein Kinase II (CK2) phosphorylation (Shen et al., 2001). A pathway for IκBα degradation which is proteasome-inhibitor resistant has been suggested to provide the mechanism of constitutive p50/c-Rel heterodimer activity in B-cells (O'Connor et al., 2004). In addition, exposure to UV radiation has been shown to lead to IκBα degradation without activation of IKK (O'Dea et al., 2007). Finally, IκBα has been shown to be cleaved by the caspase pathway during apoptosis (Barkett et al., 1997) and is a direct substrate of caspase-3. These alternate IκBα degradation pathways could provide signal-specific and cell-type specific regulation of NF-κB.

G. The Proteasome

The ubiquitin-proteasome system (UPS) is the primary pathway responsible for regulated protein degradation in the cell. Proteins meant for destruction are tagged with a 76-amino acid protein ubiquitin, which serves as a recognition signal for the 26S proteasome (Figure 1-7). The 26S proteasome is comprised of a 20S core with a 19S cap (Bochtler et al., 1999). The 20S core is a large ~700 kDa barrel-like multi-chambered enzyme formed from 4 stacks of heptameric rings, for a total of 28 subunits where the outer two rings are alpha subunits, and the inner two rings are beta subunits (Figure 1-7) (Groll and Clausen, 2003). The 19S cap recognizes K48 linked ubiquitin chains, unfolds targeted proteins in an ATP-dependent manner, and threads them through the axial pore towards the active β-subunits in the core of the proteasome. The proteasome core then cleaves the protein, producing peptides 7-10 amino acids in length. The β subunits contain three active sites, which have caspase-like (β1), trypsin-like (β2) and chymotrypsin-like (β5) activities and together can cleave proteins after almost every amino acid (Groll and Clausen, 2003).

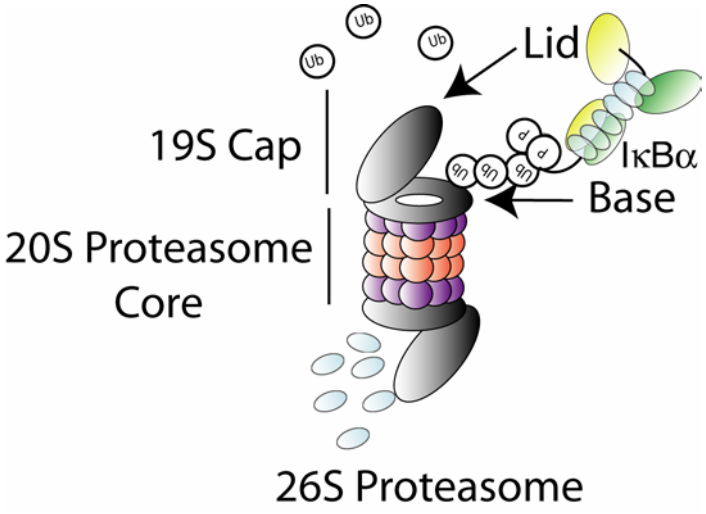

Figure 1-7. Schematic of ubiquitin recognition by the 26S proteasome
Ubiquitin-tagged proteins (example, IκBα) are recognized by the 19S cap and threaded through the 20S core where it is cleaved into 7-10mer peptides. The ubiquitin molecules are then recycled. Purple spheres represent α subunits, and pink spheres represent β-subunits.

H. Various Proteasome Complexes

Although the 26S proteasome is the most well studied proteasome complex, several other proteasome complexes have been identified which can also degrade proteins, but in an ubiquitin-independent manner. For instance, the 20S proteasome core alone has been shown to degrade proteins *in vitro*, without prior modification. In order for this degradation to occur, the α subunits which control access to the inner chamber of the proteasome by their N-terminal tails must be opened (Groll and Clausen, 2003). This can be achieved either through artificial means (addition of SDS), or through an extended peptide of the degradation target protein (Bajorek and Glickman, 2004; Takeuchi et al., 2007). The 20S core can also be activated by several regulatory subunits other than the 19S cap, such as the REG subunits (also known as 11S proteasomes), and PA200. The REGs are heptameric complexes, and have three subunits, α, β and γ, and can form either heptameric REGα/β hybrid complexes or a heptameric complex of REGγ alone. Although the function of the REGs is unclear at this point, there is preliminary evidence that REGα and REGβ participate in the production of peptide ligands for MHC class I molecules (Rechsteiner et al., 2000). The crystal structure of an 11S regulator (PA26 from *T. brucei* –has closest homology to REGα) bound to the 20S core revealed that binding of this regulator opened up the N-terminal tails of the α-subunits, providing a mechanism of proteasome accessibility (Figure 1-8) (Whitby et al., 2000). Finally, other regulatory subunits exist such as

PA200. PA200 has been shown to be involved in DNA repair, and stimulates the cleavage after acidic residues (Ustrell et al., 2002). It is clear that access to the proteasome core is highly regulated by multiple regulatory subunits.

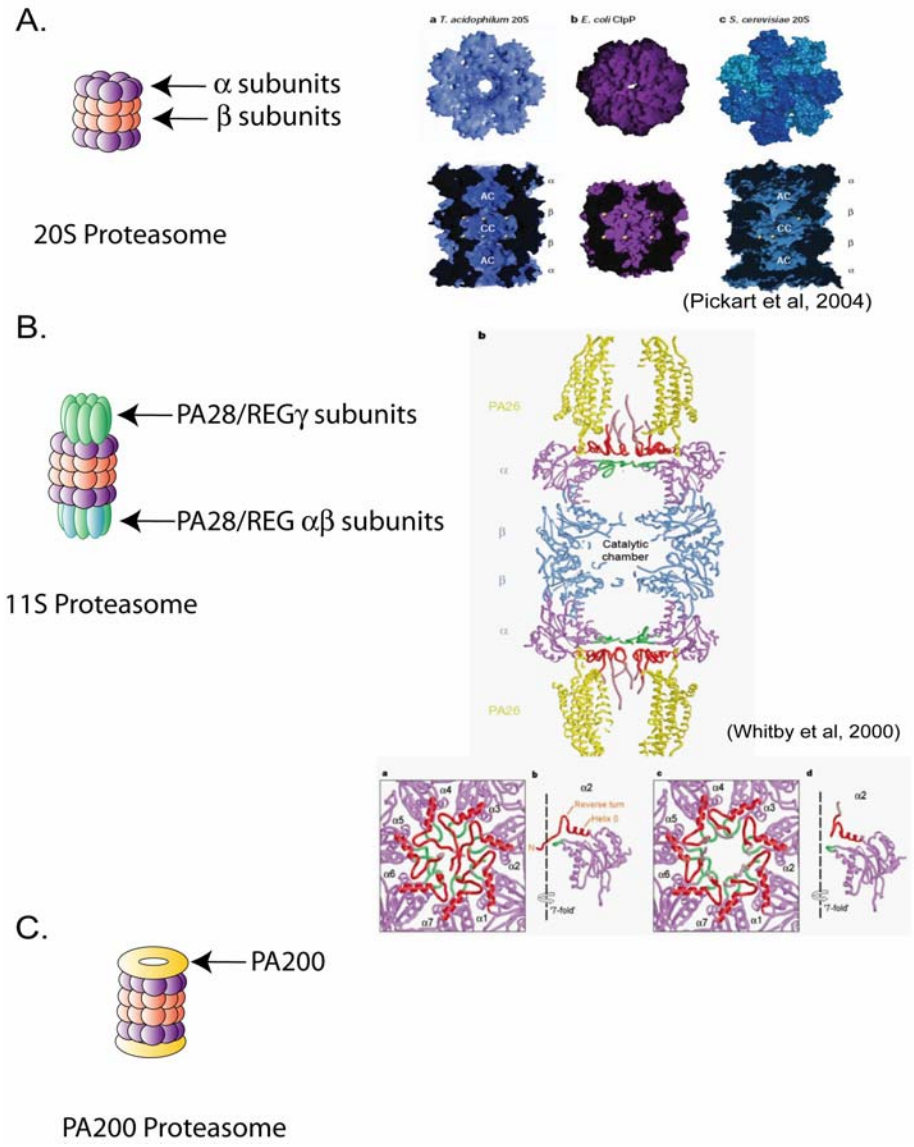

Figure 1- 8. Proteasome complexes involved in ubiquitin independent degradation

(A). Left panel: Cartoon representation of the 20S proteasome core. Right panel: structures of proteasomes from various species (Pickart and Cohen, 2004) Access to the pore of the proteasome varies in these species. (B). Cartoon representation of the 11S proteasome. (B). Crystal structure of an 11S homolog bound to the 20S core and the effect on the α-subunit N-terminal tails on pore accessibility (Whitby et al., 2000). (C). Cartoon representation of a PA200 proteasome.

I. Regulators of ubiquitin-independent proteasome degradation

In addition to proteasomal complexes that have the ability to degrade substrates without ubiquitination, there are also non-proteasomal proteins which can regulate degradation. For instance, the protein NAD(P)H quinine oxidase (NQO1) is a ubiquitous enzyme that uses NAD(P)H to reduce various quinines. NQO1 has been found to associate with the 20S proteasome (but not the 26S proteasome) during purification and regulates protein degradation (Asher et al., 2006). Several lines of evidence show that NQO1 can bind to short lived proteins such as ODC, p53 and p73α and protect them from degradation (Asher et al., 2006) both *in vitro* and *in vivo*. Inhibition of NQO1 promotes ubiquitin independent degradation of these short lived proteins.

J. Ubiquitin-independent Proteasome Substrates

The number of targets that have been identified as ubiquitin-independent substrates of the proteasome has increased significantly. Substrates include p21, ODC (orthinine decarboxylase), p53, SRC-3 and α-synuclein. For instance, ODC has been shown to be degraded in an ubiquitin independent manner by the 26S proteasome (Kahana et al., 2005). This degradation is dependent both on ATP, and the protein antizyme (AZ), which promotes binding of the C-terminal tail ODC to the 26S proteasome. In addition, ODC monomers have also been shown to be degraded by the 20S proteasome independent of ubiquitination (Asher et al., 2005) and this degradation is regulated by NQO1. Another ubiquitin independent substrate is SRC-3,

a steroid receptor co-activator, which is frequently overexpressed in breast cancers. The degradation of SRC-3 is regulated by the REGγ proteasome complex (Li et al., 2006b). Finally, the degradation of p21, a cell cycle inhibitor, has been shown to be both ubiquitin dependent and independent. This degradation can be mediated by the 20S proteasome; however, this degradation is inhibited when p21 is bound to the proliferating cell nuclear antigen (PCNA) or in the presence of the Cyclin E and Cdk2 complex (Asher et al., 2006). These substrates vary significantly in sequence and function, and so it is still unclear as to what the universal degradation mechanism is for ubiquitin-independent degradation.

K. Features of ubiquitin independent substrates

Although there is not a universal signature sequence for ubiquitin-independent substrates, one common feature is the presence of an unstructured region, which lacks three dimensional structure due to inherent features of the protein. For instance, the N-terminal transactivation domain as well as the C-terminal regulatory domain of p53 are unstructured regions (Asher et al., 2006). Also, ODC is predicted to have unstructured regions, which may serve as an additional signal for degradation. One way to induce the unfolding of proteins is through oxidation (Davies, 2001). Mild oxidation leads to unfolding of the native protein, and exposes hydrophobic residues which usually are located in the protein interior, away from solvent. Following this logic, various oxidized proteins were reported as *in vitro* substrates of the proteasome, such as oxidized glutamine synthtase, calmudulin, casein, superoxide dismutase, hemoglobin, myoglobinn, albumin and oxidized histones (Orlowski and Wilk, 2003) .

In addition, the activity of the 26S proteasome has been shown to decrease under oxidative conditions, while the activity of the 20S proteasome is increased under oxidative stress (Davies, 2001).

L. Dynamics of IκBα

Based on the examples given above, it appears that susceptibility of degradation by the proteasome without prior ubiquitination is in part determined by the structure of the protein. In the specific case of IκBα, several independent lines of investigation have lead to the conclusion that the IκBα protein exhibits a high degree of structural dynamics in solution (Croy et al., 2004; Huxford et al., 2000; Sue et al., 2008). This is in contrast to other ankyrin repeat proteins which form highly stable structures with little variation between repeats. Most folding studies have shown that ankyrin repeat structures exist either in a folded or unfolded state, and that the folding transition is highly cooperative (Mosavi et al., 2004). However, IκBα deviates from this ideal cooperative and uncooperative folding transition, and exhibits extreme flexibility in the 5^{th} and 6^{th} ankyrin repeats (Truhlar et al., 2006) as well as the N-terminus of IκBα. Therefore, it is possible that these flexible regions of IκBα may promote degradation in an ubiquitin-independent manner.

M. Degradation and Disease

There are several disease states which are directly correlated to abherrent degradation of proteins, such as Parkinson's disease, Alzheimer's disease, and Huntington's disease (Gao and Hu, 2008). Accumulation of the proteins involved in each of these disease states has been implicated in the pathogenesis. Parkinson's disease is caused by the accumulation of proteins in the neuronal or glial cytoplasm. This accumulation is comprised of mostly α-synuclein, a protein of unknown function expressed in the brain (Tofaris et al., 2001). Monomeric α-synuclein is degraded by the 20S proteasome without prior ubiquitination *in vitro*, whereas multimeric forms of α-synuclein is resistant to degradation (Tofaris et al., 2001). In Huntington's disease, accumulation of the Htt/polyQ proteins causes intranuclear inclusions in neurons, and in Alzheimer's disease, it is accumulation of amyloid-β proteins that form extracellular plaques (Tofaris et al., 2001). Therefore, the degradation of proteins is very important to understand, as misregulation of degradation pathways can have severe functional consequences.

N. Focus of Study

To fully understand NF-κB regulation, it is essential to understand how the inhibitory IκB family of proteins is regulated. The NF-κB:IκB complex is stable, and many studies have focused on NF-κB activation through signal-dependent degradation of IκBα, which includes phosphorylation, ubiquitination, and degradation by the 26S

proteasome (Karin and Ben-Neriah, 2000). However, several reports indicated that unbound IκBα is a labile protein, whose cellular levels varied with the levels of NF-κB (Pando and Verma, 2000; Rice and Ernst, 1993); (O'Dea et al., 2007). Mathematical modeling studies further postulated that free IκBα degradation is an important regulatory step in NF-κB activation (O'Dea et al., 2007). In addition, recent biophysical studies have shown that IκBα has a low folding stability with several extremely flexible regions (Ferreiro et al., 2007; Truhlar et al., 2006). Taken together, these observations suggest that IκBα can undergo two separate degradation pathways, one when bound to NF-κB, and one when not bound, or 'free'. The focus of this work is to determine the requirements of these degradation pathways, the effect of altering the 'free' IκBα degradation pathway on NF-κB activation, and how flexibility of IκBα and the presence of hydrophobic residues influence 'free' IκBα degradation.

II. Materials and Methods

A. Mammalian Cell Culture

1. Cell Culture

Immortalized 3T3 cells were grown in Dulbecco's modified Eagle's Medium (DMEM) supplemented with 10% Bovine Calf Serum (BCS) and 100 u/mL penicillin/streptomycin/glutamine. Cells were stimulated with various amounts of TNF-α (Roche Biochemicals). Cycloheximide was used at 10 μg/mL resuspended in 50% EtOH. (EMD Biosciences) For proteasome inhibition, 50 μM MG132 and 10 μM Epoximicin was used for various times (Calbiochem). 293T cells were grown in DMEM supplemented with 10% Fetal Bovine Serum (FBS).

2. Cloning and Mutagenesis

Human IκBα was used for a template in all cloning and mutagenesis reactions, a kind gift from Chris Phelps. Various fragments were generated by PCR and cloned into pBABE-puro between restriction sites of EcoRI and SalI (New England Biolabs). Digested PCR products and vector were ligated using T4 DNA ligase (New England Biolabs) and transformed into *E.coli* DH5α. Colonies obtained were screened for successful insertion of the PCR product by restriction analysis and sequencing. The 5' primers are given below with an EcoRI restriction site (underlined). A Kozak sequence was added 5' of the start site to ensure efficient translation in mammalian cells.

hIκBα (1-x) EcoRI: 5'-CGG AAT TCG CGC CAT GTT CCA GGC GGC CGA GCG- 3'

hIκBα (67-x) EcoRI: 5'-CGGAATTCGCGCCATGAAGCAGCAGCTACCGAG-3'

The 3' primers have a SalI restriction site, as well as a stop codon.

hIκBα (x-317) SalI: 5'-ACG CGT CGA CTC ATA ACG TCAGAC GCT GG-3'

hIκBα (x-302) SalI: 5'-ACGCGTCGACTCACTCGTCCTCTGTGAA

hIκBα (x-287) SalI: 5'-ACGCGTCGACTCACTCCTCATCCTCACT-3'

hIκBα (x-256) SalI: 5'-ACGCGTCGACTCAGAGCTGGTAGGGAGA-3'

hIκBα (x-241) SalI: 5'-ACGCGTCGACTCAAGCCCCACACTTCAAC-3'

hIκBα (x-206) SalI: 5'-ACG CGT CGA CTC AAC CCA AGG ACA CCA AAA G 3'

Mutagenesis primer pairs are as follows. The Stratagene Quickchange Mutagenesis protocol was followed. Successful mutations were confirmed by sequencing. S32A, S36A primers and lysine to arginine mutant primers were a kind gift from T. Huxford, and Y254L, T257A mutant primers were a kind gift from Stephanie Truhlar.

hIκBα (Y289A) F: 5'-GAG GAT GAG GAG AGC GCT GAC ACA GAG TC-3'

hIκBα (Y289A) R: 5'-GAC TCT GTG TCA GCG CTC TCC TCA TCC TC-3'

hIκBα (F295A) F: 5'- GAC ACA GAG TCA GAG GCC ACG GAG TTC ACA GAG-3'

hIκBα (F295A) R: 5'- CTC TGT GAA CTC CGT GGC CTC TGA CTC TGT GTC-3'

hIκBα (F298A) F: 5'-CAG AGT TCA CGG AGG CCA CAG AGG ACG AGC TG-3'

hIκBα (F298A) R: 5' CAG CTC GTC CTC TGT GGC CTC CGT GAA CTC TG-3'

hIκBα (F295A, F298A) F: 5'-GAC ACA GAG TCA GAG GCC ACG GAG GCC ACA GAG GAC GAG CTG-3'

hIκBα (F295A, F298A) R: 5'-CAG CTC GTC CTC TGT GGC CTC CGT GGC CTC TGA CTC TGT GTC-3'

hIκBα (L303A) F: 5'-ACA GAG GAC GAG GCT CCC TAT GAT GAC TG-3'

hIκBα (L303A) R: 5'-CAG TCA TCA TAG GGA GCC TCG TCC TCT GT-3'

hIκBα (Y305A) F: 5'-GAG GAC GAG CTG CCC GCC GAT GAC TGT GTG-3'

hIκBα (Y305A) R: 5'-CAC ACA CTC ATC GGC GGG CAG CTC GTC CTC-3'

The 1-241 4G construct was made in two steps: first, mutation of the hydrophobic residues to glycine:

hIκBα (241_4G) F: 5'-CAA AAT CCT GAC CTG GGT TCA GGC GGA GGG AAG TGT GGG GCT GAT G-3'

hIκBα (241_4G) R: 5'-CAT CAG CCC CAC ACT TCC CTC CGC CTG AAC CCA GGT CAG GAT TTT G-3'

The second step introduced a stop codon (underlined) in the mutated construct:

hIκBα (241_4Gstop) F: 5'-GAA GTG TGG GGC TTA AGA TGT CAA CAG AG-3'

hIκBα (241_4Gstop) R: 5'-CTC TGT TGA CAT CTT AAG CCC CAC ACT TC-3'

hIκBα (280_stop) F: 5'-CTT CAG ATG CTG TAA CCA GAG AGT GAG G-3'

hIκBα (280_stop) R: 5'-CCT CAC TCT CTG GTT ACA GCA TCT GAA G-3'

hIκBα (Y289G) F: 5'- GAG GAT GAG GAG AGC GGT GAC ACA GAG TCA GAG-3'

hIκBα (Y289G) R: 5'- CTC TGA CTC TGT GTC ACC GCT CTC CTC ATC CTC-3'

hIκBα (L303G) F: 5'- ACA GAG GAC GAG GGG CCC TAT GAT GAC TGT G-3'

hIκBα (L303G) R: 5'- CAC AGT CAT CAT AGG GCC CCT CGT CCT CTG T-3'

hIκBα (F295G, F298G) F: 5'GAC ACA GAG TCA GAG GGC ACG GAG GGC ACA GAG GAC GAG CTG CC-3'

hIκBα (F295G, F298G) R: 5'-GGC AGC TCG TCC TCT GTG CCC TCC GTG CCC TCT GAC TCT GTG TC-3'

The PESTA (CK2 phosphorylation sites mutated to alanine) template was a kind gift from the Hoffmann laboratory.

3. Transient Transfection and Retrovirus Production

Once clones were produced either through cloning or mutagenesis, 7 μg of pBABE DNA was co-transfected into HEK 293T cells with 3 μg of pCL-Eco, a packaging DNA (Novagen), using Lipofectamine 2000 (Invitrogen) according to the manufacturer's protocol. HEK 293T cells were seeded at ~50% confluency 24 hours prior to transfection into a 6 cm^2 plate. 42 hours after transfection, the virus-containing supernatant was filtered through a 0.45 μm filter (Millipore) and placed onto target 3T3 cells with 8 μg/mL polybrene (Calbiochem) in a 10 cm^2 plate. After cells were infected for 48 hours, they were split into 15 cm^2 plates and infected cells were se1ected using 10 μg/mL puromycin hydrochloride (Calbiochem) for 48 hours,

or until 100% of control cells died. Surviving cells were then expanded to be used for experiments. All cells were a kind gift from Alexander Hoffmann.

4. Cell Stimulation and Western Blot Detection and Quantification

After treatment with 10 μg/mL cycloheximide (Calbiochem) or various amount of TNF-α (Roche), cell extracts were prepared by removing the media, and washing cells in cold PBS 2X on ice. Cells were then harvested in the following modified RIPA buffer: 20 mM Tris-HCl pH 7.5, 0.2 M NaCl, 1% Triton-X-100, 1 mM EDTA, 2 mM DTT, 0.1 mM phenyl-methysulfonyl fluoride (PMSF), Na-O-Vanadate, and protease inhibitor cocktail (Sigma). For detection by a western blot, approximately 50 μg of total protein was separated on either a 10% or 12.5% SDS-PAGE followed by transfer onto a nitrocellulose membrane. Immunodetection was perfomed with antibodies against IκBα (Santa Cruz, sc-371 or sc-203- 1:1000 dilution, or anti-phospho IκBα from Cell Signaling, 1:5000 dilution), IκBε (sc-7156), or p65 (sc-372) followed by anti-rabbit secondary HRP-conjugated antibody (Santa Cruz, sc-1615). To detect β-actin as a loading control, sc-1615 was used.

5. Immunoprecipitation and TCA precipitation

Approximately 1 mg of total cellular protein in modified RIPA buffer was precleared with 40 μg of protein G agarose beads, and incubated overnight with α-RelA (sc 372-G) at 4^0C. Immunoprecipitates were captured with protein G beads, washed three times with 100 mM Tris pH 7.5, 250 mM NaCl, and 1% Triton-X, boiled and run on a 12.5% SDS-PAGE gel. After immunoprecipitation, the flow-through was precipitated with 5% TCA, and spun for 10' at 4^0C. The supernatant was

discarded, and the pellet was washed 3X with 1mL of acetone. The pellet was then dried and resuspended in 4X SDS dye, and run on a 12.5% SDS-PAGE gel.

6. Electrophoretic Mobility Shift Assay (EMSA)

Following stimulation with TNF-α, cells were washed twice with ice-cold Phosphate Buffered Saline (PBS) + 1mM EDTA and collected. The pellet was resuspended in 100 µL CE buffer (10mM Hepes-KOH (pH 7.9), 60 mM KCl, 1 mM EDTA, 0.54% NP-40, 1mM DTT, 1mM PMSF) and vortexed for lysis. Nuclei were pelleted at 4000*g*, resuspended in 30 µl NE Buffer [250 mM Tris (pH 7.8), 60 mM KCl, 1mM EDTA, 1 mM DTT, 1 mM PMSF], and lysed by 3 freeze-thaw cycles. Nuclear lysates were cleared by 14000*g* centrifugation and protein concentrations were normalized via Bradford assay. 2.5 µl total nuclear protein was reacted at room temperature for 15 min with 0.01 pmol of 32P-labeled 38-bp double-stranded oligonucleotide containing two consensus kappaB sites: (GCTACAA**GGGACTTTCC**GCTG**GGGACTTTCC**AGGGAGG) in binding buffer [10 mM Tris-Cl (pH 7.5), 50 mM NaCl, 10% glycerol, 1% NP-40, 1 mM EDTA, 0.1 µg/µl polydIdC], for a total reaction volume of 6 µl. Complexes were resolved on a nondenaturing 5% acrylamide (30:0.8) gel containing 5% glycerol and 1× TGE [24.8 mM Tris, 190 mM glycine, 1 mM EDTA], and were visualized using a PhosphorImager (Molecular Dynamics).

7. RNase Protection Assay

Total cellular RNA was isolated from confluent with Trizol reagent (Invitrogen). Transcript levels were monitored with α-[^{32}P]UTP–labeled probes using a

RiboQuant kit (BD Biosciences) according to the manufacturer's instructions. Data was obtained using a storage phosphor screen (GE Healthcare) and a variable mode imager (Typhoon 9400; GE Healthcare). Data was quantitated using ImageQuant TL (Amersham Biosciences) by normalization to L32 and/or glyceraldehyde- 3-phosphate dehydrogenase after local background subtraction. IκB probes were designed to select for mature mRNA species by spanning exon–exon junctions. The probe set designed against human IκBα was constructed to anneal against amino acids 180-235, and was produced using the following primers:

hIκBα RPA EcoRI: 5'-GGA ATT CAA CTA CAA TGG CCA CAC GTG-3'

hIκBα RPA HindIII: 5'-CCC CAA GCT TCA GGA GTG ACA CCA GGT CA-3'

L32, and glyceraldehyde-3-phosphate dehydrogenase probes were obtained from RiboQuant sets (BD Biosciences).

B. Proteasome Degradation Assay

1. Protein Expression and Purification

For degradation assays which involved both IκBα (residues 6-317) and p65 (residues 1-325) were purified as previously described, and were a kind gift from Tom Huxford. Degradation assays which included thermodynamically altered mutants were a kind gift from Diego Ferreiro. WT IκBα 1-317 or IκBαΔC288 constructs were cloned into pET-15b using the following primers and between restriction sites EcoRI and BamHI:

hIκBα (1-x EcoRI) 5'-GGA ATT CCA TAT GTT CCA GGC GGC CGA GCC G-3'

hIκBα (x-317 BamHI) 5'-CGG GAT CCT TAT AAC GTC AGA CGC TGG-3'

hIκBα (x-287 BamHI) 5'-CGG GAT CCT TAC TCC TCA TCC TCA CT-3'

Positive clones were transformed into BL21 (DE3) and grown up in 100 μg/mL ampicillin until OD_{600} reached ~0.4 at 37^0C. Cells were then induced with 0.1 mM IPTG and incubated at 25^0C for 16 hours, and pelleted by centrifugation at 4,000 rpm for 30' at 4^0C. Cell pellets were resuspended in 20 mM Tris pH 7.5, 150 mM NaCl, 1 mM DTT, and 0.1x protease inhibitor cocktail (Sigma) and sonicated for 30' intervals 5x at 9x90% power. After sonication, lysates were spun at 13,000 rpm for 40' at 4^0C and the soluble fraction was loaded onto a gravity flow Fast-Q column. The column was washed with the lysis buffer, and IκBα was eluted with a 200-700 mM NaCl gradient. Peak fractions were collected and loaded onto a Ni^{2+} column. The column was washed with 20 mM Tris pH 7.5, 150 mM NaCl, and 50 mM Imidazole. IκBα was eluted with increasing amounts of imidazole (100-600 mM). Peak fractions were analyzed by SDS-PAGE and Coomassie staining and were pooled, frozen and stored at -80^0C. Immediately before a proteasome degradation assay, IκBα was further purified through analytical gel filtration (SD75) in 20 mM Tris pH 7.5, 150 mM NaCl, and 1 mM DTT. A portion of the peak fraction was used directly for the degradation assay.

2. Proteasome Degradation Assay

The 20S proteasome was either a gift from Dr. Rechsteiner and Dr. Pratt, University of Utah, or Jessica Ho. The 26S proteasome was either a gift from the Pilipenko laboratory or purchased through Boston Biochemical. For degradation

reactions, the proteins and the proteasome were mixed in various molar ratios in a buffer containing 20 mM Tris pH 7.0, 250 mM NaCl, 10 mM $MgCl_2$, and 1 mM DTT. Reactions took place either at 37^0C or 25^0C and in the experiments where various truncations and/or mutations of IκBα was studied alone, samples were run through analytical gel filtration directly before proteasome degradation. Reactions which included the 26S proteasome also included 2mM ATP in the reaction buffer. Samples were removed at various time points and the reaction was stopped by adding SDS–PAGE loading dye and boiling. Protein bands were separated by SDS–PAGE and visualized by Western blotting, either with antibodies against the C-terminus of IκBα, sc-317 or sc-847. The proteasome inhibitor MG132 was used as a negative control at 1 mM (Calbiochem).

3. Native gel/Silver Stain Analysis

To determine whether the 26S proteasome was intact, a 3.5% native gel (37.5:1 Acrylamide/Bis-Acrylamide) was run in the presence of 2 mM ATP and 2 mM $MgCl_2$. Bands were detected by silver stain using the ProQuest Silver Staining Kit from Invitrogen, Inc.

III. NF-κB Dictates the Degradation Pathway of IκBα

A. Introduction

The NF-κB family of dimeric transcription factors plays a key role in many aspects of human physiology and disease. The family is composed of five members, RelA, RelB, p50, p52, and cRel that can form combinatorial hetero- and homodimers. The transcriptional activity of RelA and c-Rel containing dimers is tightly repressed by three inhibitors known as IκBα, IκBβ and IκBε through the formation of stable IκB/NF-κB complexes. In response to extracellular stimuli, such as pro-inflammatory cytokines, the signal response domain (SRD) of IκB is phosphorylated at serines 32 and 36 by activated IKK (IκB kinase), which leads to ubiquitination of IκB by ubiquitin ligases and its degradation by the 26S proteasome (Baldwin, 1996; Ghosh et al., 1998; Karin and Ben-Neriah, 2000), releasing NF-κB to activate gene transcription.

The stimulus-induced degradation of IκBα and activation of NF-κB is well characterized; however, one important feature of NF-κB regulation is its tight repression by IκB in unstimulated cells. Elevated NF-κB activity is associated with many human pathologies, including arthritis, atherosclerosis and cancer (Courtois and Gilmore, 2006). Nevertheless, the manner by which NF-κB activity is controlled in resting cells is unclear. It has been shown that IκB proteins are continuously synthesized in uninduced cells; indeed, inhibition of protein synthesis activates NF-κB and this activation requires basal IKK activity (Frankenberger et al., 1994; O'Dea et al., 2007). This implies that an IKK-dependent IκBα degradation pathway exists in

unstimulated cells and that continuous synthesis of IκBα is essential to prevent basal NF-κB activity. It is known that two distinct pools of IκBα exists in cells; the larger IκB pool is associated with NF-κB (Scott et al., 1993) and the minor pool remains as a 'free' protein. Recent studies have revealed a three order of magnitude difference in the half-life of free and NF-κB bound IκBα (O'Dea et al., 2007). Although free IκBα is degraded rapidly, it has also been reported to be a poorer substrate for IKK than NF-κB-bound IκBα (Zandi et al., 1998). The apparent contradiction between inefficient IKK phosphorylation and the short half-life of free IκBα remains unresolved.

Several studies have investigated the basal degradation pathways of both free and bound IκBα, but have come to contradictory conclusions (Krappmann et al., 1996; Pando and Verma, 2000). One study showed that the basal degradation of both free and bound IκBα occur through the same pathway that do not require IKK phosphorylation or ubiquitination (Krappmann and Scheidereit, 1997). Later, others showed that basal degradation of the bound IκBα did not require IKK phosphorylation, but could perhaps require ubiquitination. In addition, this study showed that free IκBα required ubiquitination for degradation (Pando and Verma, 2000). Considering the potential significance of free IκBα in NF-κB regulation, we sought out to clearly understand the basal degradation mechanisms of the bound and free IκBα to determine exactly how constitutive NF-κB activity is regulated.

In the present study, we address these questions with new genetic tools and a mathematical model of the reactions that determine IκBα metabolism and nuclear NF-κB activity. We find that although free IκBα can be a good substrate of IKK *in vivo*,

rapid degradation of free IκBα does not require IKK-mediated phosphorylation or lysine targeted ubiquitination, and is instead regulated intrinsically by sequences in its C-terminus. When the free IκBα degradation pathway is altered, NF-κB activation is severely dampened, proving the importance of a rapid free IκBα degradation pathway. We address the functional significance of these differential degradation rates and pathways, and find that they are critical for allowing stimulus-responsive NF-κB activation, while ensuring a low basal level of NF-κB activity.

B. Results

1. The stability of IκBα is dependent on the presence of NF-κB subunits

Although IκBα has been studied extensively as part of the IκB-NF-κB complex, the function and regulation of the free molecule remains unclear. It was reported previously that IκBα is stabilized by NF-κB (O'Dea et al., 2007; Rice and Ernst, 1993; Scott et al., 1993), but it has remained uncertain how IκBα is degraded when it is not bound to NF-κB. To characterize the degradation mechanism of IκBα proteins we used a retroviral transgenic system to introduce mutant forms of human IκBα into mouse embryonic fibroblasts (MEFs) deficient in the NF-κB proteins known to associate with it. These *nfkb1*$^{-/-}$*rela*$^{-/-}$*crel*$^{-/-}$ are referred to as *nfkb*$^{-/-}$. Consistent with these previous studies, we also find that when IκBα is reconstituted in *ikba*$^{-/-}$ cells, *nfkb1*$^{-/-}$/*rela*$^{-/-}$/*ikba*$^{-/-}$/*ikbb*$^{-/-}$ cells, and *nfkb*$^{-/-}$ cells, the protein level of IκBα decreases with the reduction of NF-κB subunits, while the mRNA level of IκBα in

nfkb$^{-/-}$ is ~75% of IκBα in *ikba*$^{-/-}$ (Figure 3-1). These results reconfirm the requirement for NF-κB to stabilize the protein level of IκBα.

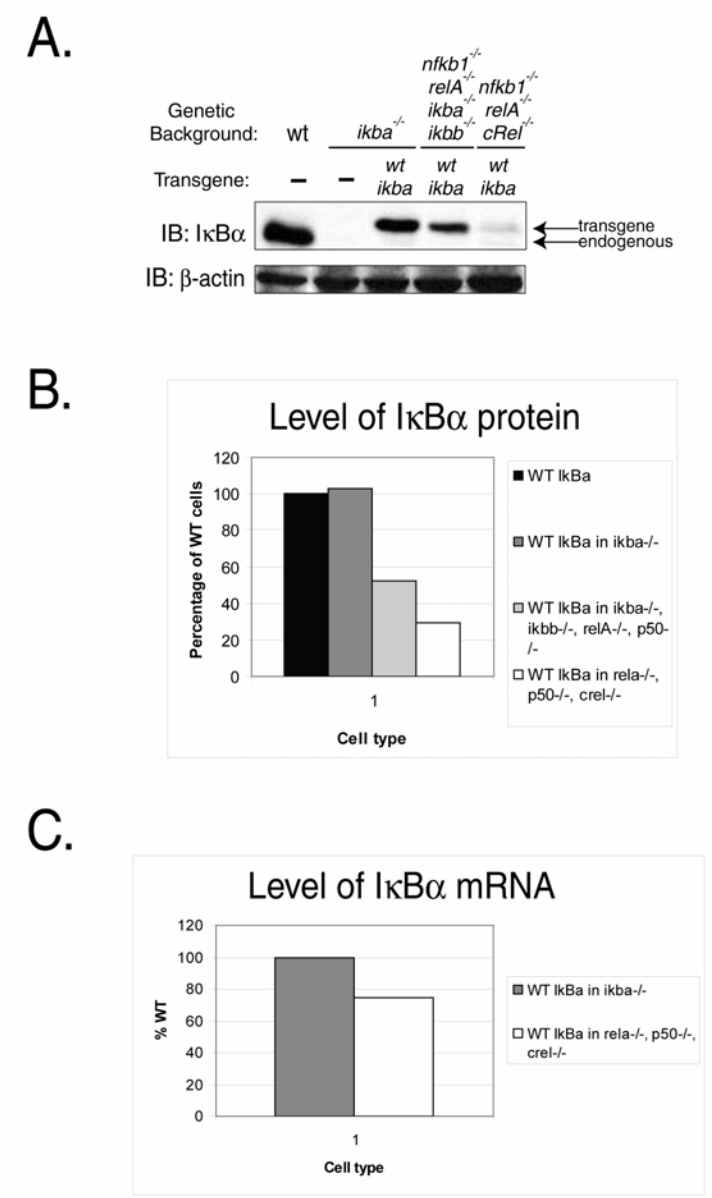

Figure 3-1. The stability of IκBα depends on the presence of NF-κB subunits Various NF-κB knock-out genetic backgrounds were used to stably transfect WT IκBα**.** (A). Cells with three different genetic backgrounds were used; *ikba*$^{-/-}$, *nfkb1*$^{-/-}$*/rela*$^{-/-}$*/ikba*$^{-/-}$*/ikbb*$^{-/-}$ *and nfkb1*$^{-/-}$*/rela*$^{-/-}$*/crel*$^{-/-}$ *(nfκb*$^{-/-}$*)*. Cell lysates were separated by SDS-PAGE and immunobloted using sc-371 (α – IκBα). Western blotting against IκBα reveals that the steady state protein level of IκBα depends on the presence of NF-κB subunits. Transgenic IκBα runs slightly higher than endogenous, so both species can be observed. (B). The level of IκBα protein in the various cell types was quantified and graphed. (C). The level of IκBα mRNA was measured both in cells containing NF-κB (*ikba*$^{-/-}$) and without NF-κB present (*nfkb*$^{-/-}$)

2. IκBα is degraded independently of IKK phosphorylation and ubiquitination

We find that when introduced into *nfkb*$^{-/-}$ cells, wild-type IκBα shows a remarkably short half-life of 10 minutes or less, similar to the half-life of endogenous IκBα in *nfkb*$^{-/-}$ deficient cells (Figure 3-2B). Since IκBα is known to be degraded in response to stimulation *via* IKK-mediated phosphorylation and specific ubiquitination, we first examined the role of these modifications by introducing specific mutations into IκBα. Several reports have also looked into the basal degradation of the free pathway; however, there is still confusion as to the role of phosphorylation and ubiquitination in the basal degradation of free IκBα (Krappmann et al., 1996; Pando and Verma, 2000). To eliminate IKK-phosphorylation, we generated a transgenic *nfkb*$^{-/-}$ cell line which expresses the S32A, S36A IκBα mutant. The degradation rates were estimated by treating these cells with cycloheximide, a translation inhibitor, and tracking the loss of IκBα protein by Western blot. We observed no difference in the apparent rates of degradation of the mutant and wild-type IκBα (Figure 3-2B). To clearly understand whether ubiquitination is required for free IκBα degradation, we created two different mutants: In one mutant, only the two lysines that have been shown to be ubiquitinated in stimulus induced degradation of NF-κB-bound IκBα were mutated to arginines (K21, 22R). In the second mutant, all nine lysines present in the IκBα protein were mutated to arginines (K9R) (Figure 3-2C). We observed that both K21R, K22R and KR9 degrade at a similar rate as wild-type IκBα. In all, our results provide a clear answer which shows that neither IKK phosphorylation nor lysine ubiquitination are required for free IκBα degradation.

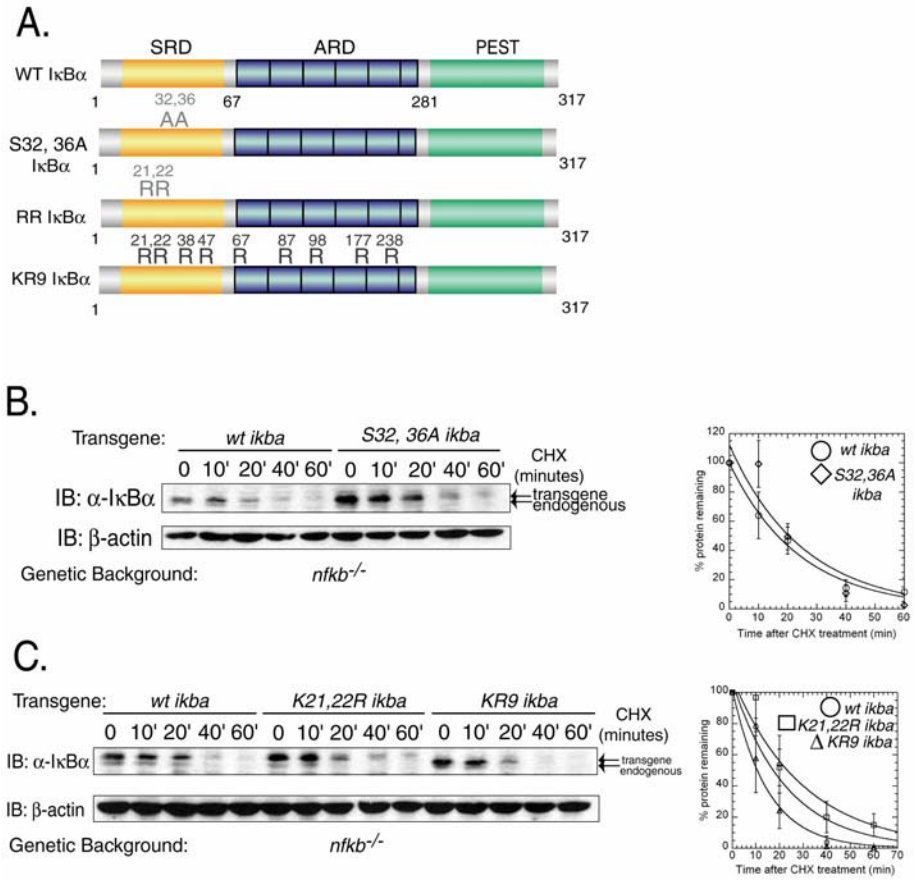

Figure 3-2. IκBα is degraded independently of IKK phosphorylation and ubiquitination

A) Schematic of IκBα primary sequence. The Signal Response Domain (SRD) is followed by the Ankryin Repeat Domain (ARD) and the PEST domain. IKK phosphorylation sites are indicated, as well as all lysines in IκBα.

B) IKK phosphorylation mutants do not inhibit free IκBα degradation. Left panel- Western blot (WB) of WT and S32, 36SA IκBα from extracts of *nfκb*$^{-/-}$ cells treated with cycloheximide for the indicated times. Endogenous IκBα and transgenic IκBα are denoted by arrows. Right panel- This is presented graphically with three separate experiments plotted with error bars signifying +/- SEM (Standard Error of the Mean). (○) represents transgenic WT IκBα and (◊) represents S32, 36A IκBα.

C) Ubiquitination mutants do not slow free IκBα degradation. Left panel- WB of WT IκBα and different lysine mutants from cell extracts prepared as described in (B). Right panel- This is presented graphically with triplicate experiments plotted with error bars signifying +/- SEM. (○) represents transgenic WT IκBα, (□) represents K21, 22R IκBα and (Δ) represents KR9 IκBα.

3. NF-κB masks the intrinsic degradation signal of IκBα

If IκBα is intrinsically unstable *in vivo*, it may also be a good substrate for purified proteasome *in vitro*. We found that the purified 20S proteasome core, which degrades many unstable proteins such p21 and ODC (Alvarez-Castelao and Castano, 2005; Asher et al., 2005; Chen et al., 2004; Touitou et al., 2001), also degrades IκBα in a ubiquitin independent manner (Figure 3-3A, lanes 1-4).

We next examined whether IκBα bound to the NF-κB dimer was also such a sensitive substrate for the 20S proteasome. We found that when IκBα is complexed to recombinant RelA, the proteasome is no longer able to degrade it (Figure 3-3A, lanes 5-8). The intrinsic instability of IκBα, which could be encoded in flexible regions of the protein, was apparently protected by NF-κB. Both the N-terminus and the C-terminal PEST region of IκBα are flexible and could potentially contribute to proteasomal recognition. Interestingly, our crystallographic and biochemical analysis of the IκBα /NF-κB complex suggests that the PEST region is protected from proteasomal degradation when bound to NF-κB (Huxford et al., 1998; Phelps et al., 2000).

Since the proteasome is required to degrade ubiquitinated IκBα in response to inflammatory stimuli, we wanted to test if the proteasome was also involved in the degradation of free, non-ubiquitinated IκBα in cells. When transgenic *nfkb*$^{-/-}$ cells were treated with the proteasome inhibitor MG132, the amount of IκBα increased rapidly in all cell lines (Figure 3-3B). This result has also been reproduced with a more specific proteasomal inhibitor, epoximicin (Figure 3-3C). These results clearly

show that even in the absence of IKK phosphorylation and ubiquitination the proteasome is essential for free IκBα degradation. We conclude that IκBα is an intrinsically unstable protein *in vivo* which can be degraded in an ubiquitin-independent manner by the proteasome in unstimulated cells.

4. Bound IκBα degradation requires IKK phosphorylation and ubiquitination in both stimulated and unstimulated cells

Does protection from ubiquitination-independent proteasomal degradation seen *in vitro* also occur *in vivo*? To that end, we introduced IκBα transgenes into *ikba*$^{-/-}$ NF-κB-containing cells, and examined their degradation in the absence of stimulation. We found indeed that wt IκBα transgenes introduced into *ikba*$^{-/-}$ cells resulted in IκBα proteins that had very long half-lives (~8 hours vs. ~10 min; compare Figure 3-6A vs. Figure 3-2B). To test the effect of IKK phosphorylation and ubiquitination in the degradation of NF-κB bound IκBα, *ikba*$^{-/-}$ cells were reconstituted with mutants defective in IKK phosphorylation and ubiquitination. These mutants abolish stimulated IκBα degradation and NF-κB activation, as shown in Figure 3-4. All of these mutants are able to bind to NF-κB in these cells, albeit with varying affinities (Figure 3-5). The levels of transgenic IκBα observed *ikba*$^{-/-}$ cells represent bound IκBα, since the half-life of bound IκBα is much longer than the free form, and all of the free IκBα is completely degraded within 60' of cycloheximide treatment. We observed that reconstituted IκBα in *ikba*$^{-/-}$ cells is only degraded when the IKK phosphorylation sites are intact (Figure 3-6). When the preferred ubiquitination sites

(K21, 22R) are mutated to arginine, degradation still occurs, which suggests that other lysines can be used for ubiquitination (Scherer et al., 1995). However, when all lysines are mutated (KR9), the degradation is slowed compared to WT IκBα. These results suggest that in unstimulated cells, NF-κB-bound IκBα undergoes slow degradation that requires both IKK phosphorylation and ubiquitination. In addition, these observations point out that the same turnover pathway pertains to NF-κB-bound IκBα in unstimulated and stimulated cells. In contrast, free IκBα turnover is determined intrinsically, independent of modifications such as phosphorylation or ubiquitination. Again, we have clearly understood the modifications required for basal degradation of free and bound IκBα.

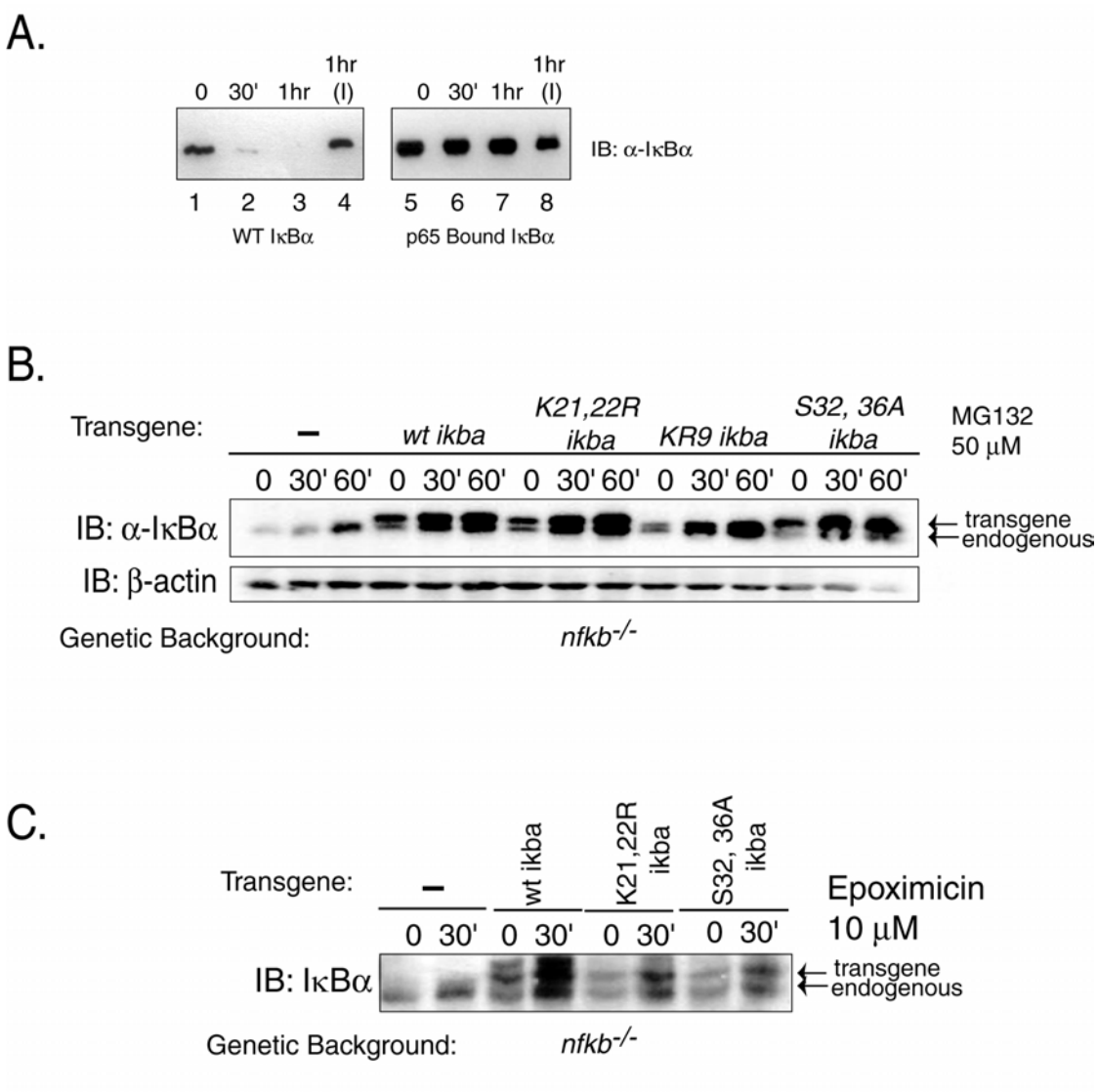

Figure 3-3. WT IκBα and mutations are degraded by the proteasome *in vitro* and in cells

(A). NF-κB protects IκBα from proteasomal degradation *in vitro*. Top: Purified 20S proteasome and IκBα were incubated at 37^0C, with or without purified p65. (I) represents the proteasome inhibitor, MG132. (B). Free IκBα is degraded by the proteasome. WB showing IκBα in the extracts of transgenic cells were treated with MG132. All protein levels increase over time, which show that the proteasome is involved in the degradation of free IκBα. (C). WB showing IκBα in the extracts of transgenic cells were treated with epoximicin, a specific proteasome inhibitor. All protein levels increase over time, which show that the proteasome is involved in the degradation of free IκBα.

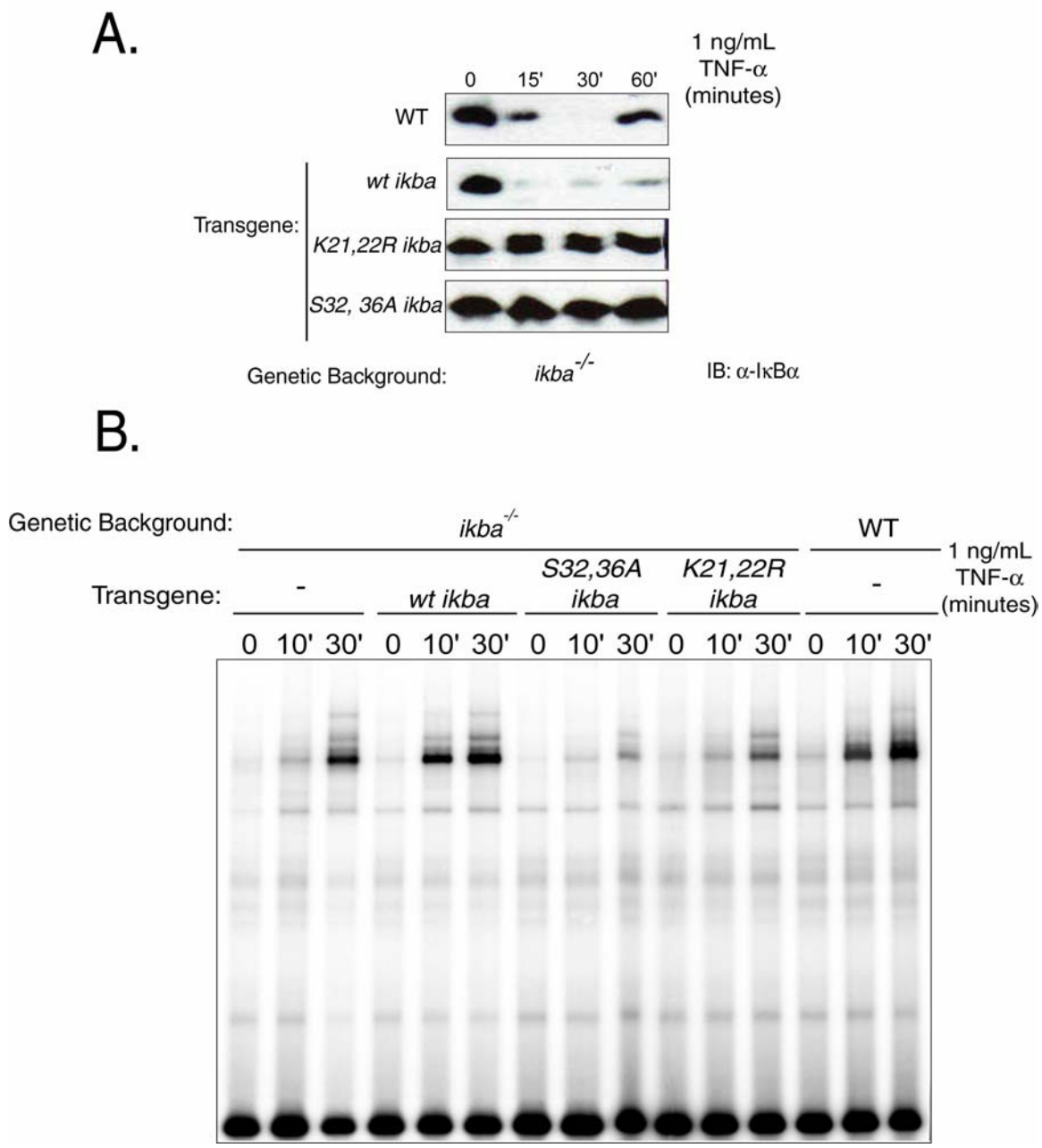

Figure 3-4. IKK phosphorylation and Ub mutations of IκBα abolish NF-κB activation

A) Transgenic WT IκBα behaves like WT IκBα, but when the main ubiquitination sites and/or Serines are mutated, signal dependent IκBα degradation does not occur

B) An EMSA comparing mutant NF-κB activation (Courtesy Alexander Hoffmann)

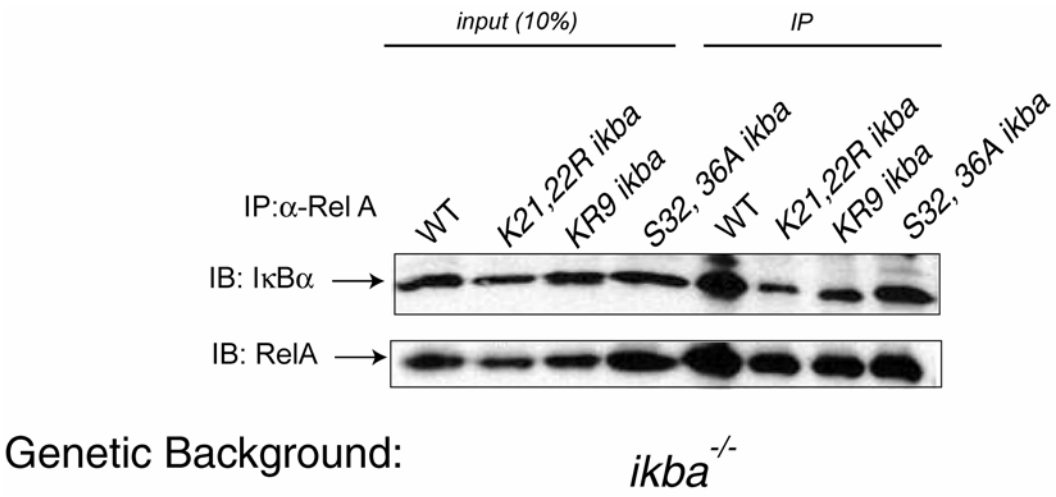

Figure 3-5. Mutants of IκBα bound to NF-κB
Cells expressing various mutants used in this study were assessed for binding to RelA. Extracts prepared from stable cell lines expressing either WT IκBα, K21, 22R IκBα, KR9 IκBα, or S32, 36A IκBα were immunoprecipitated with an antibody directed against RelA. Both inputs and immunoprecipitated proteins are visualized by western blot and probed with an α-IκBα or α-RelA antibody.

A.

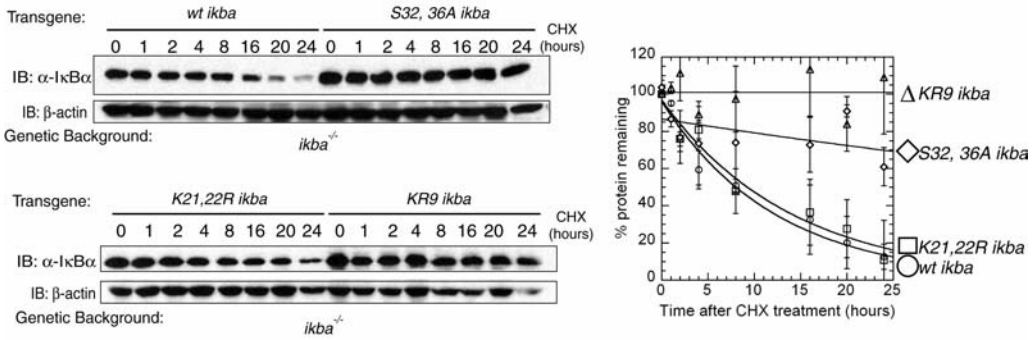

B.

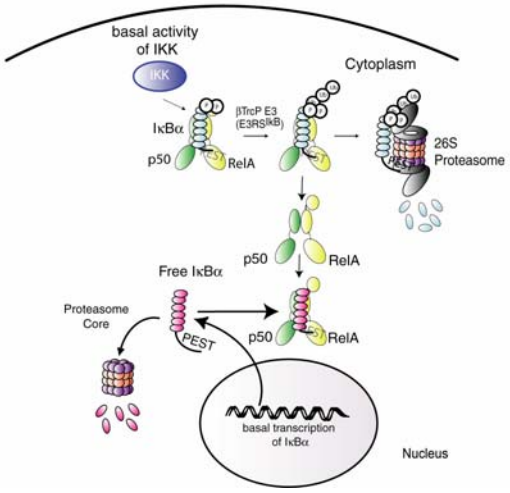

Figure 3-6. NF-κB determines the degradation pathway of IκBα
(A). IκBα is highly stable *in vivo* in the presence of NF-κB. Left panel-WB showing WT, IKK phosphorylation and ubiquitination-defective mutants introduced into *ikba*$^{-/-}$, where all NF-κB subunits are present. Cells were treated with cycloheximide for different lengths of time (up to 24 hours) and the protein levels visualized by WB. Right panel- This experiment was repeated twice and is represented graphically with error bars signifying +/- SEM (○) represents transgenic WT IκBα, (□) represents K21, 22R IκBα (Δ) represents KR9 IκBα and (◊) represents S32, 36A IκBα.
(B). A model of NF-κB repression by IκBα in pre-stimulated cells. There are two processes which control IκBα degradation. In the resting cell, basal IKK activity phosphorylates bound IκBα and targets it for ubiquitin dependent degradation. In addition, free IκBα is continuously synthesized and degraded in an IKK-and Ub independent mechanism. This keeps NF-κB from being activated in the resting cell.

5. The C-terminal PEST region regulates the degradation of free IκBα

In order to examine which segment(s) of the IκBα polypeptide determine the turnover rate *in vivo*, we generated three constructs which removed the flexible N- and C-termini to create IκBαΔN67, IκBαΔC303, and IκBαΔC288 (Figure 3-7A). *Nfkb*$^{-/-}$ cells stably expressing these mutants were generated and relative degradation rates were estimated using cycloheximide treatment. Removal of the N-terminus did not alter the degradation rate (Figure 3-7B). The removal of the last 15 amino acids (IκBαΔC303) slowed the degradation rate (Figure 3-7C), although not to the extent of IκBαΔC288 (Figure 3-8D). The segment (288-317) contains a PEST sequence, which encompasses residues 281-302. This observation is consistent with the PEST hypothesis which states that the PEST sequence is responsible for protein turnover (Rogers et al., 1986). Within the PEST region, there are six serines and threonines that have been shown to be phosphorylated by casein kinase 2 (CK2) and several reports claim that this phosphorylation affects the turnover of IκBα (Kato et al., 2003; Lin et al., 1996; McElhinny et al., 1996; Schwarz et al., 1996). We mutated these residues (S283, S288, T291, S293, T296 and T299) to alanine to generate the PESTA mutant. The PESTA mutant is degraded more slowly than wild type IκBα, but more rapidly than IκBαΔC288 (Figure 3-7D). These results suggest that phosphorylation of these residues contribute to free IκBα degradation, but other residues within the PEST domain also contribute to the rapid degradation of free IκBα. The RNA levels of all of these mutants are similar, suggesting that we have indeed altered the degradation of

free IκBα (Figure 3-8 and 3-9) Overall, our experiments show an important role of the region encompassing residues 288-302 in the turnover of free IκBα.

Figure 3-7. Rapid IκBα turnover is conferred by intrinsic C-terminal sequences (A). Schematic representation of various IκBα constructs tested for their susceptibility to degrade as a free protein. (B). The N-terminus of IκBα does not determine degradation of IκBα in the free form. Left panel- WB of IκBα in extracts of cells expressing WT and IκBα ΔN67 mutants in *nfκb*$^{-/-}$ cells after treatment with cycloheximide. Right panel- Triplicate experiments are represented graphically. Construction of stable cells and preparation of cell extracts were carried out as described in Figure 2. (●) represents transgenic WT IκBα, (▲) represents IκBα ΔN67. (C). The C-terminus of IκBα controls the rapid degradation of free IκBα. Left panel- Cells expressing transgenic IκBαΔPEST-terminus IκBαΔC288 and IκBαΔC303 were treated with cycloheximide for the indicated times and cell extracts were visualized by WB. Right panel- Triplicate experiments representing WT IκBα and IκBαΔC303 are represented graphically. (●) represents transgenic WT IκBα and (■) represents IκBαΔC303. (D). The PEST domain of IκBα is responsible for high turnover rate of free IκBα. Left panels (top and bottom) - Cells expressing transgenic WT IκBα, IκBαΔC288 and PESTA IκBα were treated with cycloheximide for the indicated times and cell extracts were visualized by WB. A (*) denotes a non-specific band. Right panel- The relative degradation rates of WT IκBα (black line), IκBαΔC288 (light gray line) and PESTA IκBα (gray line) are represented graphically.

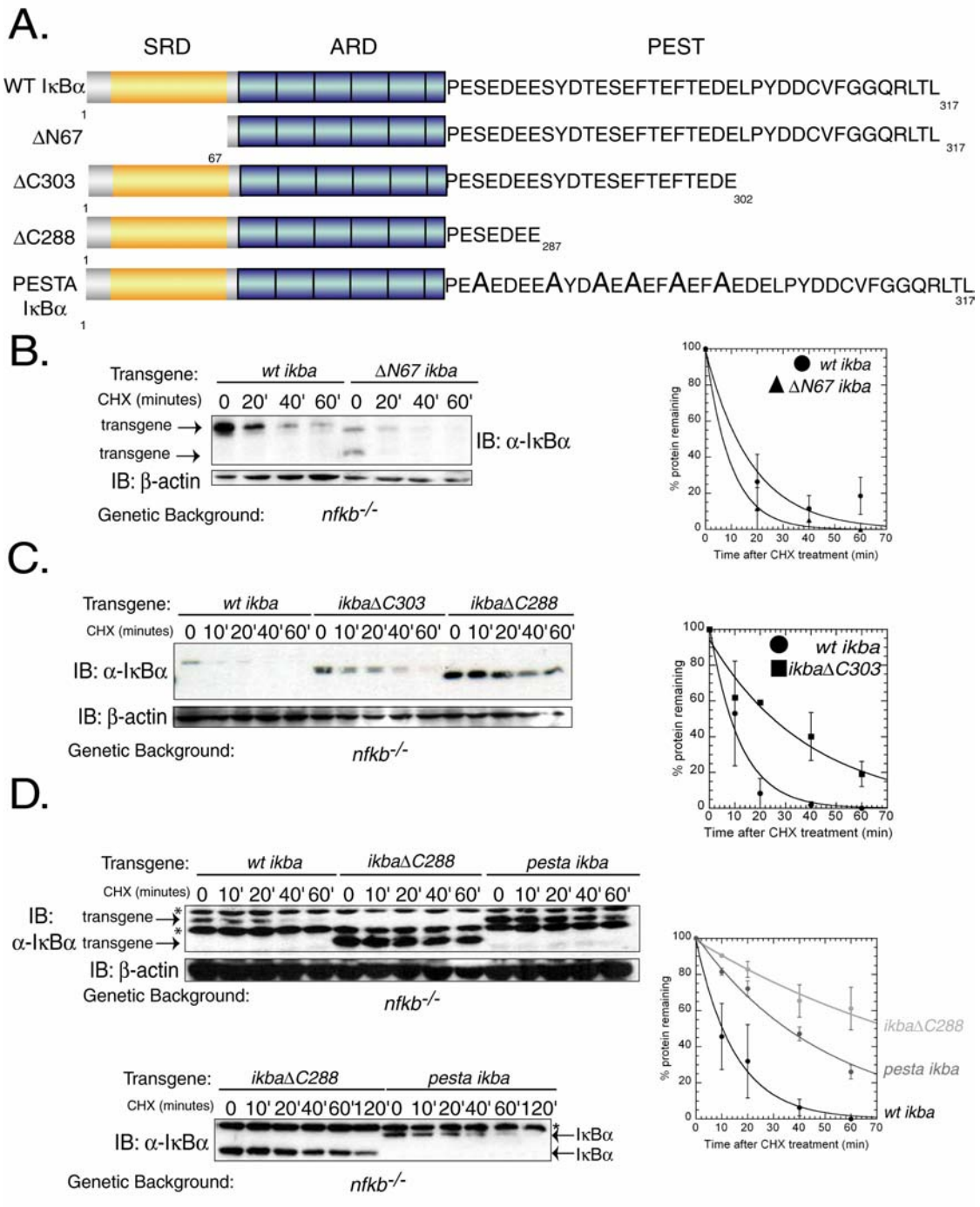
A.
SRD
ARD
PEST
WT IκBα
PESEDEESYDTESEFTEFTEDELPYDDCVFGGQRLTL
ΔN67
PESEDEESYDTESEFTEFTEDELPYDDCVFGGQRLTL
ΔC303
PESEDEESYDTESEFTEFTEDE
ΔC288
PESEDEE
PESTA IκBα
PEAEDEEAYDAEAEFAEFAEDELPYDDCVFGGQRLTL
B.
Transgene:
wt ikba
ΔN67 ikba
CHX (minutes)
0 20' 40' 60' 0 20' 40' 60'
transgene
transgene
IB: α-IκBα
IB: β-actin
Genetic Background:
nfkb-/-
wt ikba
ΔN67 ikba
% protein remaining
Time after CHX treatment (min)
C.
Transgene:
wt ikba
ikbaΔC303
ikbaΔC288
CHX (minutes)
0 10' 20' 40' 60' 0 10' 20' 40' 60' 0 10' 20' 40' 60'
IB: α-IκBα
IB: β-actin
Genetic Background:
nfkb-/-
wt ikba
ikbaΔC303
% protein remaining
Time after CHX treatment (min)
D.
Transgene:
wt ikba
ikbaΔC288
pesta ikba
CHX (minutes)
0 10' 20' 40' 60' 0 10' 20' 40' 60' 0 10' 20' 40' 60'
IB: α-IκBα
transgene
transgene
IB: β-actin
Genetic Background:
nfkb-/-
Transgene:
ikbaΔC288
pesta ikba
CHX (minutes)
0 10' 20' 40' 60' 120' 0 10' 20' 40' 60' 120'
IB: α-IκBα
IκBα
IκBα
Genetic Background:
nfkb-/-
ikbaΔC288
pesta ikba
wt ikba
% protein remaining
Time after CHX treatment (min)

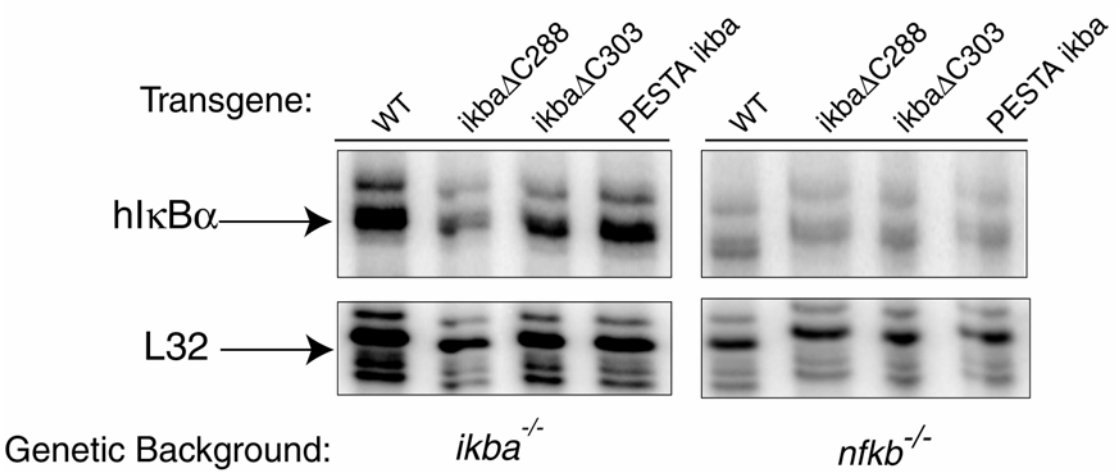

Figure 3-8. The steady state mRNA level of mutant transgenic IκBα is similar to WT IκBα

RNAse Protection assay of WT IκBα, IκBαPESTA, IκBαΔC288 and IκBαΔC303. mRNA levels of these transgenic cells are comparable, which proves that the difference in steady state protein levels is due to differential free IκBα degradation rates.

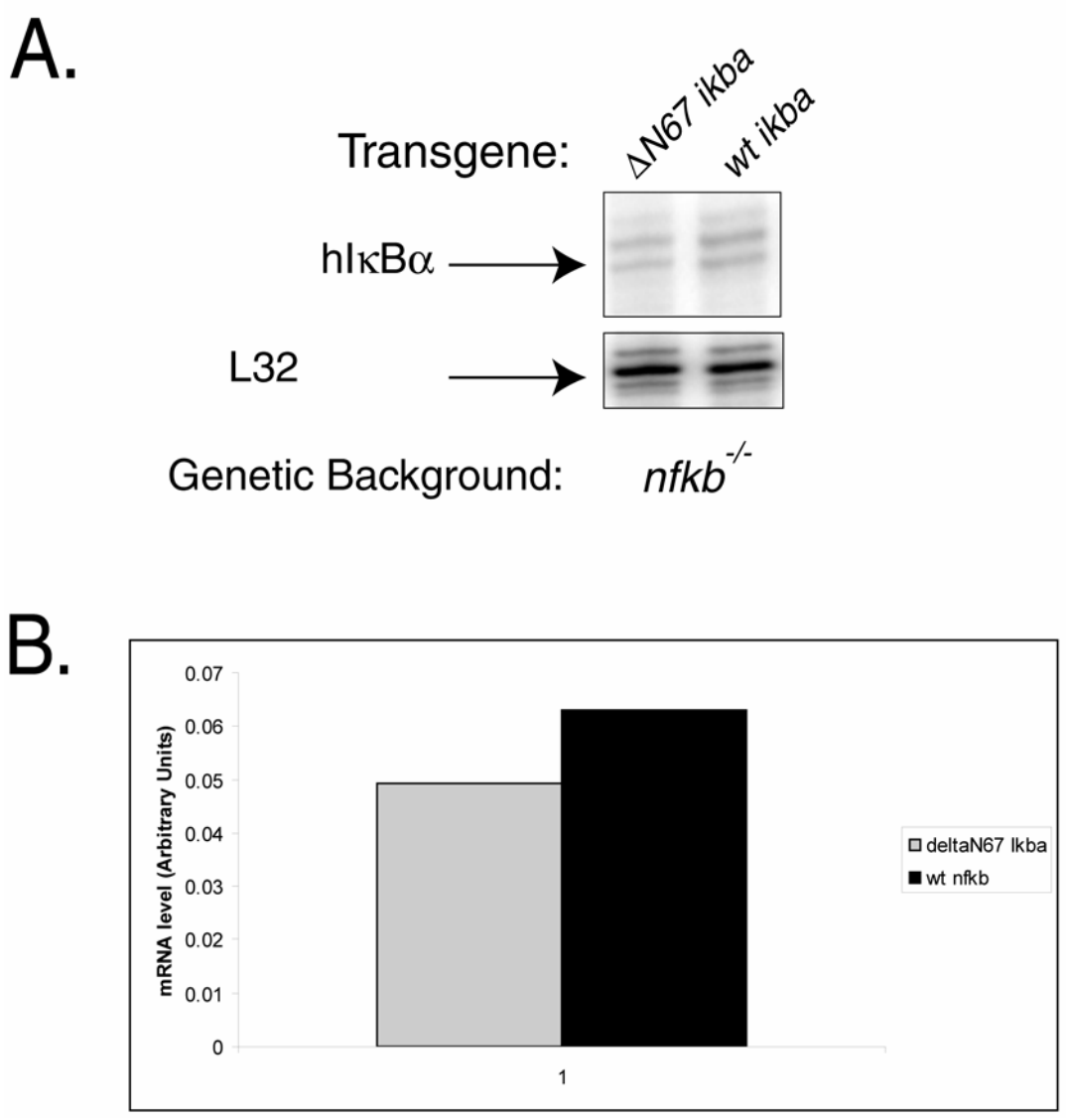

Figure 3-9. Transgenic WT IκBα and ΔN IκBα have similar mRNA levels in *nfkb*$^{-/-}$ cells.
(A). Total RNA was prepared from *nfkb*$^{-/-}$ cells expressing WT IκBα or ΔN67IκBα. RNA was then monitored using RPA.
(B) The mRNA levels were quantitated, and ΔN67IκBα has ~80% of the mRNA level as WT IκBα.

6. Efficient IKK phosphorylation of IκBα does not require NF-κB

One characteristic of the IKK-independent degradation pathway of free IκBα could be that it is a poor substrate of IKK as shown by *in vitro* experiments (Zandi et al., 1998). This substrate specificity could allow for accumulation of IκBα without being phosphorylated and degraded. We therefore wondered if indeed free IκBα is a poor substrate *in vivo*.

First, we carried out computational simulations with a mathematical model that recapitulates the kinetic reactions of IKK (Barken, 2007; Hoffmann et al., 2002b; O'Dea et al., 2007). We increased the susceptibility of the free IκBα protein for IKK-responsive degradation by increasing both IKK association rate and catalytic rate constants to match that of NF-κB-bound IκB protein. Surprisingly, we found little effect on basal or TNF-induced NF-κB activity (Figure 3-10A) (O'Dea et al., 2007). This simulation result suggests that low susceptibility to IKK-mediated phosphorylation and degradation of free IκB proteins may not be functionally important for NF-κB signaling.

We next explored in more detail whether a hypothetical mutant cell with an IKK that does not discriminate between free and NF-κB-bound IκB proteins would have different signaling behavior. Computational analysis did not reveal any significant differences in total IκBα protein levels in a simulated TNF time course (Figure 3-10B). Furthermore, the mutant cell showed very similar NF-κB activation profiles in response to inflammatory stimuli in computational simulations (Figure 3-10C).

Results from these simulations prompted us to examine whether such substrate selectivity, reported for purified proteins *in vitro*, does in fact occur *in vivo*. Utilizing *nfkb*$^{-/-}$ cells, we probed for the presence of phosphorylated IκBα protein in response to TNF. As these cells contain less total IκB protein than their wild type counterparts, we normalized the amount of protein loaded to the total amount of IκBα present in these cells. Surprisingly, we detected a strong band of p- IκBα protein in the *nfkb*$^{-/-}$ cells, which we estimate to be about half of that detected in the transduced *ikba*$^{-/-}$ cell extract diluted 10-fold to provide a roughly equal IκB protein level (Figure 3-10D). This reduction in signal may be attributed to rapid (ubiquitin-independent) proteasomal turnover of free IκBα.

Our results suggest that free and bound IκBα may be similar substrates for phosphorylation by IKK and preference of IKK for a bound IκBα may be due to stabilization of IκBα by NF-κB, rather than a difference in substrate recognition. If so, we reasoned that an IκBα protein that is intrinsically more stable may reveal IKK-induced degradation in the absence of NF-κB. Indeed, computational simulations of IκB protein levels in *nfkb*$^{-/-}$ cells indicated that while wild type IκBα levels are barely affected by TNF stimulation, the hyperstable IκBαΔC288 mutant is predicted to show a TNF induced drop in protein level that may be discernible experimentally (Figure 3-10E). Indeed, Western blotting of extracts made from TNF induced *nfkb*$^{-/-}$ cells expressing IκBαΔC288 revealed that these protein levels decrease in response to TNF over time, while those of wild type IκB protein do not in these conditions (Figure 3-10F). These results show that NF-κB binding to IκB stabilizes the IκB protein, and

stabilization is what determines IKK-mediated degradation; however, the rate of IKK phosphorylation may be similar for free and NF-κB-bound IκB proteins. The functional specificity of IKK instead is the result of the large differential in the rate of basal degradation between free and NF-κB bound IκBα.

Figure 3-10. IKK phosphorylation of free IκBα does not require NF-κB, and has no functional consequence.

(A). Computational simulations of basal NF-κB activity or of peak NF-κB activity after TNF stimulation. The IKK-dependent degradation rates of the free IκBαs were increased to match the IKK-dependent degradation rates of the NF-κB-bound IκBs. In the "wild-type" model (wt), the IKK-dependent turnover rate is 40-fold more efficient for NF-κB-bound IκB is than for free IκBα. This is decreased to 20-fold, and then finally to equal amounts of phosphorylation between free and bound IκBα. (B). Computational simulations of total IκBα levels in response to TNF for cells expressing wt IKK (black line) or a mutant IKK which does not discriminate between free IκBα and bound IκBα (gray line). (C). Computational simulations of nuclear NF-κB levels in response to TNF for cells expressing wt IKK (black line) or a mutant IKK which does not discriminate between free IκBα and bound IκBα (gray line) (D). Free IκBα is phosphorylated in response to TNF-α. Top panel- WB of p-IκB in response to TNF in *ikba*$^{-/-}$ and in *nfkb*$^{-/-}$ cells expressing WT IκBα. The amount of protein in each timecourse set was adjusted to equalize the amount of total IκBα protein in the unstimulated cell extract. Bottom panel- the amount of phospho-IκBα (normalized to total IκBα levels) is compared between *nfkb*$^{-/-}$ and diluted extracts from *ikba*$^{-/-}$ cells after 10 minutes of stimulation. (E.) Computational simulations of free IκBα levels in response to TNF for *nfκb*$^{-/-}$ cells expressing either wt IκB (black line) or a virtual IκBαΔC288 mutant with a 5-fold decrease in the IKK-independent degradation rate of free IκBα (gray line) (F). Free IκBαΔC288 is more responsive to TNF-α than WT IκBα. WB of IκBαΔC288 and WT IκBα after stimulation with 1ng/mL TNF-α. (*) denotes a non-specific band and can be used as a loading control. All computational figures are courtesy of Ellen O'Dea.

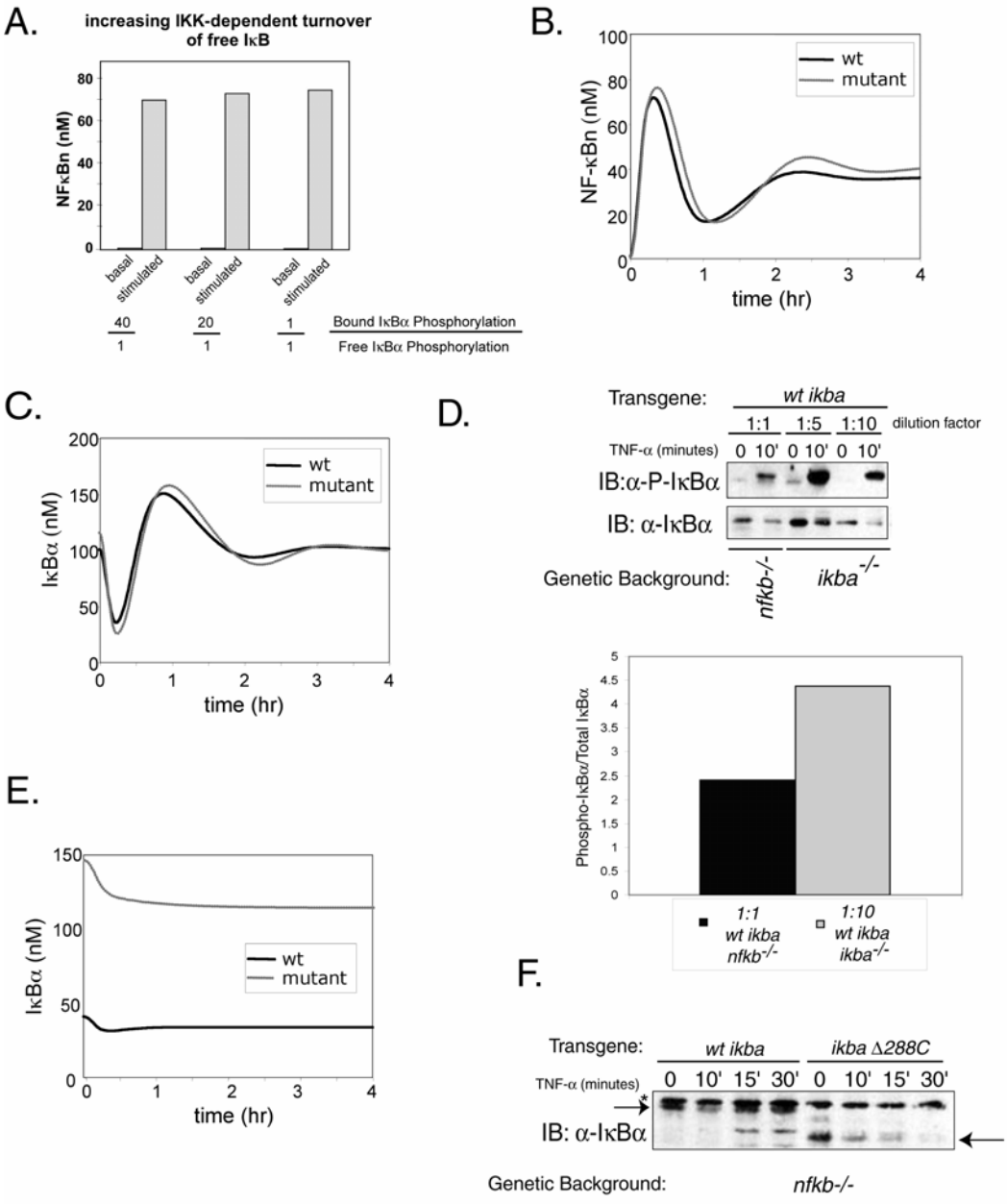
A.
increasing IKK-dependent turnover of free IκB
NFκBn (nM)
basal
stimulated
40/1
20/1
1/1
Bound IκBα Phosphorylation / Free IκBα Phosphorylation
B.
NF-κBn (nM)
time (hr)
wt
mutant
C.
IκBα (nM)
time (hr)
wt
mutant
D.
Transgene:
wt ikba
1:1
1:5
1:10
dilution factor
TNF-α (minutes)
0 10' 0 10' 0 10'
IB:α-P-IκBα
IB: α-IκBα
Genetic Background:
nfkb-/-
ikba-/-
Phospho-IκBα/Total IκBα
1:1 wt ikba nfkb-/-
1:10 wt ikba ikba-/-
E.
IκBα (nM)
time (hr)
wt
mutant
F.
Transgene:
wt ikba
ikba Δ288C
TNF-α (minutes)
0 10' 15' 30' 0 10' 15' 30'
IB: α-IκBα
Genetic Background:
nfkb-/-

7. Rapid degradation of free IκBα is critical for NF-κB activation.

If the amount of the free protein is altered significantly, this could have a detrimental effect on NF-κB activation. To test this hypothesis, we introduced the longer half-life mutant IκBαΔC288 into *ikba*$^{-/-}$ cells and measured if a significant amount of this mutant remains free compared to WT IκBα. RelA was immunoprecipitated and the amount of bound IκBα was observed by western blot. Both IκBαΔC288 and WT IκBα bound to RelA similarly (Figure 3-11A, lanes 3 and 4). The flow-though was TCA precipitated and proteins were separated by SDS-PAGE followed by WB and probed for IκBα and RelA. We clearly observe an excess of IκBαΔC288 compared to WT (Figure 3-11A, lanes 5 and 6), suggesting that we have indeed enhanced the free pool of IκBα in the IκBαΔC288 mutant.

We then explored the functional effect of the IκBαΔC288 mutant with higher *in vivo* stability; measuring NF-κB activation by electrophoretic mobility shift assay (EMSA) of nuclear extracts, we found that the IκBαΔC288 mutation caused a significant dampening of the NF-κB activation profile. We also observed a lag in NF-κB activation in cells expressing the IκBαΔC288 mutant. (Figure 3-11C, 1-30 minutes). To further understand how the stable IκBαΔC288 mutant negatively affects stimulus-dependent NF-κB activation, we stimulated cells expressing WT IκBα, IκBαΔC288, and IκBαPESTA with TNF-α and probed for phosphorylated IκBα. We find a slower phosphorylation rate of the IκBαΔC288 mutant compared to WT IκBα. However, by 10' and 15', IκBαΔC288 is eventually phosphorylated and

degraded (Figures 3-11D and 3-11E). This slight shift in phosphorylation and degradation could account for lower NF-κB activation at the early time point (20'). At the later time points, NF-κB activation in cells expressing the IκBαΔC288 never reach the same maximum as WT IκBα expressing cells. This dampening effect is therefore due to the excess free IκBα that never gets degraded (Figure 3-11E). Although the total amount of IκBαΔC288 phosphorylation is similar to WT IκBα, the total amount of IκBαΔC288 mutant is significantly higher (Figure 3-11D). This explains why most, but not all of IκBαΔC288 is degraded even after 1 hour of stimulation (Figures 3-11E). Our results thus suggest that the lag in NF-κB activation might be due to the delay in IKK phosphorylation and that the lower level of overall NF-κB activity at all times is due to the excess amount of free non-degraded IκBα. The PESTA IκBα mutant (which has slower free IκBα degradation) also has dampened NF-κB activation (Figure 3-11B), and its phosphorylation is intact, if not more efficient than WT IκBα (Figure 3-11E). Overall, our results demonstrate for the first time that the rapid degradation pathway is essential for rapid and robust NF-κB activation. Our combined computational and experimental results demonstrate that the constitutive degradation pathway of free IκBα exists and is critical in allowing for appropriate activation of NF-κB in response to a stimulus.

Figure 3-11. IKK-independent IκB degradation is critical for signal responsiveness

(A). IκBαΔC288 accumulates as a free protein. Cells were immunodepleted with an α-RelA antibody and immunoprecipitates and flow-through samples were analyzed by WB. (*) Denotes non-specific bands.(B). NF-κB activation is dampened due to stabilized free IκBα. EMSA for NF-κB activity in response to TNF stimulation in cells expressing WT IκBα, IκBαΔC288, and PESTA IκBα transgenes. (C). Quantitation of the EMSA in (5B). Two separate experiments are graphed. WT IκBα is represented by black lines (solid and dashed), PESTA IκBα is represented by gray lines (solid and dashed), and IκBαΔC288 is represented by light gray lines (solid and dashed). Stimulus induced IKK dependent phosphorylation of IκBαΔC288 and PESTA IκBα compared to WT IκBα. Phosphorylation of IκBαΔC288 is slightly slower than WT IκBα, while phosphorylation of PESTA IκBα is slightly faster than WT IκBα. Western blot showing phosphorylated IκBα after stimulation with 1ng/mL TNF-α. (*) denotes a non-specific band. (D). Stabilized IκBα degrades more slowly than WT IκBα. Left panel- IκBαΔC288, and WT IκBα transgenes in *ikba*$^{-/-}$ were treated with 1 ng/mL TNF-α and whole cell extracts were run on SDS-PAGE, and analyzed by WB. Right panel- Quantification of the left panel. WT IκBα is represented by a black line, while IκBαΔC288 is represented by a light gray line.

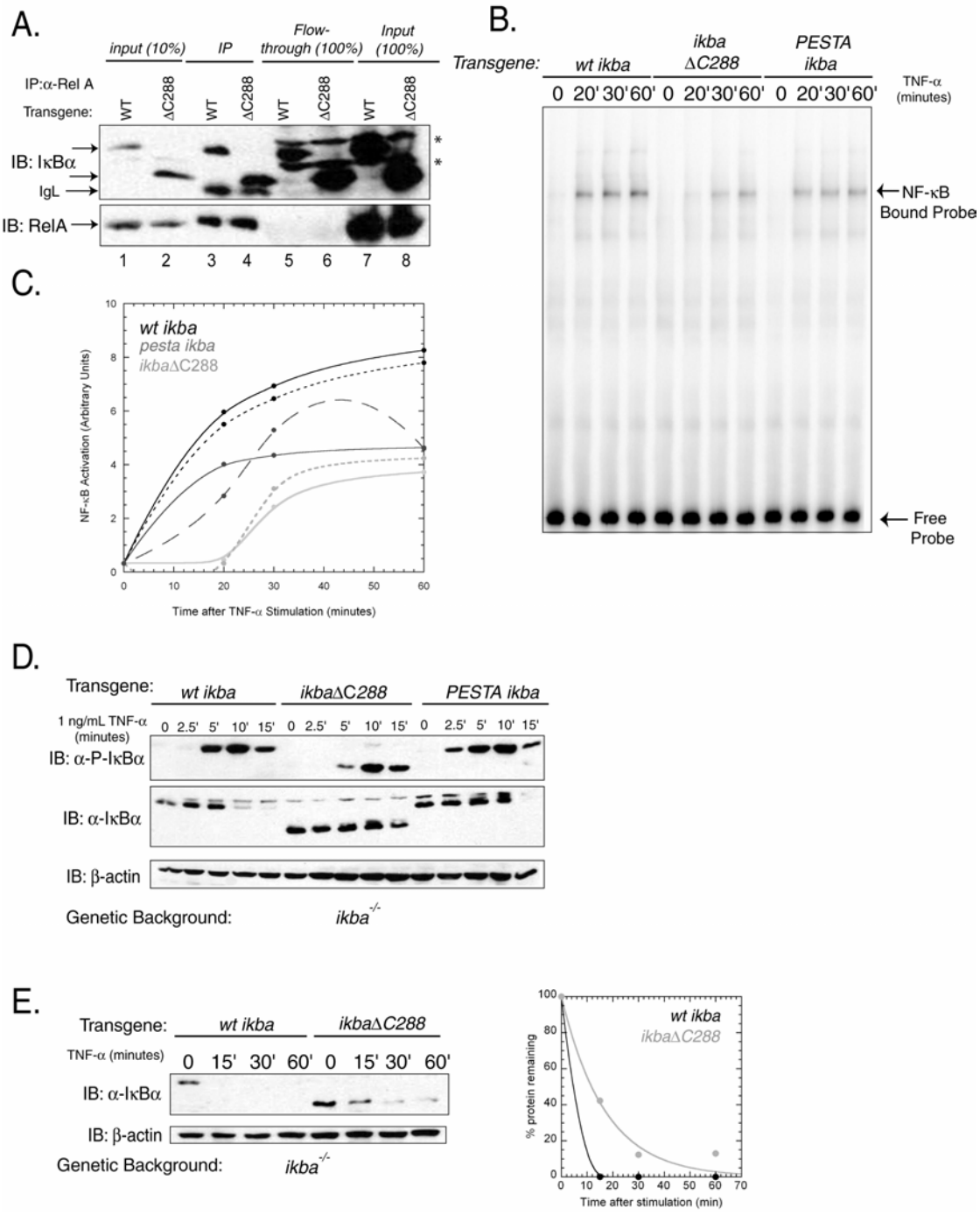
A.
input (10%)
IP
Flow-through (100%)
Input (100%)
IP:α-Rel A
Transgene:
WT
ΔC288
IB: IκBα
IgL
IB: RelA
1 2 3 4 5 6 7 8
B.
Transgene:
wt ikba
ikba ΔC288
PESTA ikba
TNF-α (minutes)
0 20' 30' 60' 0 20' 30' 60' 0 20' 30' 60'
NF-κB Bound Probe
Free Probe
C.
wt ikba
pesta ikba
ikbaΔC288
NF-κB Activation (Arbitrary Units)
Time after TNF-α Stimulation (minutes)
D.
Transgene:
wt ikba
ikbaΔC288
PESTA ikba
1 ng/mL TNF-α (minutes)
0 2.5' 5' 10' 15' 0 2.5' 5' 10' 15' 0 2.5' 5' 10' 15'
IB: α-P-IκBα
IB: α-IκBα
IB: β-actin
Genetic Background: ikba-/-
E.
Transgene:
wt ikba
ikbaΔC288
TNF-α (minutes)
0 15' 30' 60' 0 15' 30' 60'
IB: α-IκBα
IB: β-actin
Genetic Background: ikba-/-
wt ikba
ikbaΔC288
% protein remaining
Time after stimulation (min)

8. Comparison of 20S and 26S Proteasome Mediated Degradation of IκBα.

These results have clearly shown the importance of the residues 289-317 in the degradation of free IκBα. However, these experiments do not address how the proteasome can specifically target unbound IκBα. There have been reports that both the 26S proteasome and 20S proteasome can degrade proteins in an ubiquitin independent manner (Baugh et al., 2009; Murakami et al., 2000). The 26S proteasome is comprised of the 20S catalytic core as well as 19S regulatory subunits, which cap either end or both ends of the 20S core. As shown previously, IκBα can be degraded by the 20S proteasome *in vitro,* although specificity has not been addressed. Can we recapitulate the results observed in cells *in vitro* with the 20S proteasome? We incubated both 1-317 and IκBαΔC288 with the 20S proteasome, but observed no difference in degradation rates (Figure 3-12A), unlike what we observed in cells. Interestingly, a stable intermediate was noted at 15' when IκBα (1-287) was used as the substrate for degradation, suggesting the proteasome may use slightly different mechanisms to degrade full length and IκBαΔC288.

Although the result observed in cells was not reproduced with the 20S proteasome core, it is possible that the 26S proteasome can degrade IκBα in an ubiquitin independent manner and the 19S cap can confer specificity. When we incubated both 1-317 and IκBαΔC288 with the 26S proteasome in a 1:10 molar ratio, both full length and truncated proteins are degraded at a similar rate, although overall degradation rate was slower than 20S proteasome (Figure 3-12B). To confirm that

the 26S used was pure, the proteasome was run on a native gel and silver stained (Figure 3-12C). Indeed, we observe several bands which could correspond to the 26S proteasome, either 20S core alone, 19S cap alone, or a 19S:20S:19S complex or a singly capped 19S:20 complex. This experiment was repeated again with two sources of 26S proteasome, both purchased from Boston Biochemical and a gift from the Pilipenko group at the University of Chicago (Baugh et al., 2009) (Figure 3-13) . These results suggest that the 26S proteasome is capable of degrading IκBα in an ubiquitin independent manner, although the specificity between the degradation rate of 1-317 and IκBαΔC288 in cells has yet to be resolved.

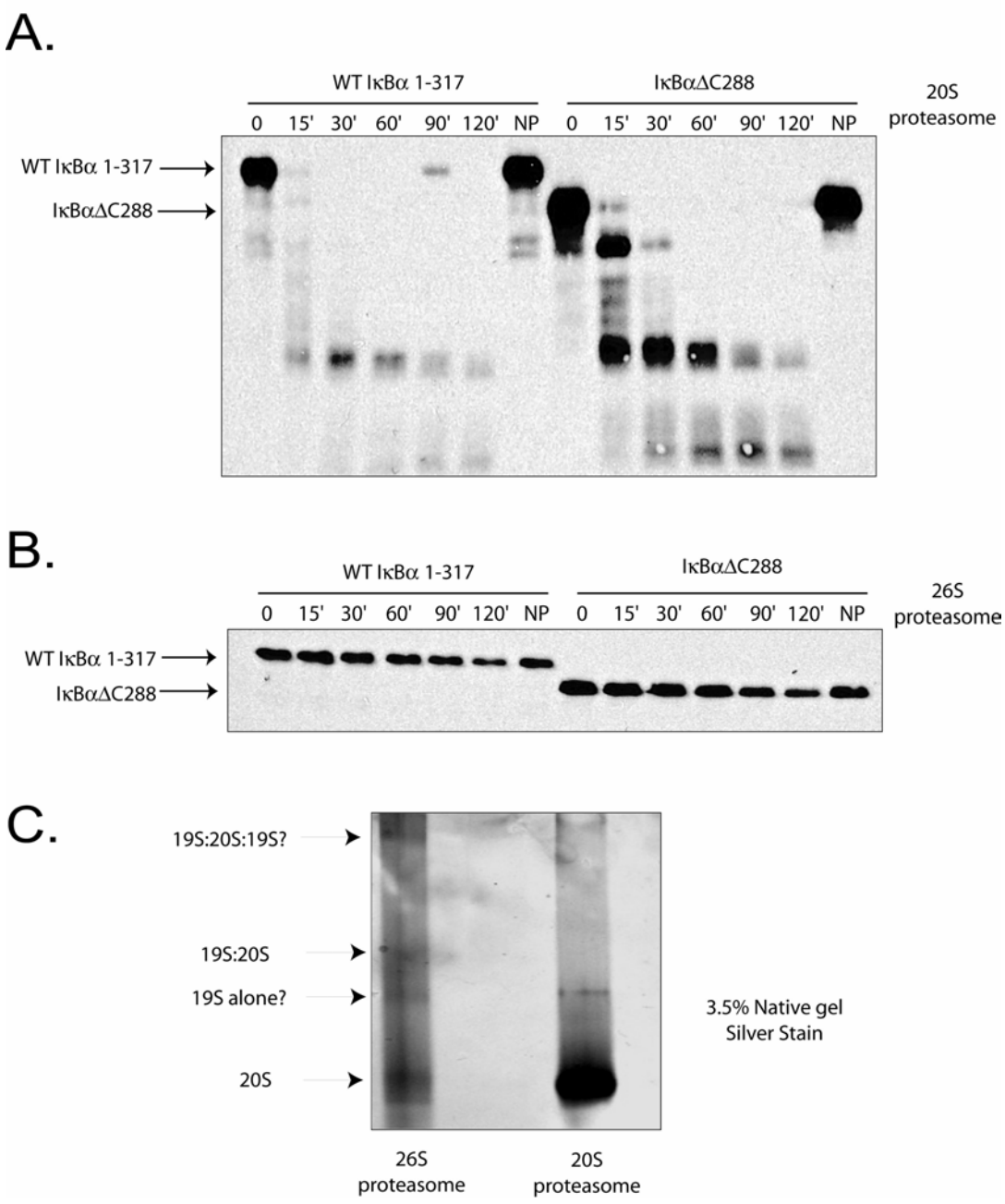

Figure 3-12. Both the 20S and 26S proteasome can degrade free IκBα
(A). Approximately 2.5 μg of either 1-317 IκBα or IκBαΔC288 IκBα were incubated with latent 20S proteasome (a gift from Jessica Ho) in a 1:10 molar ratio and incubated at 25^0C for the indicated times. Degradation of the proteins was visualized through Western Blot with an antibody against the entire IκBα protein. (B). The same experiment as in (A), but the 26S proteasome was used. (C). A native gel silver stained to show that the 26S is intact during this experiment as shown by a distinct banding pattern. However, the exact identity of each band is not known.

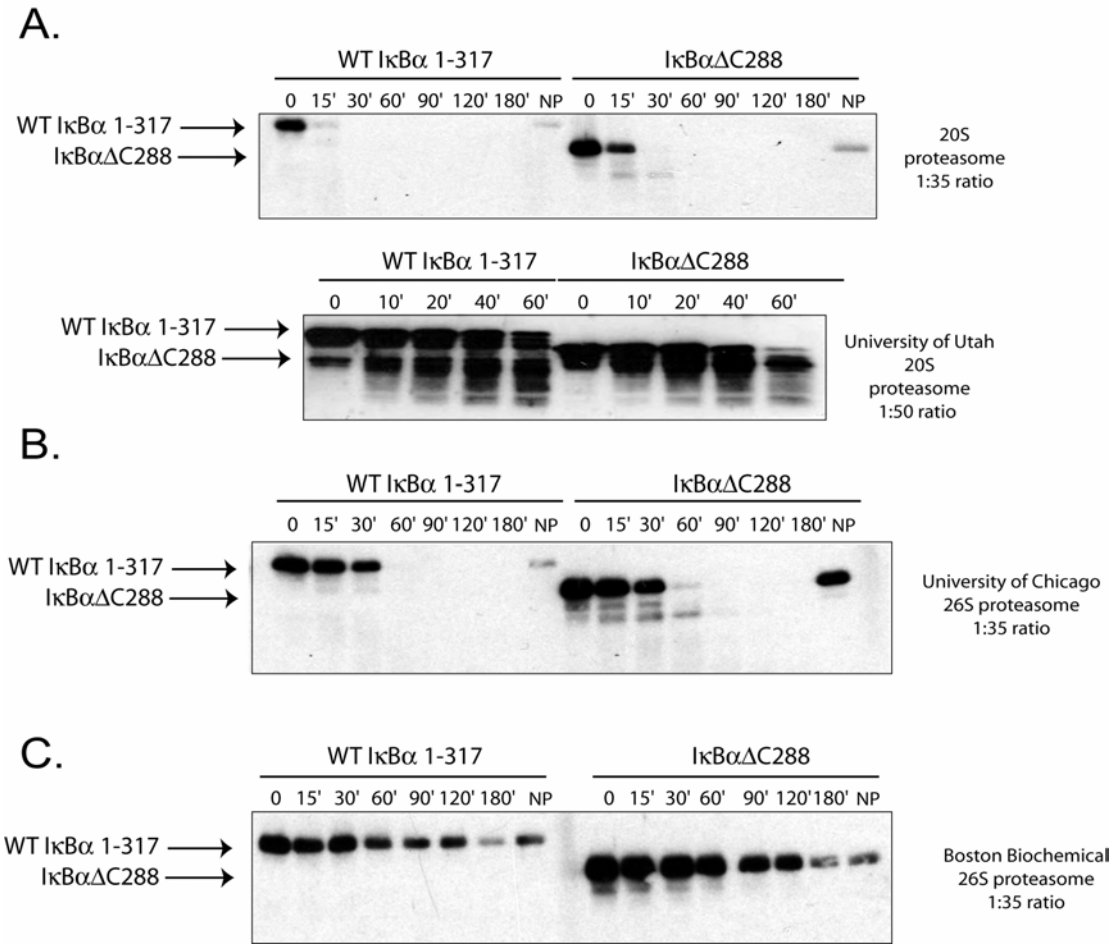

Figure 3-13. Both 20S and various sources of 26S proteasome can degrade IκBα (A). Purified IκBα either FL (1-317) or truncated IκBαΔC288 was incubated with the 20S proteasome in a 1:35 molar ratio (top panel-gift from Jessica Ho) or a 1:50 ratio (bottom panel-gift from Dr. Rechsteiner and Dr. Pratt, University of Utah) from various sources for the indicated times. NP=no proteasome added. (B). As in (A), but with 26S proteasome given as a gift from the Pilipenko lab at the University of Chicago. (C). As in (A) and (B), but with 26S proteasome purchased from Boston Biochemical.

C. Discussion

Contrary to previous overexpression or cell-free biochemical based analyses (Alvarez-Castelao and Castano, 2005; Krappmann et al., 1996; Lin et al., 1996; Miyamoto et al., 1994; Pando and Verma, 2000; Schwarz et al., 1996; Tergaonkar et al., 2003; Van Antwerp and Verma, 1996) the experimental work presented here using a clean genetic system delineates the free IκBα degradation pathway as separate from the well-described IKK- and ßTRCP-axis. We were able to 1) establish that IκBα which is not bound to NF-κB is an intrinsically unstable protein *in vivo*, 2) show that IKK phosphorylation and ubiquitination are not necessary for free IκBα degradation, 3) identify the region of IκBα responsible for the rapid degradation of free IκBα and, 4) demonstrate that a stable free IκBα negatively affects stimulus-dependent NF-κB activation (Figure 3-14).

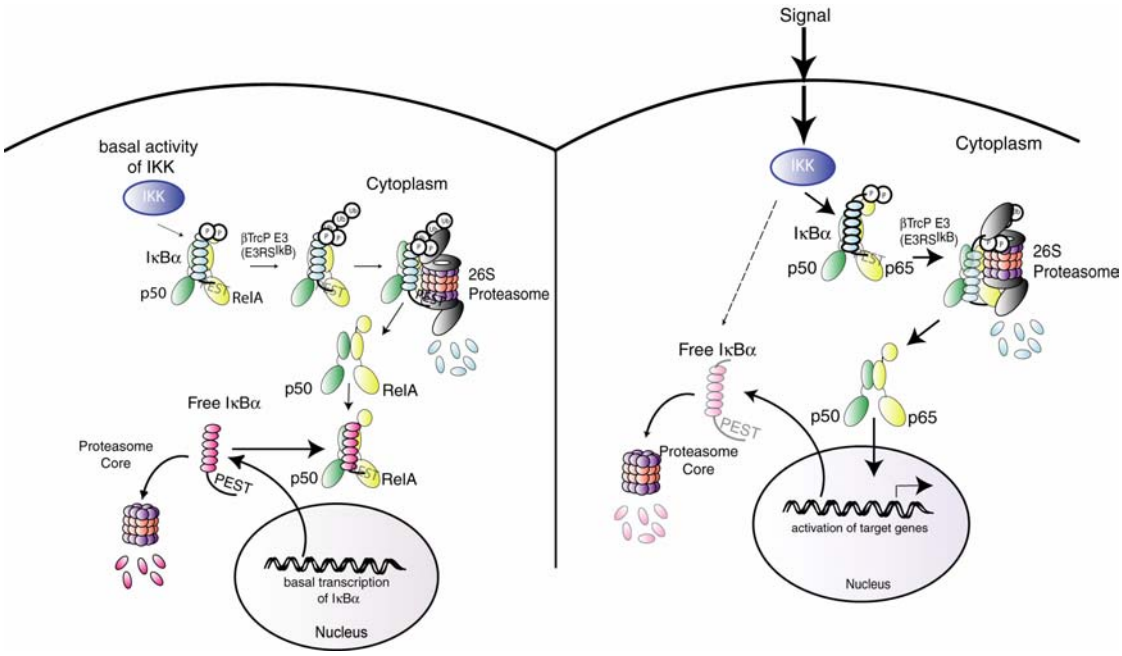

Figure 3-14. A final model of the degradation pathways controlling IκBα in basal and stimulated cells.
In the resting cell, enough IκBα is synthesized that it can rebind any NF-κB released due to slow basal IKK activity. Free IκBα is degraded very rapidly, and only represents ~15% of the total IκBα in the cell (Transparent IκBα). When IκBα binds to NF-κB, it is stabilized, and must go through IKK-dependent phosphorylation and degradation (Bold IκBα). Upon stimulation, the activity of IKK is increased such that most (if not all) IκBα is rapidly degraded and allows for NF-κB activation. Free IκBα must be continously degraded in order to allow for this rapid and robust NF-κB activation.

1. IκBα degradation is rapid and regulated via the C-terminal PEST region

We show that the PEST sequence of free IκBα is important for proteasomal degradation and that the primary degradation pathways of free and NF-κB-bound IκBα are different in unstimulated cells. Whereas bound IκBα is degraded by the IKK-initiated ubiquitin-proteasome pathway in both stimulated and unstimulated cells, free IκBα does not require phosphorylation by IKK nor ubiquitination for degradation. This conclusion is subject to the caveat that ubiquitination of the N-terminus may be possible, but such a modification remains controversial (Bloom et al., 2003; Coulombe et al., 2004; Sheaff et al., 2000). Instead, we identified the PEST sequence containing C-terminal region of IκBα as a determinant of its short half-life. In addition, we find (consistent with other reports) (Alvarez-Castelao and Castano, 2005) that the 20S core particle alone is able to degrade IκBα *in vitro*, but we have been unable to establish its sufficiency *in vivo*. It is possible that other regulators of the 20S core particle are required for recognition of the PEST sequence, or perhaps even the entire 26S proteasome is responsible for the ubiquitin-independent degradation, as has been shown for p21 (Liu et al., 2006a).

The current knowledge of Ub-independent protein degradation proposes that one of the criteria for Ub-independent protein degradation is the lack of high folding stability of the target substrate (Asher et al., 2006). IκBα, not bound to NF-κB, has a partially folded ARD and PEST sequence that is relatively unstructured (Croy et al., 2004). Upon binding to NF-κB, both these regions of the protein become more folded (Huxford et al., 1998; Truhlar et al., 2006). In the x-ray crystal structure of the

IκBα/NF-κB complex, the residues corresponding to most of the PEST region (residues 281-291) display clear electron density, and are involved in neutralizing the DNA-binding residues of the RelA/p50 heterodimer (Huxford et al., 1998). Chemical cross-linking experiments also revealed interactions between the PEST of IκBα and the DNA binding domain of NF-κB which confirmed the structural studies (Phelps et al., 2000).

As such, we now understand the molecular interactions that show the interdependency between NF-κB and IκBα. While IκB proteins mask the DNA binding and nuclear localization sequences of NF-κB, NF-κB masks the intrinsic degradation signals in IκBα preventing its rapid degradation.

2. The degradation kinetics of IκBα determine IKK's functional specificity for NF-κB bound IκBα

NF-κB appears to direct the degradation of bound IκBα through IKK-mediated N-terminal phosphorylation, since only NF-κB-bound IκBα levels drop significantly in response to IKK-inducing stimuli. Yet, our analysis of IκBα phosphorylation in NF-κB-deficient cells indicates that free IκBα is also a good substrate for IKK. We find that IκBα -susceptibility to IKK-mediated degradation is dependent on its stabilization by NF-κB. Indeed, stabilizing IκB by introducing appropriate mutations in its C-terminus also sensitizes the protein for IKK-mediated degradation. Our results refine a previous model that suggests that negative feedback regulation by IκBα

requires a build-up of the free protein that is not sensitive to IKK-mediated degradation (Zandi et al., 1998). Since then, TNF-induced IKK activity was shown to be attenuated at 25 min after stimulation which may allow for the build-up of newly synthesized IκBα (Cheong et al., 2006; Werner et al., 2005).

Instead, the functional specificity of IKK for NF-κB-bound IκB is achieved through a large difference in basal degradation rates rather than a preference of the kinase for the NF-κB bound protein. As of yet, there is no information on the interaction between NF-κB and IKK, nor any data suggesting that there are conformational changes of the IκB N-terminus triggered by NF-κB binding, either of which would provide a platform for IKK preferential phosphorylation. Thus, NF-κB determines the fate of IκBα through stabilization; not only does the physical interaction with NF-κB preclude its rapid degradation; this stabilization allows phosphorylation by IKK and thereby stimulus-responsive NF-κB activation.

3. The instability of IκB tunes the cellular responsiveness to inflammatory stimuli

Although stabilization of IκB by NF-κB is a hallmark of the NF-κB signaling module, we found that stabilization of free IκBα through disruption of the free IκBα degradation pathway can inhibit NF-κB activation. Although free IκBα is not responsive to stimulus, this degradation pathway is nonetheless a determinant of stimulus-responsive NF-κB signaling (Figure 3-14). This finding may be rationalized

by the fact that high constitutive IκB transcription and translation ensure an excess of IκB synthesis. High degradation rates of free IκBα ensure a low level of excess IκBα, which is estimated to be about 15% of the total (O'Dea et al., 2007; Rice and Ernst, 1993). Tuning the level of free IκBα in the cell by controlling either synthesis or degradation may therefore provide opportunities for signaling crosstalk. That is, non-inflammatory signals, such as those derived from environmental or metabolic stress conditions, may affect the responsiveness of the cell to inflammatory stimuli that regulate NF-κB *via* IKK by affecting either the free or bound degradation pathway. Finally, as demonstrated in our study, using a combined approach in which quantitative biochemical studies interface with mathematical modeling may therefore help understand the differential responsiveness of cells in stressed conditions often found in pathological contexts.

4. Proteasome Specificity of IκBα Degradation

To address the proteasome specificity in recognition of WT IκBα and IκBα ΔC288, we tested both the 20S and 26S to test whether we can recapitulate the results that we observe *in vivo* using an *in vitro* system. First, we used the latent 20S proteasome, as we knew that IκBα could be degraded rapidly by this enzyme without prior modifications such as ubiquitin. However, we did not see a striking difference between the degradation rates of the two constructs with 20S mediated degradation. Next we tested the 26S proteasome, which thought to be primarily involved in ubiquitin-dependent protein degradation, but has also has been shown to degrade some

proteins without ubiquitin modification (Asher et al., 2006; Baugh et al., 2009; Murakami et al., 2000). It was possible that the 19S cap gave specificity toward the full-length protein rather than IκBα ΔC288. However, the two proteins degraded at a very similar rate when incubated with the 26S proteasome. It is possible that other forms of the 20S proteasome such as the ones bound to different 11S regulatory particles might be responsible for free IκBα degradation *in vivo*. One cannot however rule out the presence of yet unidentified protein or proteins that target the PEST sequence for proteasomal degradation.

This chapter includes text and figures from the publication: Mathes, E, O'Dea, E, Hoffmann A, and Ghosh, G. 'NF-κB Dictates the Degradation Pathway of IκBα' with permission. The dissertation author was the primary investigator and author of this material.

IV. Consensus design of IκBα affects ubiquitin independent degradation and NF-κB activation

A. Introduction

One of the most abundant classes of proteins which mediate protein-protein interactions is the repeat protein (Li et al., 2006a). There are more than 20 different classes of repeat proteins, including leucine-rich repeats proteins (LRR), armadillo/HEAT repeat proteins, and ankyrin repeat (AR) proteins. Ankyrin repeats are found in proteins which are involved in transcriptional regulation, cytoskeletal architecture, cell cycle progression, cellular development and differentiation, and toxins (Li et al., 2006a). Ankyrin repeats have an extended protein structure, rather than a globular protein structure, which allows for short range contacts and interactions between ankyrin repeats, rather than long range interactions as seen in globular proteins (Barrick et al., 2008). Each repeat contains a structural motif of ~30-40 amino acids which fold into a helix-loop-helix motif with a β-hairpin extending from one repeat and into the next. Repeats with the 33 amino acid sequence GXTPLHLAXXGHXXXVXXLL were first identified within the sequence of yeast Swi6p, Cdc10p, and the *D. melanogaster* protein, Notch in 1987 (Li et al., 2006a). Later, this repeat was named ankyrin, after the discovery of 24 such repeats in a cytoskeletal protein 'ankyrin'.

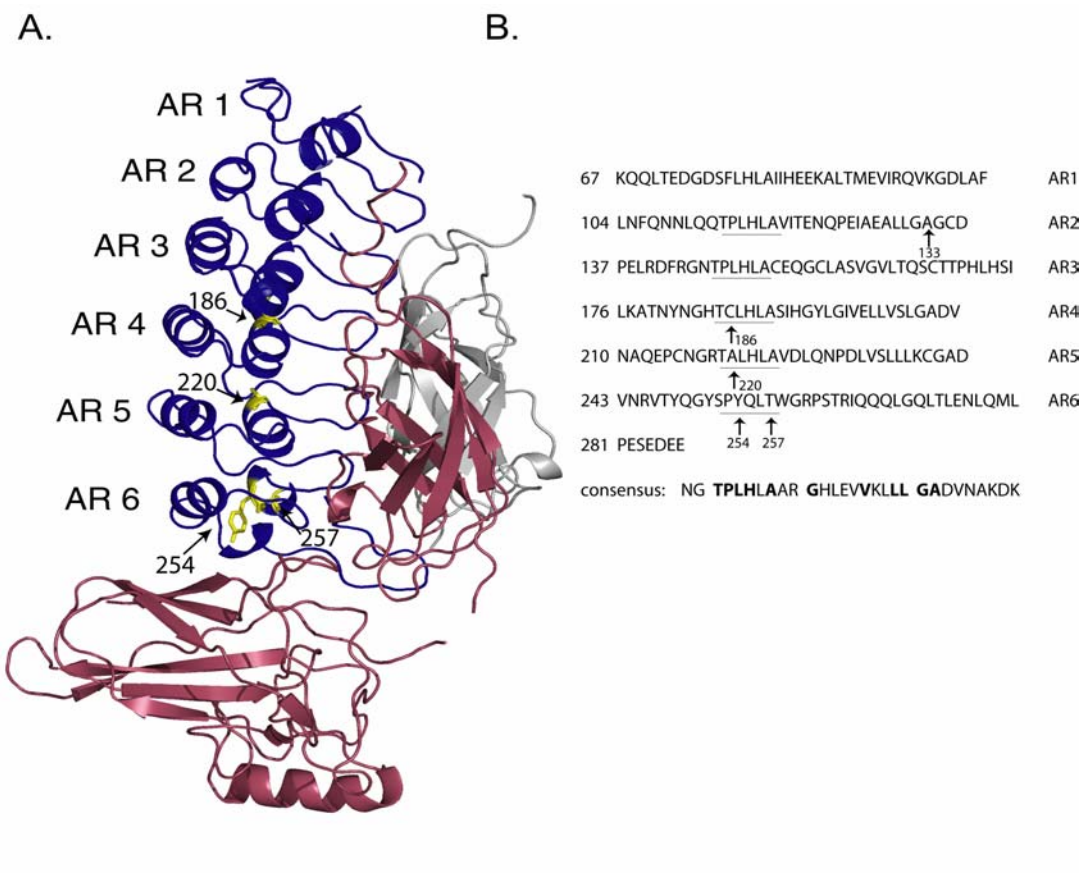

Figure 4-1. Overall structure of IκBα and ankyrin repeat sequence (A). Structure of IκBα (blue) bound to NF-κB (p65 in purple and p50 in silver) (B). The ankyrin repeat sequence of IκBα is shown compared to the consensus ankyrin repeat sequence (Ferreiro et al., 2007). Mutations made in this chapter (C186P, A220P, Y254L, T257A) which conform IκBα to the consensus ankyrin repeat sequence are highlighted both in A and B with arrows. A133W is also marked with an arrow.

IκBα contains 6 ankyrin repeats (AR), of which the 1st and 6th deviate most significantly from the consensus sequence (Ferreiro et al., 2007) (Figure 4-1). The folding and stability of IκBα when not bound to NF-κB has been studied extensively (Croy et al., 2004; Ferreiro et al., 2007). The folding of IκBα nucleates at AR2 and AR3 and propagates outward towards AR1 and AR4, all as part of the first folding transition (Ferreiro et al., 2007; Ferreiro et al., 2005). The second folding transition includes AR5 and AR6. This model of nucleation and folding has been supported by experimental evidence (Ferreiro et al., 2007) which shows that unfolding of IκBα occurs through a pre-transition state involving AR 5 and 6 and then the full unfolding of the stable core of AR 1-4. In addition, in the free IκBα protein, AR 5 and 6 are known to be extremely flexible, and fold upon binding to NF-κB (Truhlar et al., 2006). Overall these studies suggest IκBα has two independently folded modules; one involving AR 1-4, and the other involving AR 5-6 (Ferreiro et al., 2007).

To make several ARs within IκBα conform more closely to the ankyrin repeat consensus sequence, mutations were made both in AR4 and AR5 (C186P, A220P) as well as in AR6 (Y254L, T257A). These mutations had various effects on folding and dynamics. The C186P, A220P double mutation stabilized IκBα by ~1.5 kcal/mol (as determined by urea denaturation) and increased the T_m by ~5^0C. The Y245L, T257A double mutation, located in AR6, increased the ΔG of unfolding by only ~0.7 kcal/mol. Therefore, all of these consensus mutations increased the stability of IκBα, albeit to varying degrees. However, one significant difference was noted between these two double mutations. In the case of the C186P, A220P mutation, the unfolding

of AR6 was not cooperative, much like WT IκBα (Ferreiro et al., 2007). However, the Y254L, T257A double mutation displayed a single unfolding transition in AR6, as assayed by a single tryptophan in the 6th ankyrin repeat (Ferreiro et al., 2007; Truhlar et al., 2008). In addition, H/D exchange experiments of the Y254L, T257A double mutation showed that AR 5 and 6 are no longer inherently flexible, suggesting that these mutations have converted IκBα into a single folding module, by 'pre-folding' AR 5 and 6 (Truhlar et al., 2008).

It is known that free IκBα can be degraded *in vitro* by the 20S proteasome, and can be degraded in an ubiquitin-independent manner in cells. Many ubiquitin-independent substrates are known to be flexible which facilitates degradation (Liu et al., 2003; Prakash et al., 2004). Therefore, we used the C186P, A220P and Y254L, T257A double mutations in IκBα to determine how these ankyrin repeat consensus mutations affect ubiquitin-independent proteasomal degradation. Although both consensus double mutations stabilize IκBα thermodynamically, only the Y254L, T257A double mutation creates an IκBα that has a single cooperative unfolding transition in AR 6. Also, due to the 'pre-folded' nature of the Y254L, T257A mutation, binding to NF-κB was significantly impaired as measured *in vitro*, and so binding of this mutant in cells was also tested (Truhlar et al., 2008). Finally, the functional consequences of this NF-κB binding defect in the IκBα Y254L, T257A mutation was determined in both basal and stimulated cells.

B. Results

1. *In vitro* Degradation of the Stabilized C186P, A220P IκBα

There are multiple examples where unfolded proteins are degraded in an ubiquitin independent manner (Asher et al., 2005; Sheaff et al., 2000). Therefore, since the consensus C186P, A220P mutant stabilized IκBα by increasing both the T_m (by ~ 5^0C) and the ΔG of unfolding by 1.5 kcal/mol, it was intuitive to speculate that these mutants would be resistant to proteasomal degradation. The degradation rate of this mutant was compared to WT IκBα *in vitro* using the 20S proteasome which has been previously shown to degrade IκBα. Two different conditions were tested, in which either the reaction proceeded at 25^0C or 37^0C, and with a gel filtration step immediately preceding the degradation experiment to exclude any aggregate (Figure 4-2 A, and B). Surprisingly, the C186P, A220P protein actually degraded faster than WT IκBα (Figure 4-2). The rapid rate of C186P, A220P mutant degradation was unexpected, since this mutant was overall more thermodynamically stable than WT IκBα.

2. *In vitro* Degradation of the Destabilized A133W IκBα

To monitor the folding transitions of the N-terminal ankyrin repeats, a local mutation was made in AR2 of A133W. This mutation was not a consensus mutation, but destabilized IκBα by ~3 kcal/mol as measured by urea denaturation and lowered the T_m by 8 ^{0}C. Therefore, it was intuitive to speculate that this mutant would degrade

faster than WT IκBα. Intriguingly, this mutation degraded similarly to WT IκBα, and much slower than the C186P, A220P mutation (Figure 4-2 A and B). A triple mutant was created where both the double and single mutants were combined (A133W, C186P, A220P) and its *in vitro* degradation was tested. This mutant showed a degradation pattern similar to the C186P, A220P double mutant, suggesting that the consensus mutations play a more significant role in degradation than the A133W mutant. Taken together, the determining factor of degradation is clearly not overall thermodynamic stabilization as shown by these *in vitro* degradation assays. However, these experiments were performed *in vitro*, and not in the context of the cell.

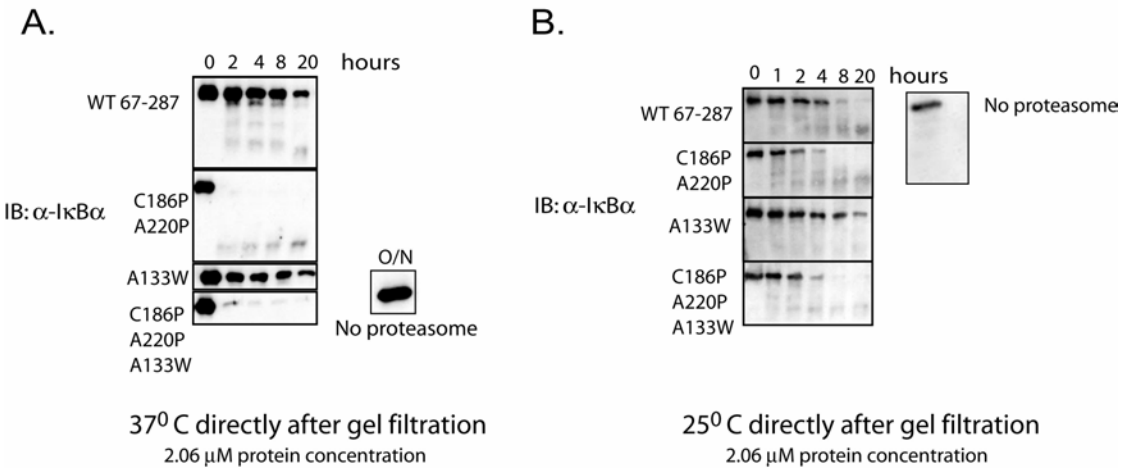

Figure 4-2. Overall thermodynamic stabilization does not correlate to a slower degradation rate *in vitro*.
(A). Various IκBα mutants (67-287) were incubated with 20S proteasome at 37^0C in a 1:12 molar ratio, and stopped at indicated times. Protein was detected by western blot using an antibody directed against the entire IκBα protein. (B). As in (A), but repeated at 25^0C.

3. Degradation of C186P, A220P in cells

Although the C186P, A220P double mutation degraded faster than WT IκBα *in vitro*, it is possible that this double mutation will behave differently in the context of the cell. Therefore, we tested whether the C186P, A220P mutation would slow free IκBα degradation when expressed in cells which lack the NF-κB subunits p50, c-Rel and RelA (*nfkb*$^{-/-}$). These transgenic cells were treated with the translational inhibitor cycloheximide (CHX) and the degradation rate of both WT and C186P, A220P were visualized by Western Blot. The C186P, A220P mutation did not slow the degradation of unbound IκBα (Figure 4-3) as compared to WT IκBα, although it is overall more thermodynamically stable. This suggests that it is not overall thermodynamic stability which determines the degradation rate of IκBα.

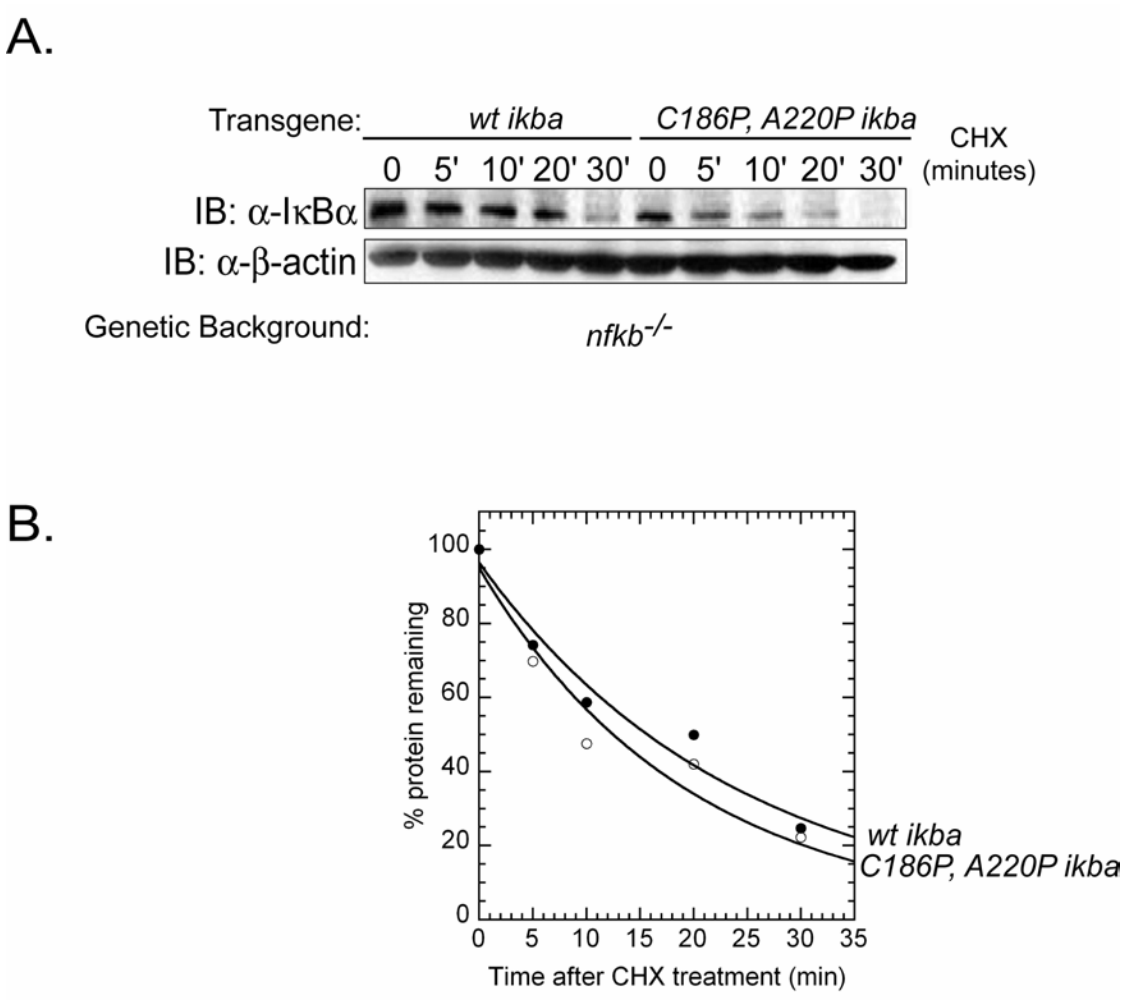

Figure 4-3. Overall thermodynamic stabilization does not correlate to a slower degradation rate in cells

(A). *nfkb*$^{-/-}$ cells expressing either WT IκBα or C186P, A220P IκBα were treated with cycloheximide and the rate of IκBα degradation was detected by Western blot. (B). Graphical representation of (A), normalized by β-actin levels. (●) represents WT IκBα, and (○) represents C186P, A220P IκBα.

4. Degradation of the stabilized Y254L, T257A IκBα

Since the C186P, A220P double mutation did not slow free IκBα degradation *in vitro* or in cells, mutations were made in AR6 to conform to the consensus AR sequence (Truhlar et al., 2008). This double mutation (Y254L, T257A) causes AR 5 and 6 to fold cooperatively into a conformation similar to that found in NF-κB bound IκBα (Truhlar et al., 2008). When the Y254L, T257A IκBα mutation was incubated with the 20S proteasome *in vitro*, there was a ~ 3-fold increase in stability as compared to WT IκBα (Truhlar et al., 2008). To determine whether free Y254L, T257A IκBα was also stabilized in the cell, this mutant was expressed in *nfkb*$^{-/-}$ cells (Figure 4-4). These transgenic cells were treated with cycloheximide and the degradation rate was compared to WT IκBα. Similar to the *in vitro* data result, free IκBα containing the Y254L, T257A mutation degraded more slowly than WT IκBα (Figure 4-4). This result, together with the C186P, A220P degradation result, suggests that it is flexibility in the 5th and 6th ankyrin repeats which determines proteasome mediated degradation, rather than overall thermodynamic stability.

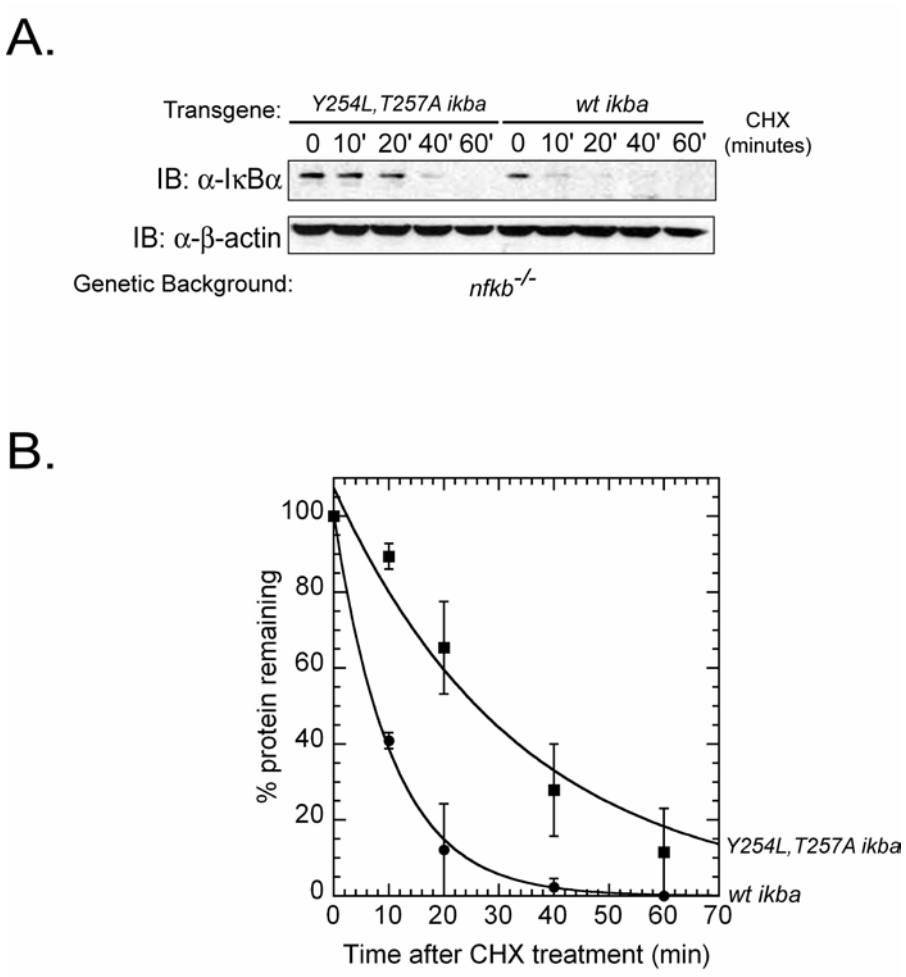

Figure 4-4. Consensus mutations in the 6th ankyrin repeat of IκBα slow IκBα degradation

(A). *nfkb*$^{-/-}$ cells expressing WT IκBα or Y254L, T257A containing IκBα were treated with CHX for the indicated times and remaining IκBα was detected by Western Blot. (B). Average of two separate experiments is graphed, as well as the s.e.m. (●) represents WT IκBα, and (■) represents Y254L, T257A IκBα.

5. Functional consequences of the Y254L, T257A double mutant

Another consequence of the Y254L, T257A double mutation and 'pre-folded' AR6 is a significantly reduced binding affinity to NF-κB (Truhlar et al., 2008). This result suggests that the ability of the 5th and 6th repeats to fold upon binding to NF-κB is an important characteristic of IκBα (Truhlar et al., 2008). To see whether this result is recapitulated in cells, *ikba*$^{-/-}$ cells were reconstituted with WT IκBα as well as the Y254L, T257A IκBα mutation. We found that binding of the full-length mutant protein to NF-κB was diminished compared to WT IκBα (Figure 4-5), as shown by immunoprecipitation of RelA and Western Blot against IκBα.

Since the affinity of NF-κB binding to the Y254L, T257A IκBα mutation was significantly diminished, it is possible that the NF-κB activation pathway is altered and will not have the same NF-κB activation profile as cells expressing WT IκBα. In fact, it is possible that the activation profile will look similar to cells which lack IκBα altogether. When Y254L, T257A transgenic cells were stimulated with TNF-α, a potent inducer of the NF-κB activation pathway, NF-κB translocation was significantly dampened in the Y254L, T257A expressing cells compared to cells expressing WT IκBα, although phosphorylation by IKK was very similar to WT IκBα (Figure 4-6A and B). In this Y254L, T257A double mutation, two significant features of IκBα have been altered by simply making AR6 fold cooperatively. One feature is the binding to NF-κB, and another is slowing of the free IκBα degradation pathway. Therefore, the NF-κB activation profile seen in the Y254L, T257A

expressing mutants could be attributed to both stabilization of free IκBα, and the weaker binding affinity to NF-κB (Figure 4-7).

Another functional consequence of the Y254L, T257A mutant IκBα is the amount of basal NF-κB activation. Since this double mutation does not bind as efficiently to NF-κB, not all of NF-κB is inhibited. Therefore, even without stimulation, a higher level of NF-κB could be present in the nucleus. This is precisely what is observed in Y254L, T257A expressing cells (Figure 4-6C). The increased amount of basal NF-κB could result in higher levels of IκBε, which is also a NF-κB dependent gene. To test this, a western was done with extracts prepared from WT and Y254L, T257A expressing cells, and indeed, there was a much higher level of IκBε protein (Figure 4-7A). Cells lacking *ikba*$^{-/-}$ have been shown to have an increase in IκBε levels (Kearns et al., 2006; O'Dea et al., 2007). This is an example of how alteration of IκBα folding can have a ripple effect on many parameters of NF-κB signaling.

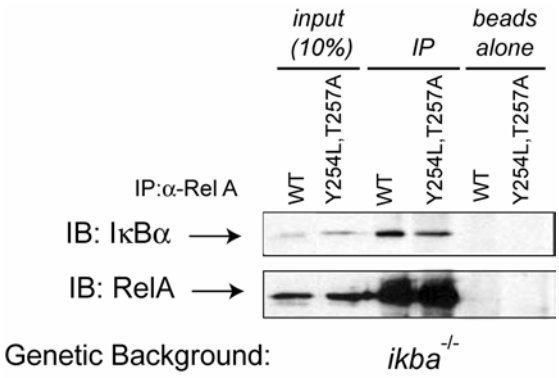

Figure 4-5. Y254L,T257A mutation binds more weakly than WT IκBα to NF-κB. NF-κB was immunoprecipitated with an α-RelA antibody and binding to IκBα was visualized with Western blot. The beads alone lanes show no non-specific binding of IκBα.

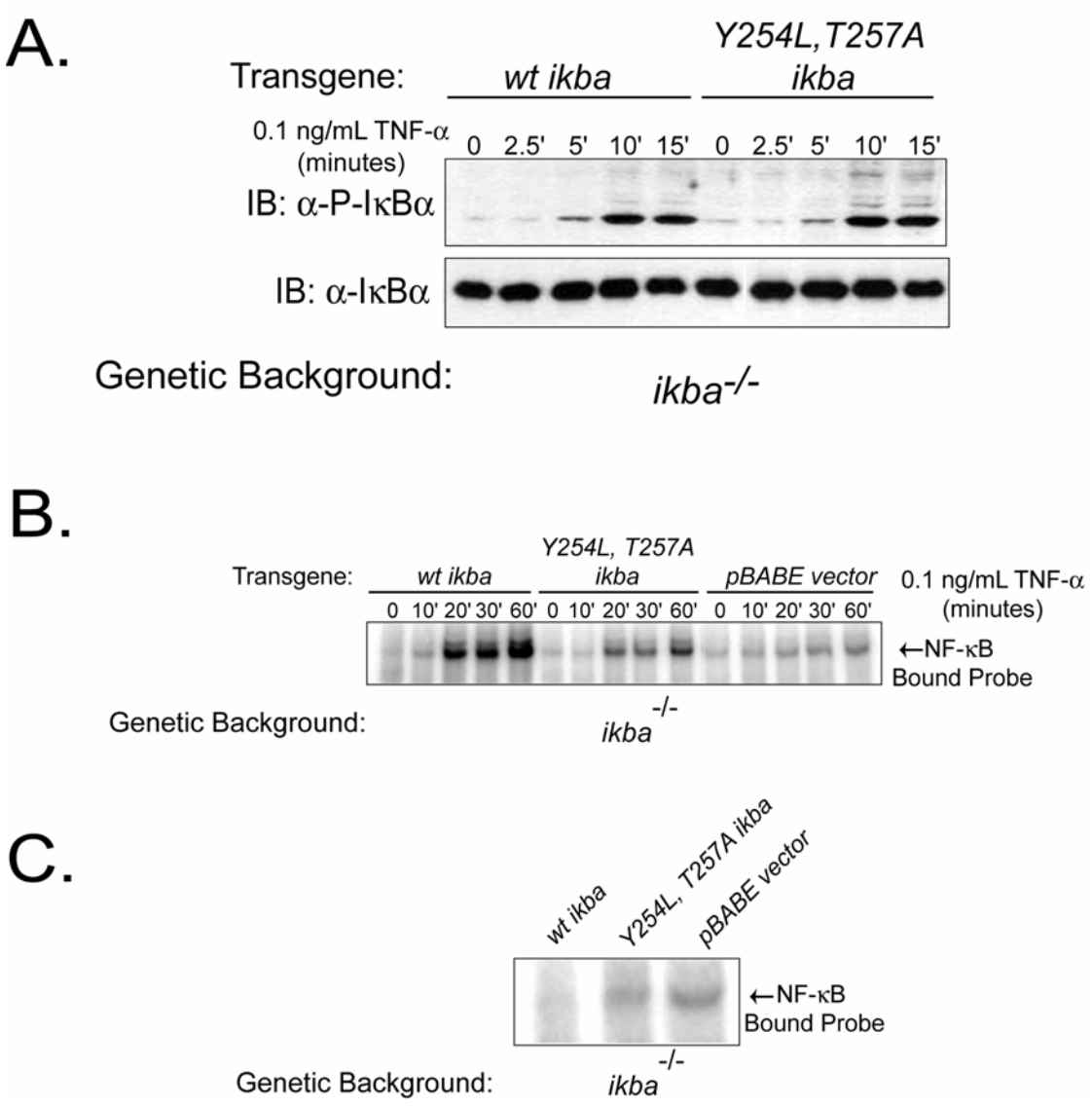

Figure 4-6. The Y254L, T257A IκBα affects both activated and basal NF-κB activation.
(A). Upon stimulation with TNF-α, WT IκBα and Y254L, T257A IκBα are phosphorylated to a similar level by IKK. (B). EMSA using nuclear extracts from stimulated cells shows that there is a significant decrease in nuclear translocation of the mutant IκBα, similar to a vector alone (pBABE) control in *ikba*$^{-/-}$ cells. (C). In resting cells, there is an increase in nuclear NF-κB, due to the decreased binding affinity of the Y254L, T257A mutation to NF-κB.

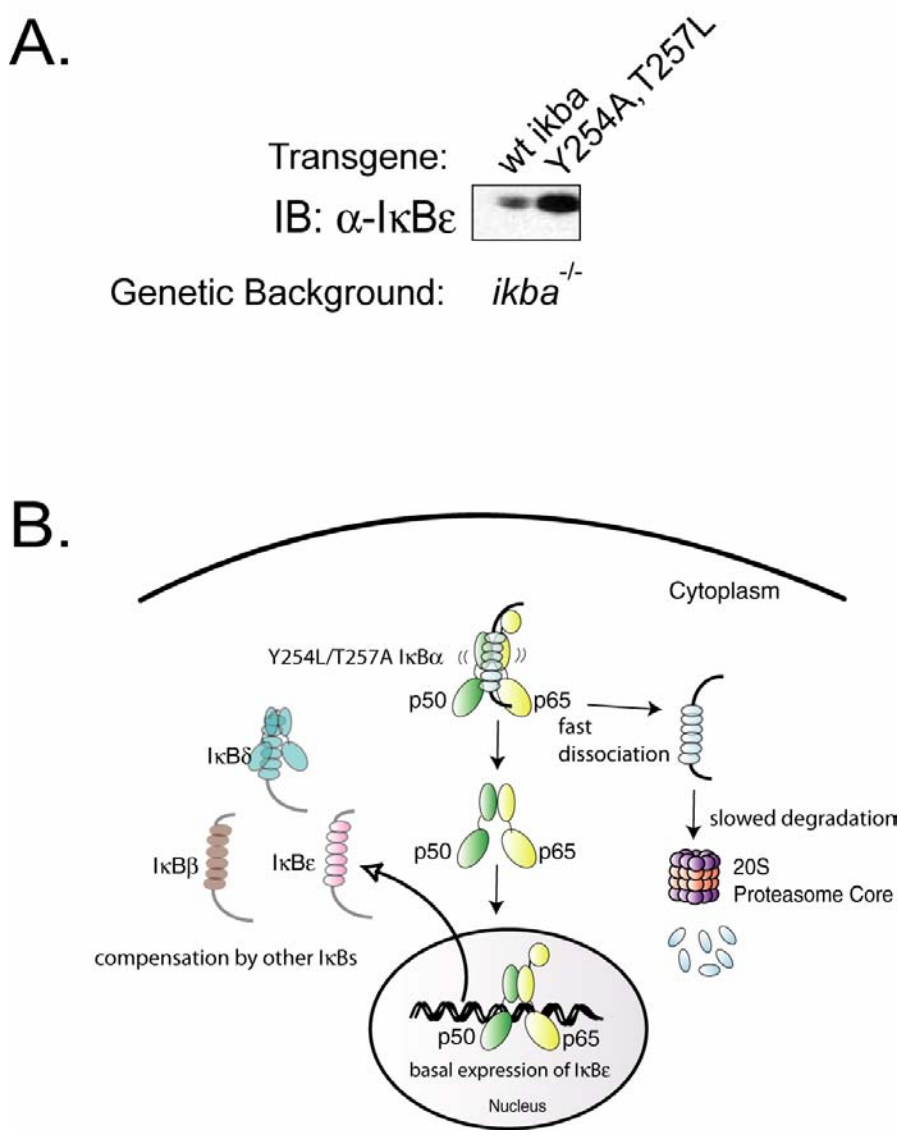

Figure 4-7. In mutant cells, there is an increase in basal IκBε protein levels. (A). Whole cell extracts from *ikba*$^{-/-}$ cells expressing either WT IκBα or Y254L, T257A IκBα were run on SDS-PAGE and probed with an α-IκBε antibody. The increase of IκBε due to higher basal NF-κB levels may explain the NF-κB activation profile. (B). Cartoon representing the effect of both reduced binding affinity of the Y254L, T257A mutant and slowed ubiquitin independent degradation.

C. Discussion

1. Only Mutation of IκBα in the 6th Ankyrin Repeat Alters Free IκBα Degradation

Although the use of repeat proteins as a protein-protein interaction module is apparent, the functional significance for variations between repeats has not been explored thoroughly. However, the repeat protein IκBα provides us with a unique opportunity to test the role of the sequence deviations from the ankyrin repeat consensus. Although the X-ray structure of IκBα-bound to NF-κB has been determined, the evolutionary pressure of ankyrin repeat variation is not clear.

More recently, the biophysical characteristics of IκBα folding have been studied in detail (Ferreiro et al., 2007; Ferreiro et al., 2005; Truhlar et al., 2006). These studies showed that changing the IκBα primary sequence to a perfect AR repeat sequence has severe consequence in its folding-unfolding transition and NF-κB binding property *in vitro*. However, the effect of these perturbations on proteasome mediated degradation in cells have not yet been explored. It is thought that for ubiquitin-independent degradation, an unfolded protein or extended peptide is necessary for the initiation of proteasome degradation, and that a defined structure precludes this degradation (Asher et al., 2006; Takeuchi et al., 2007).

In this study, we have shown through consensus mutations of the ankyrin repeats, that ubiquitin independent degradation of IκBα is not determined by overall thermodynamic stability, but rather targeted stability in ARs 5 and 6. The C186P,

A220P double mutant degraded faster than WT IκBα *in vitro* although cell based studies showed this mutant degrades similarly as WT IκBα. Interestingly, although the ΔG of unfolding is altered, M/D simulations showed that the AR6 of both the C186P,A220P mutant protein and the WT protein displayed large fluctuations (Ferreiro et al., 2007). The mutant may degrade faster *in vitro* for two reasons; first, the 20S proteasome may not be the true enzyme *in vivo* that is responsible for ubiquitin independent degradation of IκBα. *In vitro*, 20S proteasome degradation is largely mediated by thermodynamic stability. Secondly, IκBα has a greater tendency to aggregate, therefore differential aggregation of WT and C186P, A220P protein *in vitro* may alter degradation kinetics. Interestingly, the A133W destabilizing mutation degraded at a similar rate to WT IκBα, rather than faster as would be expected for a more unstable protein. However, the influence of this mutation on the flexibility of the 5^{th} and 6^{th} ankyrin repeat is not known.

Finally, the only mutant which shows a correlation between thermodynamic stability and slower degradation is one that mutates the variant 6^{th} ankyrin repeat to the consensus ankyrin repeat sequence at Y254 and T257. Introduction of these mutations created a pre-folded mutant which slowed degradation *in vitro* and was recapitulated in cells (Truhlar et al., 2008). These proteasome degradation studies show that the flexibility in the 5^{th} and 6^{th} repeats of IκBα determine the rate of proteasomal degradation, rather than overall thermodynamic stability.

2. Functional Consequences of Pre-folding IκBα

The consequences of the Y254L, T257A mutation in IκBα are far reaching. First, the binding of this mutant to NF-κB is perturbed significantly *in vitro* and recapitulated in cells with full-length proteins as shown by immunoprecipitation. Second, this reduced binding affinity leads to an increased level in basal NF-κB. This perturbs the entire NF-κB activation system by increasing the amount of NF-κB dependent gene products, and inhibitors, such as IκBε or p100 (IκBδ). Therefore, the reason for the uniqueness of the 6th ankyrin repeat is to ensure effective NF-κB binding and to lead to rapid ubiquitin independent degradation.

Chapter IV, in part, is as it appears in: Truhlar SM, Mathes E, Cervantes CF, Ghosh G, Komives EA. "Pre-folding IkappaBalpha Alters Control of NF-kappaB Signaling." J Mol Biol. 2008 Jun 27;380(1):67-82. Epub 2008 Mar 4.
The dissertation author was a co-author on this publication.

V. Hydrophobic Residues in Flexible Regions Influence the Rate of Free IκBα Degradation

A. Introduction

When not bound to NF-κB, IκBα has marginal thermodynamic stability (Croy et al., 2004; Ferreiro et al., 2007). While it is known that the N-terminal SRD and C-terminal PEST domain are flexible, (Croy et al., 2004; Huxford et al., 1998; Jacobs and Harrison, 1998) differences between the flexibility of the ankyrin repeats have also been observed. The ankyrin repeat region (ARD) of IκBα contains 6 ankyrin repeats, which altogether do not form a compact folded domain (Ferreiro et al., 2007). Both folding studies and H/D exchange experiments show that ankyrin repeats 2-4 are less flexible than ankyrin repeats 1, 5 and 6 when not bound to NF-κB (Ferreiro et al., 2007; Truhlar et al., 2006). The flexibility of ankyrin repeats 5 and 6 has been shown to be important for NF-κB binding and for degradation of unbound IκBα (Truhlar et al., 2006).

In addition to a correlation between flexibility and protein degradation, there is also a correlation between hydrophobic residues and proteasomal degradation. For instance, 20S proteasome activity is stimulated when incubated with peptides containing a 4-mer hydrophobic motif (Kisselev et al., 2002). In addition, it has been shown that proteasomal degradation of proteins such as Huntington protein (Htt), androgen receptor (AR) , SGK-1 and MATa-2 are also determined by hydrophobic motifs (Bogusz et al., 2006; Chandra et al., 2008; Johnson et al., 1998). Finally, exposure of hydrophobic residues in mildly oxidized proteins has been shown to increase proteasomal activity (Shringarpure and Davies, 2002). Taken together, these

studies suggest that hydrophobic residues contribute to efficient proteasomal degradation.

The PEST region within proteins has been defined as a stretch of sequences which are enriched with (P) proline, (E) glutamic acid, (S) serine, and (T) threonine residues. The PEST sequence is thought to serve as a signal for the degradation of proteins (Rogers et al., 1986). IκBα has a C-terminal PEST region which has been shown to be phosphorylated by CK2 on serines and threonines and this phosphorylation is thought to contributeto IκBα turnover. However, the role of residues other than (P) (E) (S) and (T) in IκBα degradation has not been explored.

In this study, we show that certain flexible regions of IκBα can act as degradation signals and these degradation signals are dependent on hydrophobic residues. Truncations of IκBα that end at the flexible 5th or within the 6th ankyrin repeat significantly increase the degradation rate of free IκBα. In contrast, when IκBα is designed to end at the less flexible 4th ankyrin repeat, degradation is drastically slowed. Mutation of a hydrophobic patch within the 5th ankyrin repeat significantly stabilizes unbound IκBα, but this effect can only be observed in a truncated form of IκBα. Therefore, the primary degradation signal of full-length free IκBα is included in the C-terminal PEST region. When examining the contribution of residues within the PEST domain to IκBα degradation, we found that Y289, whether mutated to glycine or alanine, altered the degradation rate of unbound IκBα significantly. In contrast, mutation of F295 and F298 of IκBα to alanine caused stabilization, while mutation to glycine abolished this effect. We speculated that

mutation from phenylalanine to alanine induced a helical structure, and this was confirmed by secondary structure prediction, while mutation to glycine eliminated any secondary structure within the PEST domain. Overall, both flexibility and residue type are paramount in determining the ubiquitin independent degradation of IκBα.

B. Results

1. Inherent flexibility in IκBα leads to rapid degradation.

It was previously shown that in the absence of NF-κB subunits, the inhibitor protein IκBα degrades rapidly, (Mathes et al., 2008; Pando and Verma, 2000; Rice and Ernst, 1993). While removal of the N-terminal domain (residues 1-67) does not affect rapid degradation, removal of residues 287-317 (the C-terminus) significantly reduced free IκBα degradation (Mathes et al., 2008). However, this truncation does not remove the entire PEST domain, and so, we set out to determine whether the deletion of the entire PEST region further stabilized free IκBα. Using NF-κB deficient cells (cells lacking the NF-κB subunits, p65, cRel, p50-hereafter will be referred to as *nfkb*$^{-/-}$), we expressed a construct which removed the entire PEST domain (IκBαΔC281). By treating cells with cycloheximide (CHX), a translational inhibitor, one can determine the approximate half-life of unbound IκBα. Unexpectedly, this truncated mutant slightly increases the degradation rate of IκBα (Figure 5-1B). Intrigued, we created three more constructs of IκBα which further truncate the C-terminus of IκBα: ΔC257, ΔC242, and ΔC207 (Figure 5-1A and C). The ΔC257 truncation removes the entire PEST domain as well as half of the 6th ankyrin repeat, and has been shown to slow free IκBα degradation *in vitro* (Kroll et

al., 1997). The ΔC242 truncation removes entire 6th repeat and ends at the 5th ankyrin repeat of IκBα. Finally, the ΔC207 truncation removes all residues C-terminal to the 4th ankyrin repeat. Surprisingly, removal of residues N-terminal to the PEST domain (ΔC256 and ΔC242) enhanced the degradation rate of free IκBα (Figure 5-1C). Only when both the 5th and 6th ankyrin repeats of IκBα are entirely removed in the construct IκBα ΔC206, is the degradation of free IκBα stabilized (Figure 5-1C). This observation can be explained by the inherent flexibility of the 5th and 6th ankyrin repeats of IκBα, which in this case, correlates to a rapid degradation rate (Truhlar et al., 2006).

Figure 5-1. Truncations in flexible regions of IκBα increase the rate of proteasome mediated free IκBα degradation

(A). Structure of IκBα from the crystal structure bound to NF-κB (PDB ID:1IKN). Only IκBα is shown, with truncations and ankyrin repeats indicated on the structure. (B). Left panel: *nfkb*$^{-/-}$ cells expressing WT IκBα, IκBα ΔC288 and IκBα ΔC281 were treated with CHX and detected by western blot using an antibody directed against the N-terminus of IκBα. (*) indicate non-specific bands associated with this antibody. Right panel: Left panel quantitated, normalized to β-actin, and graphed. Error bars indicate s.e.m. from at least three experiments. (●) represents WT IκBα, (○) represents IκBαΔC281, and (●) represents IκBαΔC288. (C). Top left panel: *nfkb*$^{-/-}$ cells expressing WT IκBα, IκBα ΔC281 and IκBα ΔC257 were treated with CHX and protein levels were detected by western blot. Bottom left panel: *nfkb*$^{-/-}$ cells expressing WT IκBα, IκBα ΔC242 and IκBα ΔC206 were treated with CHX and protein levels detected by western blot. Right panel: Averages from at least two experiments were quantitated and graphed. Error bars indicate s.e.m. from at least two experiments. (■) represents IκBα ΔC207, (●) represents WT IκBα, (●) represents IκBα ΔC257, and (○) represents IκBα ΔC242. (D). *nfkb*$^{-/-}$ cells expressing WT IκBα, IκBαΔC257, or IκBαΔC242 were treated with MG132, a proteasomal inhibitor for the indicated periods of time. All IκBα protein levels increase, suggesting that the proteasome is involved in this degradation pathway.

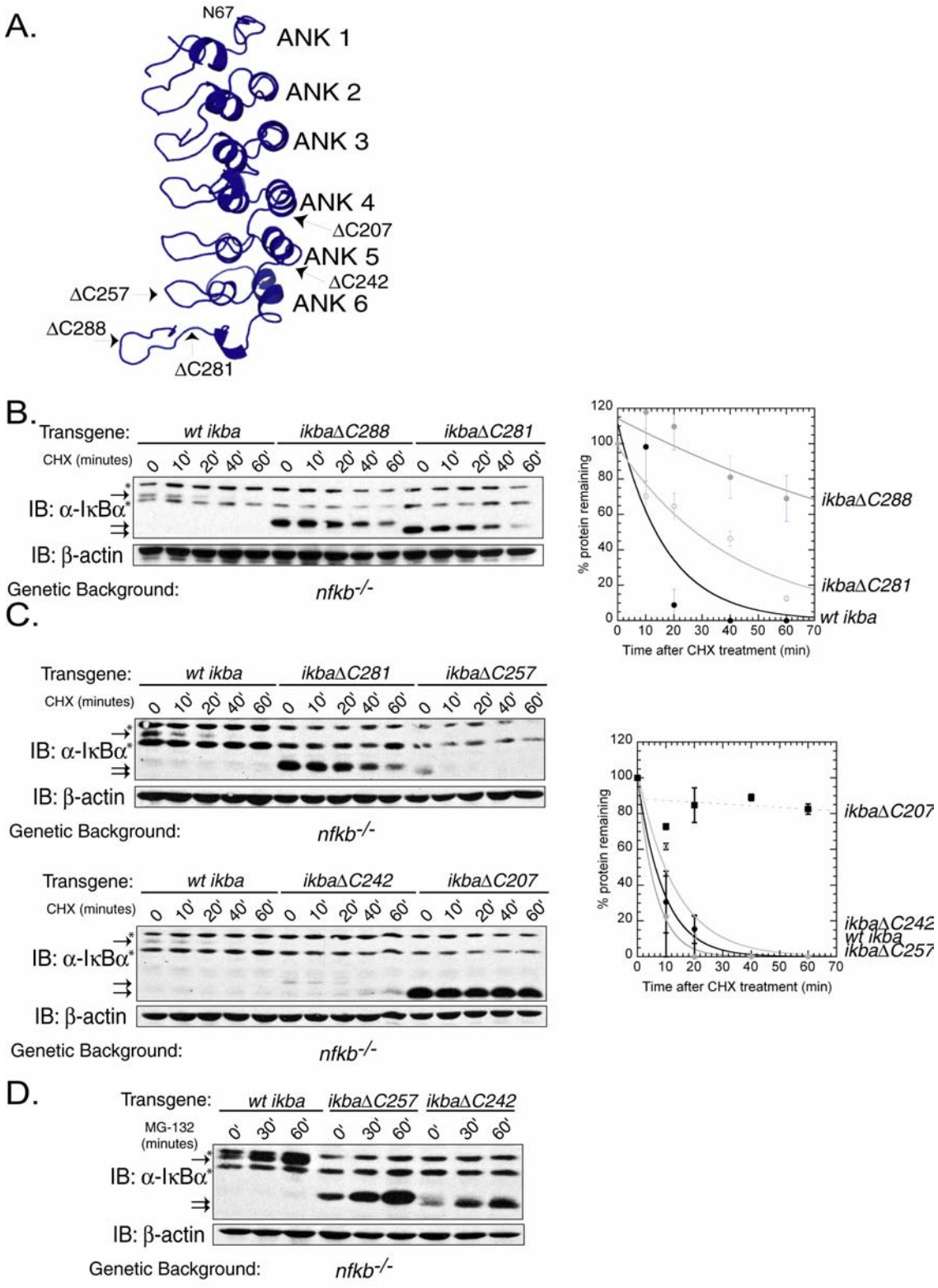
A.
N67
ANK 1
ANK 2
ANK 3
ANK 4
ΔC207
ANK 5
ΔC242
ΔC257
ANK 6
ΔC288
ΔC281
B.
Transgene:
wt ikba
ikbaΔC288
ikbaΔC281
CHX (minutes)
0 10' 20' 40' 60' 0 10' 20' 40' 60' 0 10' 20' 40' 60'
IB: α-IκBα
IB: β-actin
Genetic Background:
nfkb-/-
% protein remaining
Time after CHX treatment (min)
ikbaΔC288
ikbaΔC281
wt ikba
C.
Transgene:
wt ikba
ikbaΔC281
ikbaΔC257
CHX (minutes)
0 10' 20' 40' 60' 0 10' 20' 40' 60' 0 10' 20' 40' 60'
IB: α-IκBα
IB: β-actin
Genetic Background:
nfkb-/-
Transgene:
wt ikba
ikbaΔC242
ikbaΔC207
CHX (minutes)
0 10' 20' 40' 60' 0 10' 20' 40' 60' 0 10' 20' 40' 60'
IB: α-IκBα
IB: β-actin
Genetic Background:
nfkb-/-
% protein remaining
Time after CHX treatment (min)
ikbaΔC207
ikbaΔC242
wt ikba
ikbaΔC257
D.
Transgene:
wt ikba
ikbaΔC257
ikbaΔC242
MG-132 (minutes)
0' 30' 60' 0' 30' 60' 0' 30' 60'
IB: α-IκBα
IB: β-actin
Genetic Background:
nfkb-/-

2. Truncated IκBα is degraded by the proteasome

Although IκBα ΔC257 and IκBα ΔC242 degrade rapidly, it is not known whether these proteins are degraded by the proteasome, although WT IκBα expressed in *nfkb*$^{-/-}$ cells has been shown to be degraded by the proteasome without prior ubiquitination, as well as *in vitro* by the 20S proteasome core (Alvarez-Castelao and Castano, 2005; Mathes et al., 2008). To test whether the truncated forms of IκBα are degraded by the proteasome, the proteasome inhibitor MG132 was added to *nfkb*$^{-/-}$ cells expressing WT IκBα, IκBα ΔC257 or IκBα ΔC242. After addition of MG132 to these cell lines, the protein level increases over time, showing that degradation of these proteins is mediated by the proteasome (Figure 5-1D). Unfortunately, the degradation reactions cannot be recapitulated *in vitro* due to the tendency of these constructs to aggregate, which could lead to slowed proteasomal degradation (Ferreiro et al., 2007). Together, these results suggest that proteasome-dependent degradation signals in IκBα are exposed in flexible regions of the protein.

3. The 5th ankryin repeat degradation signal is dependent on hydrophobic residues

Since the IκBα ΔC242 truncation degrades at a faster rate as compared to IκBα ΔC206 (Figure 5-1C) a degradation signal must exist in the 5th ankyrin repeat. It is known that the 5th ankyrin repeat is flexible, and it is possible that a degradation signal is exposed in the IκBα ΔC242 truncation of IκBα. It has also been hypothesized that hydrophobic residues play a role in proteasomal recognition and activation (Bogusz et al., 2006; Chandra et al., 2008; Johnson et al., 1998; Kisselev et

al., 2002; Shringarpure and Davies, 2002). For instance, a 4-mer hydrophobic peptide can stimulate the gate opening of the α subunits of the 20S proteasome, leading to the activation of the inner catalytic sites of the β subunits (Kisselev et al., 2002). Therefore, we mutated four residues (V233, L235, L236 and L237) which are located in a C-terminal hydrophobic patch of IκBα in the 5th ankyrin repeat to glycine (Figure 5-2A). We introduced this mutation (4G) into either the full-length protein or IκBα ΔC242. When IκBα 4G ΔC242 was introduced into *nfkb*$^{-/-}$ cells, the degradation was significantly slowed compared to wt IκBα ΔC242, suggesting that hydrophobic residues are very important in proteasomal recognition and degradation in a flexible region (Figure 5-2B). This is the first time that the requirement for both a flexible region and hydrophobic residues has been observed for IκBα. However, when the 4G mutation is introduced into full-length IκBα, only a small decrease in the degradation rate was observed (Figure 5-2C). It is possible that that the 5th ankyrin repeat is not completely exposed for proteasomal recognition when the rest of the protein is present, which then suggests that the most influential degradation signal in the full-length protein is the C-terminal segment from 287-317.

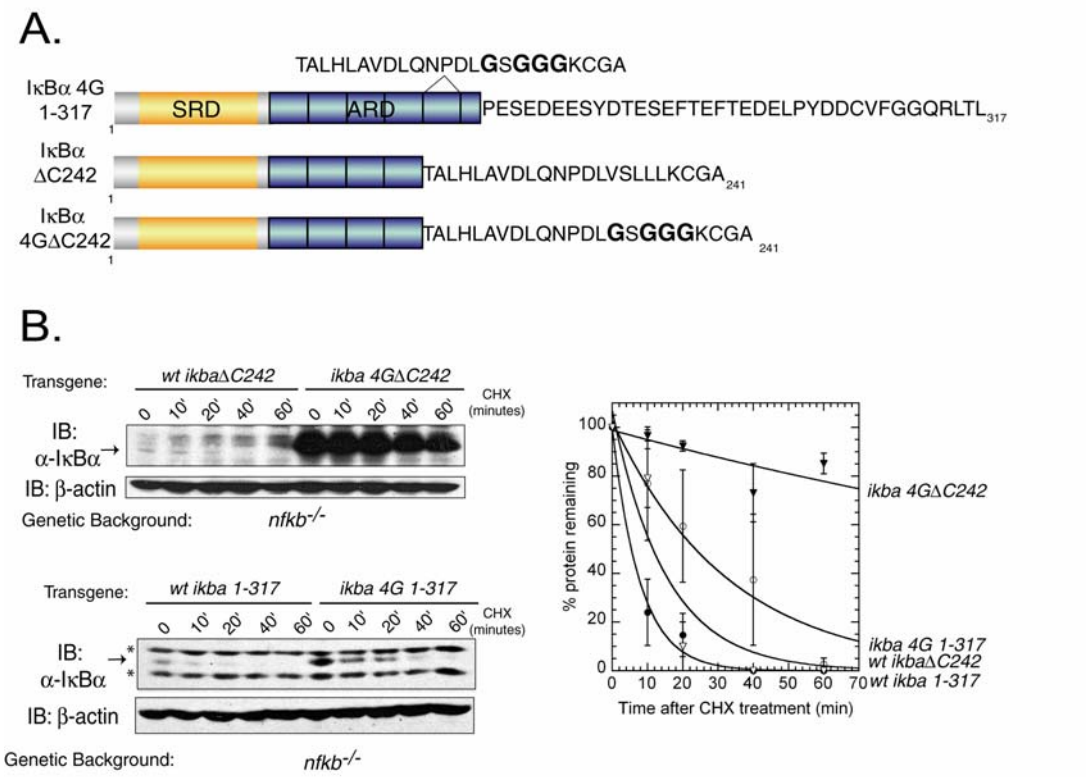

Figure 5-2. The 5th ankyrin repeat degron is influenced by hydrophobic residues

(A). Schematic detailing the location of the hydrophobic residues mutated to glycine (4G), either in the full-length or IκBαΔC242 background. (B).Top left panel: *nfkb*$^{-/-}$ cells expressing WT IκBαΔC242 or IκBα 4GΔC242 were treated with CHX and degradation was observed by western blot. Bottom left panel: *nfkb*$^{-/-}$ cells expressing WT IκBα 1-317 or IκBα 4 G 1-317 C242 were treated with CHX and degradation was detected by western blot. (*) indicates n.s. band associated with the antibody directed against the N-terminus of IκBα. Right panel: Quantification of left panels (▽) represents wt IκBαΔC242, (▼) represents IκBα 4GΔC242. (●) represents WT IκBα 1-317, and (○) represents IκBα 4G 1-317. Error bars indicate s.e.m. and are representative of at least two individual experiments.

4. Residues within the PEST domain of IκBα contribute to rapid free IκBα degradation

In all, the above experiments suggest that the primary degradation signal of free IκBα is located within the C-terminal 20 residues 288-317. This region, which includes most of the PEST domain, is known to be flexible (Huxford et al., 1998), (Croy et al., 2004; Phelps et al., 2000). The PEST region of IκBα is defined within P281 and D307 (Sun et al., 1996), is negatively charged, and becomes more so upon CK2 phosphorylation at sites S283, S288, T291, S293, T296, T299. However, mutation of all CK2 phosphorylation sites does not stabilize free IκBα to the same degree as the truncation of IκBαΔC288. Located between these negatively charged residues are hydrophobic residues. To determine whether these residues contribute to unbound IκBα degradation, they were mutated to alanine (Y289A, F295A, F298A, L303A and Y305A). Unlike the 5th ankyrin repeat hydrophobic patch, these residues are scattered throughout the C-terminal PEST region, so we examined the effect of these residues individually (Figure 5-3A). All of the mutations increased the half-life of IκBα to varying degrees (Figure 5-3B-D). IκBα Y305A slightly slowed the degradation of IκBα, as compared to WT IκBα ($t_{1/2}$~15', Figure 5-3B). L303A had a moderate effect on free IκBα stabilization ($t_{1/2}$~30') (Figure 5-3B). The F295A and F298A single mutations also had a moderate effect on IκBα degradation ($t_{1/2}$ ~30' WT-Figure 5-3C top panel). The F295A, F298A double mutant was created due to the presence of an 'EFT' insert in human IκBα, and perhaps these phenylalanines could have a more significant impact on degradation when combined (Figure 5-4). Indeed,

the double mutant enhanced the stability of IκBα ($t_{1/2}$ =40', Figure 5-3C, top panel). The last mutant, Y289A, showed the most significant effect on IκBα stability ($t_{1/2}$=60', Figure 5-3D). These results clearly establish a role of the hydrophobic residues as a determinant of free IκBα stability. In addition, these results show that mutation of residues within the PEST region other than (P) (E) (S) or (T) also can contribute significantly to ubiquitin independent degradation of IκBα.

Figure 5-3. Mutations in the PEST domain alter free IκBα degradation

(A) Top, Schematic representing IκBα and the C-terminal PEST domain with residues that were mutated indicated in bold. Bottom, left panel: Transgenic *nfkb*$^{-/-}$ cells expressing WT IκBα, IκBα ΔC288, or PESTA IκBα were treated with cycloheximide (CHX) and IκBα protein levels were detected by western blot. Right panel: Western blot quantitated, normalized to β-actin levels, and graphed as a percentage of protein remaining. (●) -WT IκBα, (●)-PESTA IκBα, and (●)-IκBα ΔC288. (Adapted from Mathes, 2008.) (B) Left panel: Transgenic *nfkb*$^{-/-}$ cells expressing either WT IκBα, L303A IκBα, or Y305 IκBα were treated with cycloheximide (CHX) and IκBα protein levels were detected by western blot. Right panel: Left panel quantitated, normalized with β-actin, and graphed as percentage of protein remaining with 0' equal to 100% for each cell line. (□) - L303A IκBα, (●) WT IκBα, (◇) Y305A IκBα. (C). Top left panel: Transgenic *nfkb*$^{-/-}$ cells expressing F295A IκBα, F298A IκBα, or the combined F295A, F298A IκBα mutants were treated with CHX and degradation was detected through western blot. Bottom left panel: Transgenic cells expressing WT IκBα or F295A, F298A IκBα were treated with CHX and degradation monitored by western blot. Right panel: Quantification and graphical representation of averages from both top and bottom panels. (●) represents WT IκBα, (□) represents F295A IκBα, (□) represents F298A IκBα, and (■) represents F295A, F298A IκBα. Error bars represent s.e.m., and are representative of at least two experiments. (C). Left panel: Western blot of CHX treated *nfkb*$^{-/-}$ cells expressing WT IκBα, or Y289A IκBα. Right panel: Quantification and graphical representation of left panel. (●) represents WT IκBα, and (Δ) represents Y289A IκBα. Error bars represent s.e.m., and are representative of at least two experiments.

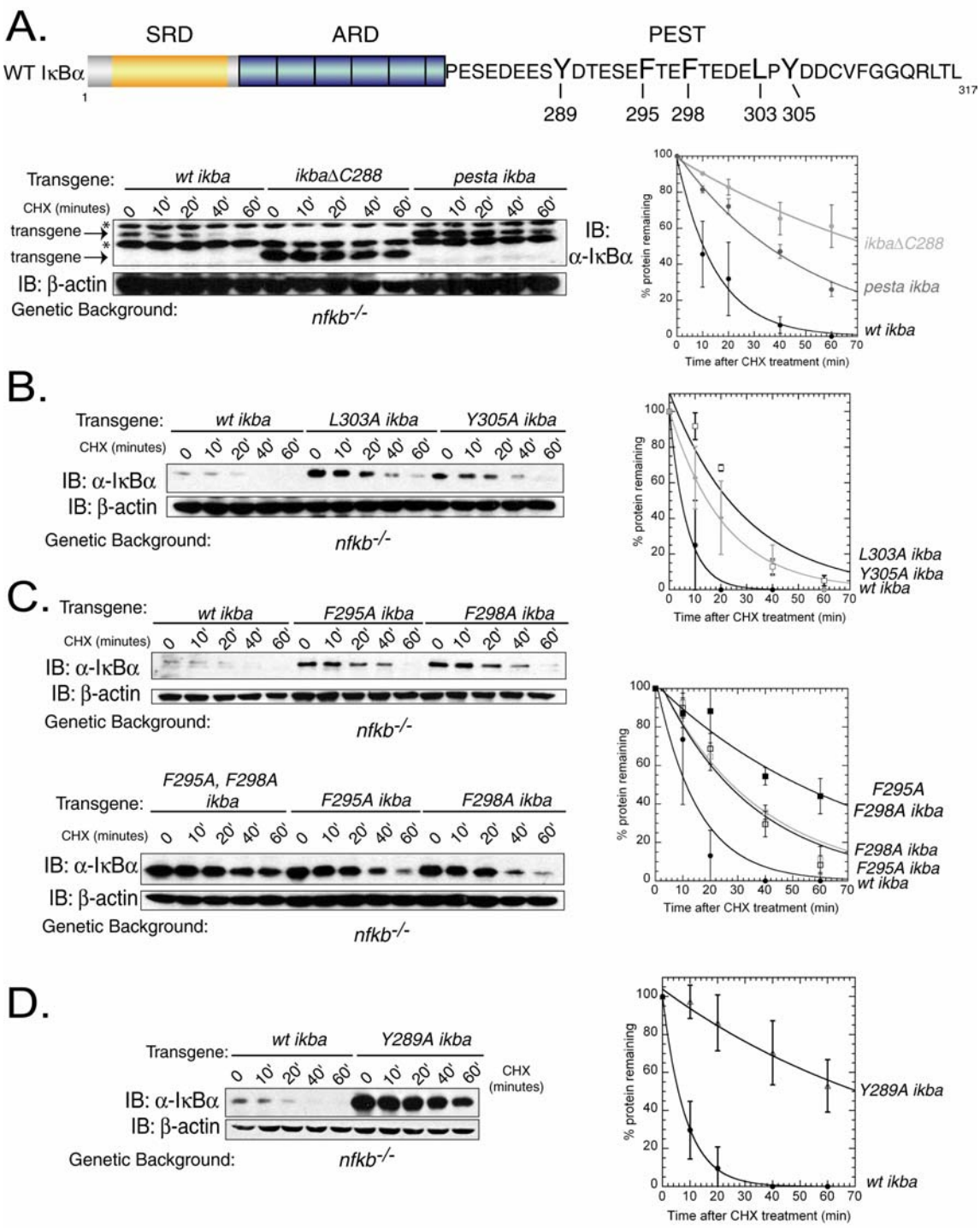
A.
SRD
ARD
PEST
WT IκBα
PESEDEESYDTESEFTEFTEDELPYDDCVFGGQRLTL
1
317
289
295
298
303
305
Transgene:
wt ikba
ikbaΔC288
pesta ikba
CHX (minutes)
0 10' 20' 40' 60' 0 10' 20' 40' 60' 0 10' 20' 40' 60'
transgene
transgene
IB: α-IκBα
IB: β-actin
Genetic Background:
nfkb-/-
% protein remaining
Time after CHX treatment (min)
ikbaΔC288
pesta ikba
wt ikba
B.
Transgene:
wt ikba
L303A ikba
Y305A ikba
CHX (minutes)
0 10' 20' 40' 60' 0 10' 20' 40' 60' 0 10' 20' 40' 60'
IB: α-IκBα
IB: β-actin
Genetic Background:
nfkb-/-
% protein remaining
Time after CHX treatment (min)
L303A ikba
Y305A ikba
wt ikba
C.
Transgene:
wt ikba
F295A ikba
F298A ikba
CHX (minutes)
0 10' 20' 40' 60' 0 10' 20' 40' 60' 0 10' 20' 40' 60'
IB: α-IκBα
IB: β-actin
Genetic Background:
nfkb-/-
F295A, F298A ikba
Transgene:
F295A ikba
F298A ikba
CHX (minutes)
0 10' 20' 40' 60' 0 10' 20' 40' 60' 0 10' 20' 40' 60'
IB: α-IκBα
IB: β-actin
Genetic Background:
nfkb-/-
% protein remaining
Time after CHX treatment (min)
F295A F298A ikba
F298A ikba
F295A ikba
wt ikba
D.
Transgene:
wt ikba
Y289A ikba
CHX (minutes)
0 10' 20' 40' 60' 0 10' 20' 40' 60'
IB: α-IκBα
IB: β-actin
Genetic Background:
nfkb-/-
% protein remaining
Time after CHX treatment (min)
Y289A ikba
wt ikba

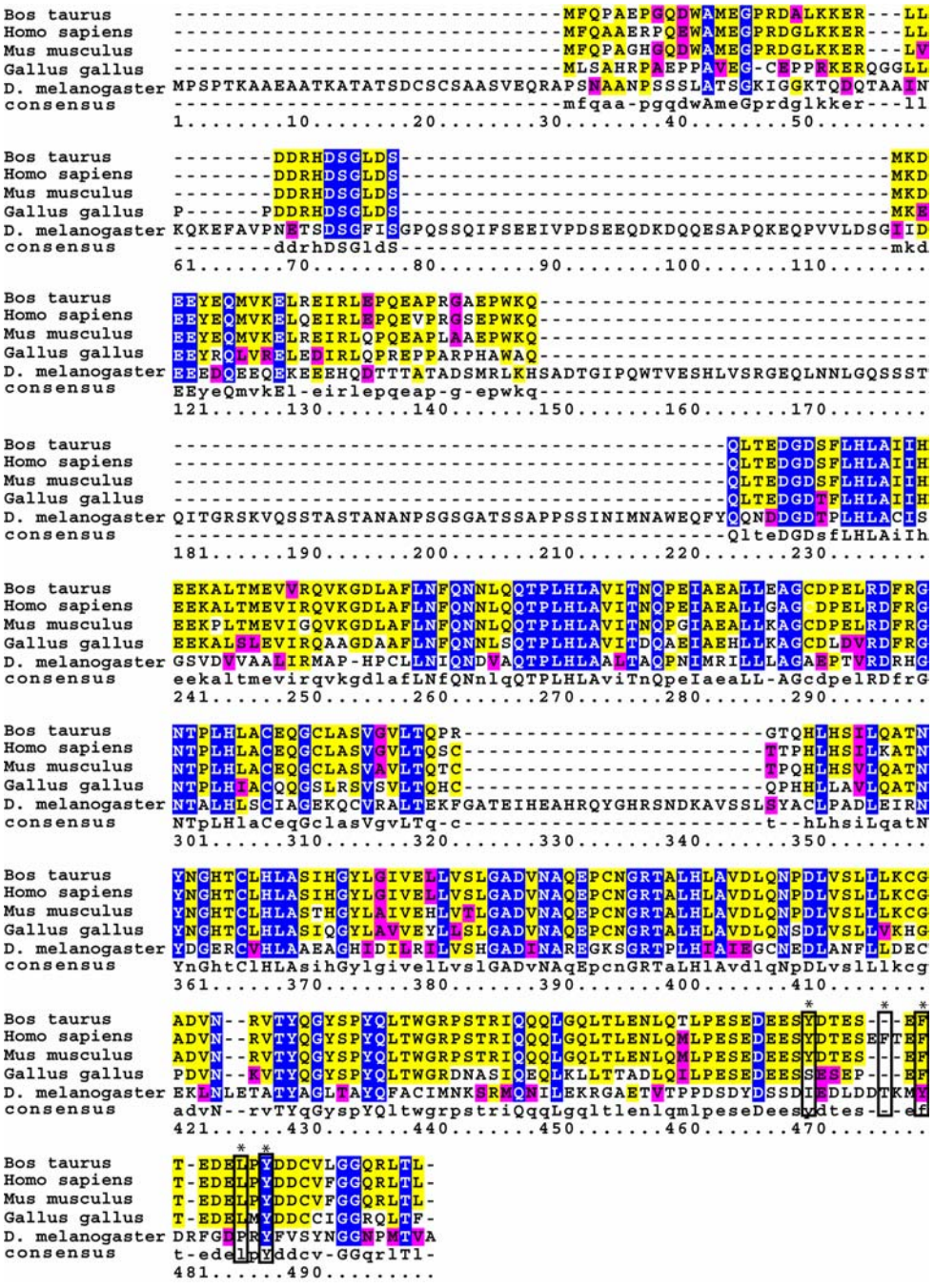

Figure 5-4. Sequence alignment across species for IκBα

Sequences from *B. taurus*, *H. sapiens*, *M. musculus*, *G. gallus*, and *D. melanogaster* were aligned using CLUSTALW (Thompson) Mutations made in this study are boxed and marked with an (*). Yellow shading indicates identical residues across several species, purple indicates similar residues, and blue shading with white text indicates complete conservation.

5. The PEST hydrophobic residues regulate IκBα stability through different mechanisms

In order to ensure that the effect of mutating F295 and F298 to alanine is a specific, rather than an indirect effect, these residues were also mutated to glycine. Surprisingly, F295G, F298G double mutant did not have the same stabilization effect as F295A, F298A double mutation (Figure 5-5A). Therefore, these phenylalanines are most likely not involved in a specific interaction leading to proteasomal degradation. To explain this differing degradation rate, secondary structure analysis was performed both on the F295A, F298A and F295G, F298G mutations using the San Diego Supercomputer PELE program (http://workbench.ucsd.edu) and the JOI program which combines all secondary structure algorithms in a 'winner takes all' manner. As shown in Table 5-1, the F295A and F298A mutations increased the helical propensity of the PEST region as compared to the F295G and F298G mutations and WT IκBα. As described previously, flexibility within the C-terminus of IκBα is important for rapid degradation (Truhlar et al., 2008), and so alteration of this flexibility/secondary structure within the PEST domain could have a direct effect on the degradation rate. In addition, a study done on the PEST domain of the E2 enzyme from papillomavirus showed that phosphorylation disrupts the overall structure, and this thermodynamic stability corresponds to degradation rates (Garcia-Alai et al., 2006). Likewise, L303G did not slow IκBα degradation as compared to WT IκBα (Figure 5-5B).

Unlike the phenylalanine and leucine residues, mutation of Y289 to glycine had the same stabilizing effect as the Y289A mutation, even though according to secondary structure prediction, Y289G has less helical propensity than Y289A (Table 5-1). Therefore, Y289 does have a specific role to play in free IκBα degradation. However, the exact mechanistic role that this tyrosine plays is still unknown. One possibility is that this tyrosine is phosphorylated, and so the program NetPhos 2.0 (Blom et al., 1999) was used to predict phosphorylation sites of IκBα (Table 5-2). Out of eight tyrosines found throughout IκBα, three were found to be possible phosphorylation sites, Y42, Y305 and Y289. Experimental evidence has shown Y42 to be phosphorylated by Syk in response to H_2O_2 and found this phosphorylation leads to IκBα:NF-κB dissociation and NF-κB activation (Takada et al., 2003). Y305, has been experimentally shown to be phosphorylated by c-Abl (Kawai et al., 2002). In contrast, Y289 has not identified as a phosphorylation site *in vivo*; however, using the Group Based Phosphorylation Scoring Method (GPS) (Xue et al., 2005), Syk had the highest score and is a putative kinase, although six other kinases (EGFR, RYn/Yes, IR, LCK, LYN, SRC were also listed as possible kinases for Y289). This could provide an attractive regulatory mechanism for the degradation of unbound IκBα, since Y289 might not be available for phosphorylation when IκBα is bound to NF-κB (Figure 5-6). However, when not bound to NF-κB, IκBα could present Y289 as a phosphorylation site, and this phosphorylation could lead to rapid degradation as mutation to either alanine or glycine slows IκBα degradation significantly. It is also possible that this phosphorylation has not been identified, because the unbound IκBα

is degraded so quickly. Although this is highly speculative, the putative phosphorylation of Y289 is a possible mechanism of regulating unbound IκBα degradation.

Figure 5-5. Y289 is the key residue within the PEST domain that determines degradation rate

(A) Left panel: Transgenic *nfkb*$^{-/-}$ cells expressing WT IκBα, F295G, F298G IκBα or F295A, F298A IκBα were treated with cycloheximide (CHX) and IκBα protein levels were detected by western blot. Right panel: Western blot quantitated, normalized to β-actin levels, and graphed as a percentage of protein. (●) represents WT IκBα, (■) represents F295A, F298A IκBα, and (□) represents F295G, F298G IκB (B). Left panel: *nfkb*$^{-/-}$ cells expressing either WT IκBα, L303A IκBα or L303G IκBα were treated with CHX. Right panel: Average and s.e.m. of at least two experiments are quantitated and graphed. (●) represents WT IκBα, (□) represents L303A IκBα, and (■) represents L303G IκBα. (C). Left panel: Transgenic *nfkb*$^{-/-}$ cells expressing either WT IκBα, Y289A IκBα, or Y289G IκBα were treated with CHX. Right panel: Average and s.e.m of at least three experiments are quantitated and graphed. (●) represents WT IκBα, (Δ) represents Y289A IκBα, and (◆) represents Y289G IκBα.

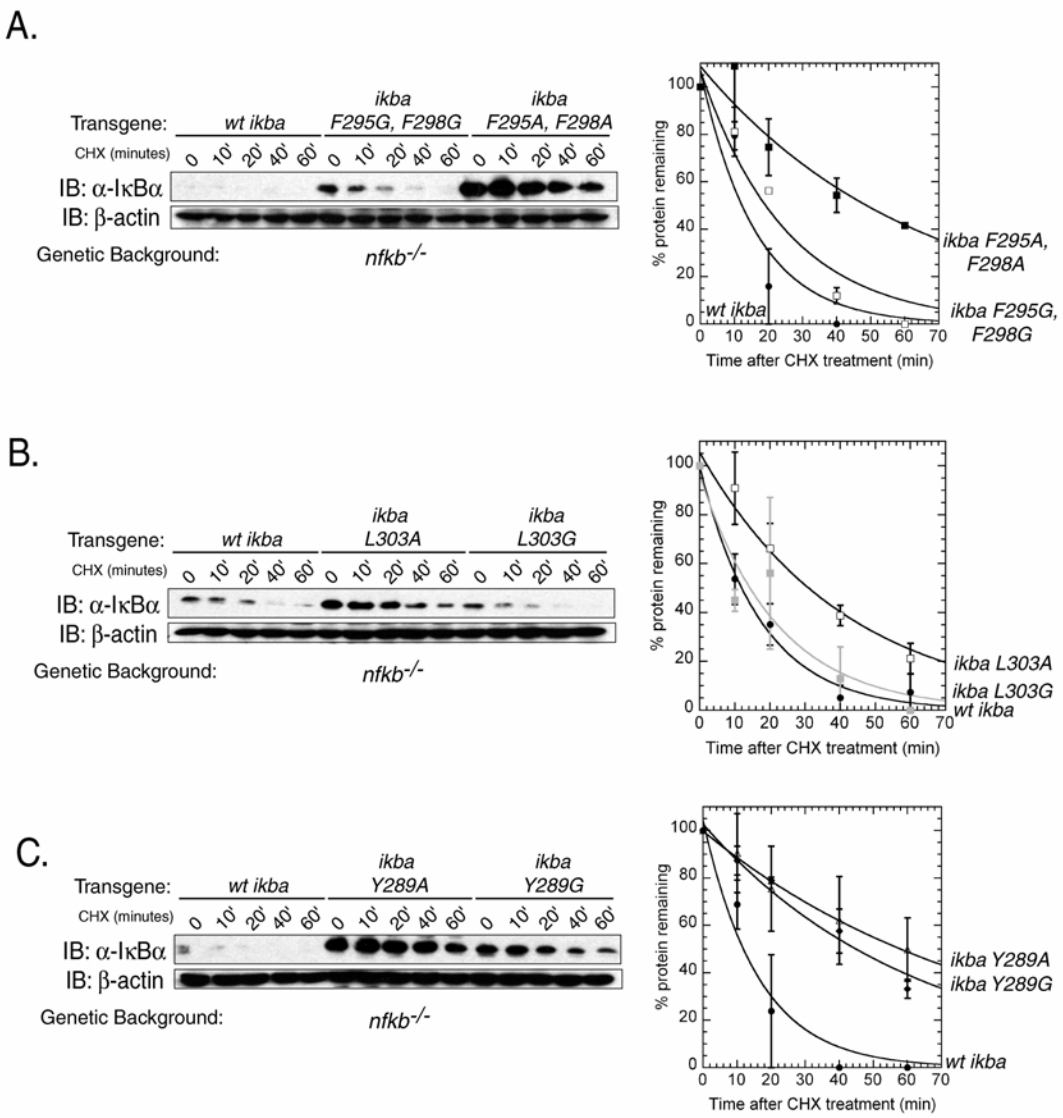
A.
Transgene:
wt ikba
ikba F295G, F298G
ikba F295A, F298A
CHX (minutes)
0 10' 20' 40' 60' 0 10' 20' 40' 60' 0 10' 20' 40' 60'
IB: α-IκBα
IB: β-actin
Genetic Background:
nfkb-/-
% protein remaining
Time after CHX treatment (min)
ikba F295A, F298A
wt ikba
ikba F295G, F298G
B.
Transgene:
wt ikba
ikba L303A
ikba L303G
CHX (minutes)
0 10' 20' 40' 60' 0 10' 20' 40' 60' 0 10' 20' 40' 60'
IB: α-IκBα
IB: β-actin
Genetic Background:
nfkb-/-
% protein remaining
Time after CHX treatment (min)
ikba L303A
ikba L303G
wt ikba
C.
Transgene:
wt ikba
ikba Y289A
ikba Y289G
CHX (minutes)
0 10' 20' 40' 60' 0 10' 20' 40' 60' 0 10' 20' 40' 60'
IB: α-IκBα
IB: β-actin
Genetic Background:
nfkb-/-
% protein remaining
Time after CHX treatment (min)
ikba Y289A
ikba Y289G
wt ikba

Table V-I. Secondary structure prediction of mutant IκBα

Sequences were run through the PELE structure prediction program available with the Biology Workbench (http://workbench.sdsc.edu) and listed with their approximate $t_{1/2}$s. As shown, the helical propensity increases with the F295A, F298A double mutation, and this propensity is abolished when glycines are introduced. (C)=random coil, (H)=helical region, and (E)=β-sheet

Secondary Structure Prediction Table

Construct	PESEDEESYDTESEFTEFTEDELPYDDCVFGGQRLTL	Approximate Half-life
WT IκBα	CCCCCCCCCCCHHHHCCCCCCCCCCCCCCCCCCCC	~ 10 minutes
F295A, F298A IκBα	CCCCCCCCCCCHHHHHHHHHCCCCCCCCCCCCCCCC	~ 40 minutes
F295G, F298G IκBα	CCCCCCCCCCCCCCCCCCCCCCCCCCCCCCCCCCCC	~ 20 minutes
Y289A IκBα	CCCCCCCCCCHHHHHHHHHCCCCCCCCCCCCCCCCC	~ 45 minutes
Y289GIκBα	CCCCCCCCCCCCCHHCHHCCCCCCCCCCCCCCCCC	~ 40 minutes
L303A IκBα	CCCCCCCCCCCHHHHCCCCCCCCCCCCECCCCCCC	~ 30 minutes
L303G IκBα	CCCCCCCCCCCCHHCCCCCCCCCCCCCEEECCCCEEE	~ 15 minutes
PESTA IκBα	CHHHHHHHHHHHHHHHHHHHCCCCCCCCCCCCCCCC	~ 35 minutes

Table V-II. Predicted phosphorylation sites of IκBα

The WT sequence of IκBα was run through the NetPhos 2.0 Server (Blom et al., 1999) to determine putative tyrosine phosphorylation sites. These are listed with their flanking sequences and putative tyrosine kinase as described by Group-based Phosphorylation Scoring Method (Xue et al., 2005).

Phosphorylation Prediction Table
as predicted by NetPhos 2.0 Server

Tyrosine	Context	Predicted Phosphorylation? (YES/NO-KINASE)
Y42	KDEE**Y**EQMV	YES (SYK)
Y181	YKATN**Y**NGHT	NO
Y195	SIHG**Y**LGIV	NO
Y248	NRVT**Y**QGYS	NO
Y251	TYQG**Y**SPYQ	NO
Y254	GYSP**Y**QLTW	NO
Y289	DEES**Y**DTES	YES (POSSIBLY SYK)
Y305	DELP**Y**DDCV	YES (c-Abl)

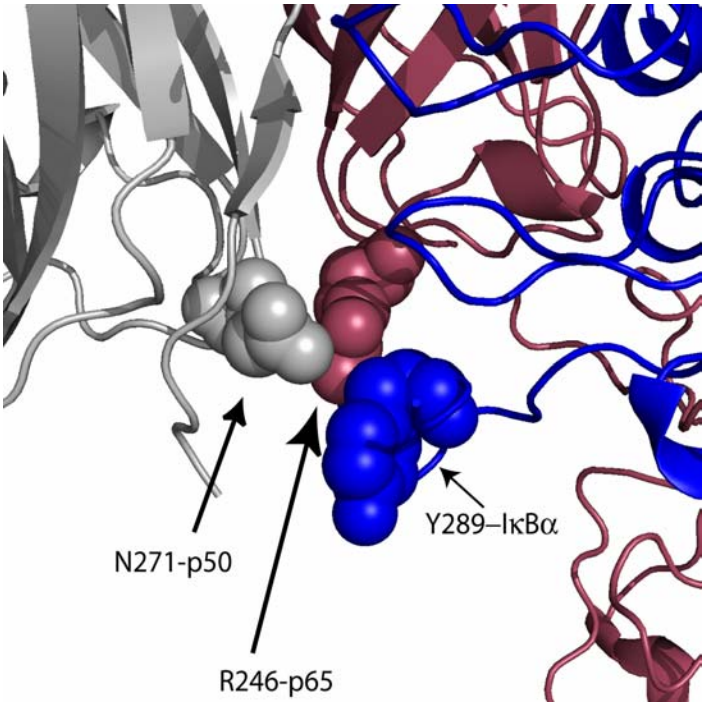

Figure 5-6. Y289 of IκBα is in close proximity with p50 and p65.

IκBα is colored blue, p65 is colored in magenta, and p50 is colored silver. Y289 of IκBα is in close proximity with N271 of p50 and R246 of p65, suggesting that Y289 is capable of interacting with NF-κB.

6. Effect of Y289 mutations on NF-κB activation

Since we have now determined that a single residue, Y289 has a specific effect on free IκBα degradation, we tested how this mutation would affect NF-κB activation. Therefore, *ikba*$^{-/-}$ cells were reconstituted with both Y289A and Y289G IκBα and compared to transgenic wt IκBα expressing cells. Stimulation with TNF-α led to rapid nuclear NF-κB translocation in WT expressing cells, while Y289A expressing cells had a slightly dampened NF-κB activation profile (Figure 5-7A). Finally, Y289G expressing cells had a very similar NF-κB activation profile as WT IκBα expressing cells. Therefore, although Y289A and Y289G mutants exhibit similar degradation rates in *nfkb*$^{-/-}$ cells, the impact on NF-κB activation are different.

In an attempt to understand this difference in NF-κB activation, several aspects of the IκB:NF-κB signaling system were tested. First, induced phosphorylation of IκBα by IKK on serines 32 and 36 was monitored with an α-phospho- IκBα antibody. All cell lines had approximately the same amount of phosphorylation (Figure 5-7B). In addition, the induced degradation of WT IκBα expressing cells was much more obvious than the degradation in the Y289G IκBα and Y289A IκBα expressing cells, presumably due to the increased amount of total IκBα by slowing down the free IκBα degradation pathway (Figure 5-7C). Finally, binding of the mutants was tested through immunoprecipitation with an α-RelA antibody. This experiment revealed that all IκBα mutants bound to NF-κB with similar affinity as WT IκBα. The amount of free IκBα observed in the IP flow-through could account for the slight difference in

NF-κB activation. Since Y289A has an excess of IκBα in the flow-through, this could show that excess free IκBα has an important role to play in NF-κB activation. This could be due to the slightly higher overall level of the Y289A mutant as compared to the Y289G mutant. This is not due to an increase is mRNA levels, since mRNA levels are very similar (Figure 5-9). Finally, the levels of other IκBs were detected with both RPA and western blot in the various cell lines (Figure 5-10). These analyses revealed that the level of IκBε much lower in the Y289G expressing cells, both at the mRNA and protein level. A reasonable argument could be made that Y289G IκBα could bind slightly better to NF-κB than WT IκBα. This could lead to less NF-κB basal activity, and consequently less expression of IκBε (Figure 5-10). Although these analyses are far from conclusive, it may provide an insight into the difference in NF-κB activation between Y289A and Y289G expressing cells. Nonetheless, Y289 is an important residue for unbound IκBα degradation.

Figure 5-7. Tyrosine mutations have differing effects on NF-κB activation. (A). EMSA showing NF-κB activation with *ikba*$^{-/-}$ cells expressing either WT IκBα, Y289A IκBα, or Y289G IκBα. (B). Transgenic cells were stimulated with TNF-α (0.1 ng/mL) and phosphorylation of IκBα was detected through western blot with an α-phospho IκBα antibody. All cell lines were phosphorylated similarly. (C). Degradation of IκBα is slower in Y289A and Y289G expressing cells. (D). Immunoprecipitation with α-RelA antibody shows that Y289A, Y289G and WT IκBα all bind to NF-κB similarly, but Y289A expressing cells have more 'free' IκBα than Y289G or WT IκBα.

A.

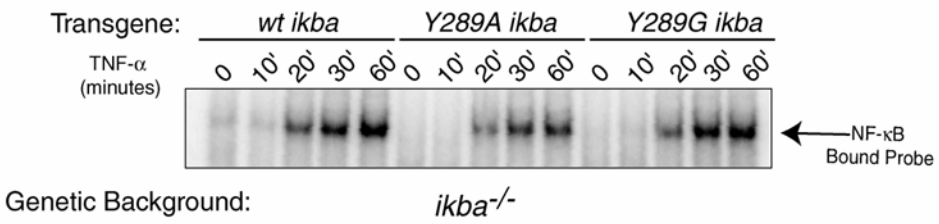
Transgene:
wt ikba
Y289A ikba
Y289G ikba
TNF-α (minutes)
0 10' 20' 30' 60' 0 10' 20' 30' 60' 0 10' 20' 30' 60'
NF-κB Bound Probe
Genetic Background:
ikba-/-

B.

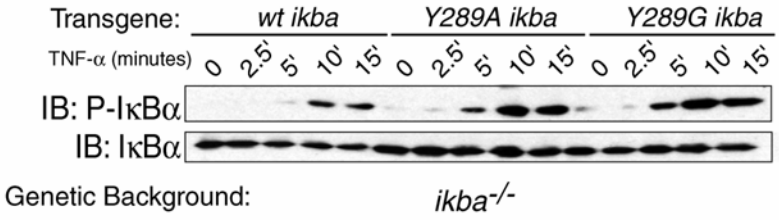
Transgene:
wt ikba
Y289A ikba
Y289G ikba
TNF-α (minutes)
0 2.5' 5' 10' 15' 0 2.5' 5' 10' 15' 0 2.5' 5' 10' 15'
IB: P-IκBα
IB: IκBα
Genetic Background:
ikba-/-

C.

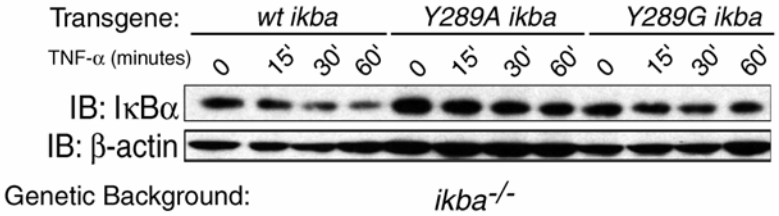
Transgene:
wt ikba
Y289A ikba
Y289G ikba
TNF-α (minutes)
0 15' 30' 60' 0 15' 30' 60' 0 15' 30' 60'
IB: IκBα
IB: β-actin
Genetic Background:
ikba-/-

D.

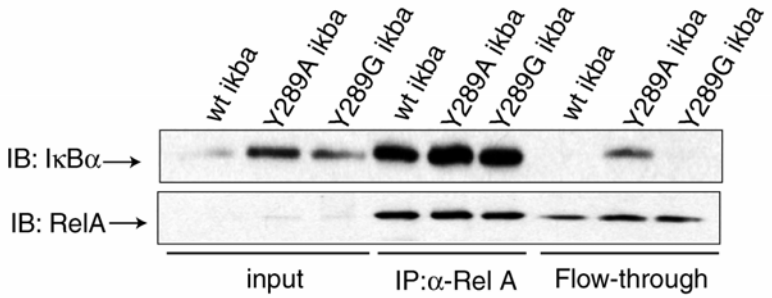
wt ikba
Y289A ikba
Y289G ikba
wt ikba
Y289A ikba
Y289G ikba
wt ikba
Y289A ikba
Y289G ikba
IB: IκBα
IB: RelA
input
IP:α-Rel A
Flow-through

7. Induced structural changes in IκBα alter NF-κB activation and NF-κB dependent gene expression

Although mutation of F295 and F298 in IκBα to alanine leads to an increase in protein level and stability due both to induced structural changes and an increase in the mRNA level (Figure 5-9), we characterized the F295A, F298A double mutation in the presence of NF-κB subunits to determine whether this mutant would affect NF-κB activation.

First, the binding of this double mutant and WT IκBα to RelA was compared. Transgenic cells expressing the F295A, F298A double mutant was generated in *ikba*$^{-/-}$ 3T3s (where all NF-κB subunits are present) (Figure 5-8A). Immunoprecipitation of RelA revealed that wt and mutant IκBα bound to RelA with similar affinity. However, a large fraction of mutant IκBα came out in the IP flow through. This suggests that unlike WT IκBα where ~90% remains NF-κB-bound, a significant amount of IκBα F295A, F298A mutant remains unbound. Therefore, we have increased the amount of free IκBα, which could influence NF-κB activation. To ensure that IKK phosphorylation and subsequent degradation remained intact, stimulation of these cells with TNF-α showed proportionately similar amounts of IKK phosphorylation but varying degradation rates, as expected due to an excess of IκBα (Figure 5-8B top and bottom panel) . These observations confirm that the IκBα F295A, F298A double mutant is able to bind NF-κB, responds to stimulus-dependent degradation when bound to NF-κB and accumulates in its free form.

Figure 5-8. F295A, F298A mutation leads to increased levels of IκBα and decreased NF-κB activation.

(A). *ikba*$^{-/-}$ cells reconstituted with either WT or F295A, F298A IκBα were immunoprecipitated with an α-RelA antibody and probed with an antibody against the C-terminus of IκBα. 10% of the flow-through was loaded and as shown, the level of unbound IκBα is increased significantly. (B). WT or F295A, F298A reconstituted cells were treated with TNF-α, and IκBα phosphorylation and degradation was detected by western blot. (C). EMSA using nuclear extracts after transgenic cells were treated with either 0.1 ng/mL TNF-α or 0.01 ng/mL TNF-α. NF-κB bound probe and free probe are indicated. (D). EMSA from transgenic cells treated with either 10 ng/mL LPS or 50 ng/mL LPS. (E). RNase Protection Assay (RPA) using several NF-κB dependent gene targets as indicated. Transgenic cells were treated with 0.1 ng/mL TNF-α and RNA was isolated at the indicated time points. L32 was used as a loading control. (F). Quantification of RPA. (▲-solid line)- cells expressing WT IκBα, (■-dashed line)- cells expressing F295A, F298A IκBα.

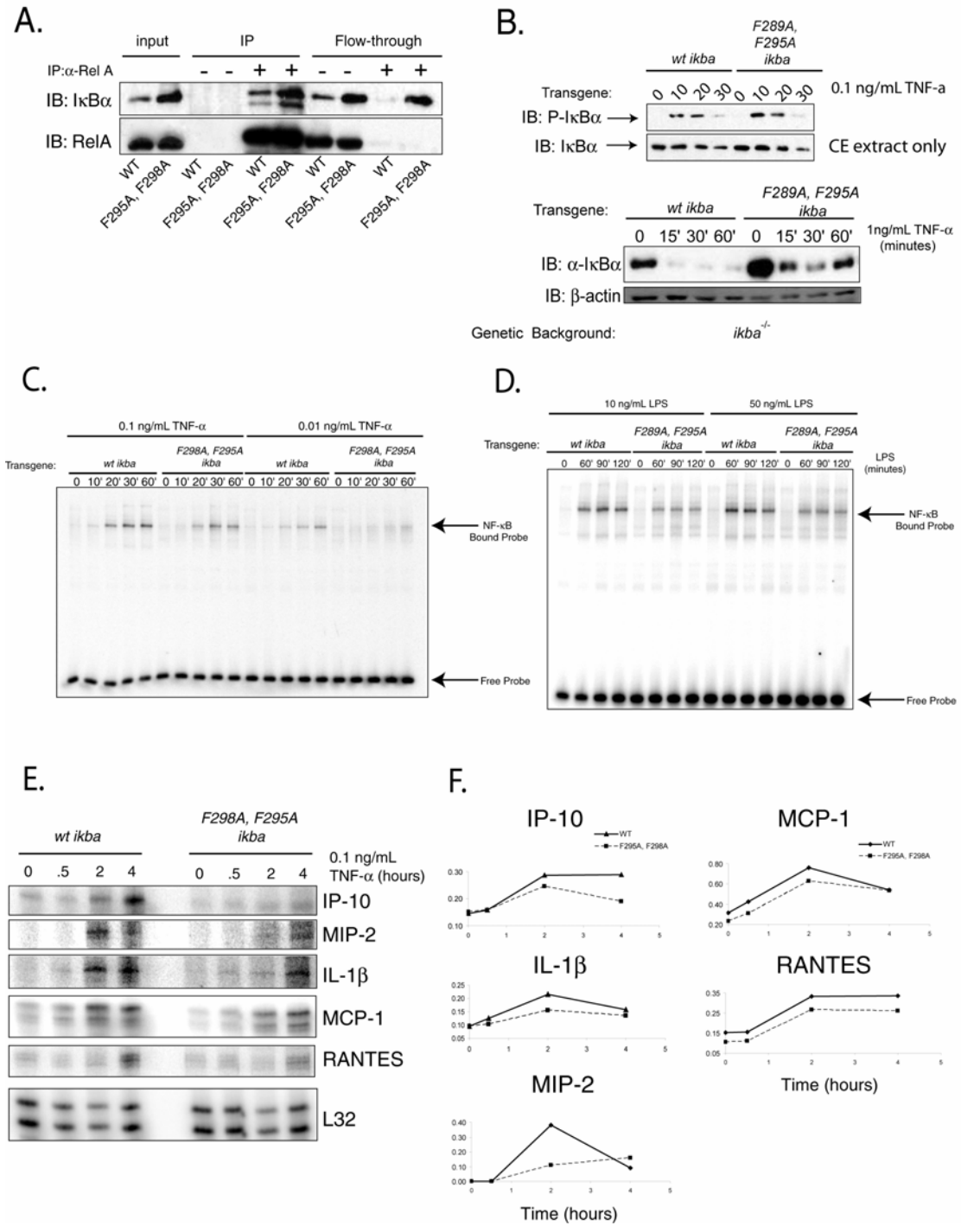
A.
input
IP
Flow-through
IP:α-Rel A
IB: IκBα
IB: RelA
WT
F295A, F298A
B.
wt ikba
F289A, F295A ikba
Transgene:
0.1 ng/mL TNF-a
IB: P-IκBα
IB: IκBα
CE extract only
1ng/mL TNF-α (minutes)
IB: α-IκBα
IB: β-actin
Genetic Background:
ikba-/-
C.
0.1 ng/mL TNF-α
0.01 ng/mL TNF-α
NF-κB Bound Probe
Free Probe
D.
10 ng/mL LPS
50 ng/mL LPS
LPS (minutes)
E.
0.1 ng/mL TNF-α (hours)
IP-10
MIP-2
IL-1β
MCP-1
RANTES
L32
F.
Time (hours)

We next tested if the altered degradation rate and increase in protein level of IκBα F298A, F298A double mutant could potentially alter NF-κB activation after stimulation. Transgenic cells expressing IκBα F295A, F298A double mutant were stimulated with different concentrations of TNF-α. As shown in Figure 5-8C, NF-κB activation is dampened in the F295A, F298A as compared to WT IκBα. Although the dampening effect of NF-κB activation by the IκBα mutant is more pronounced when cells are treated with 0.01 ng/ml of TNF-α, the effect is also clear at a 0.1 ng/mL TNF-α concentration (Figure 5-8C). NF-κB activation is also impaired in cells expressing the F285A/F298A double mutant treated with LPS, another inducer of the NF-κB pathway (Figure 5-8D). These results suggest that the dampening of NF-κB activation is not signal specific. Overall, we have established a system in which we can clearly observe the effect of stabilizing unbound IκBα on NF-κB activation

We then tested how stimulus-dependent gene transcription was affected in cells expressing the IκBα F295A, F298A mutant. We monitored the expression of five different cytokine genes (IP-10, MIP-2, MCP-1, IL-1β and RANTES) after stimulation with TNF-α. Promoters of these genes are well characterized and are known to contain binding sites for NF-κB dimers (Hoffmann et al., 2003). They are activated primarily by NF-κB RelA containing dimers that are predominantly inhibited by IκBα. Our results show that all of the tested genes are affected in cells expressing IκBα F295A, F298A mutant (Figure 5-8E and F). However, the magnitude and kinetics of inhibition are markedly different. For instance, although the expression of MCP-1 is similar at later time points of induction, basal expression is

dampened, suggesting that NF-κB plays a role in basal gene expression at this promoter. The expression of both IP-10 and RANTES peak at later time points and both are markedly inhibited in cells expressing the stable IκBα mutant. The expression of both MIP-2 and IL-1β peak at earlier time points, and in cells expressing the IκBα F295A, F298A mutant, levels of MIP-2 and IL-1β are significantly dampened at 2 hours. These results clearly demonstrate that the amplitude and kinetics of NF-κB activation can be inhibited by stabilizing free IκBα.

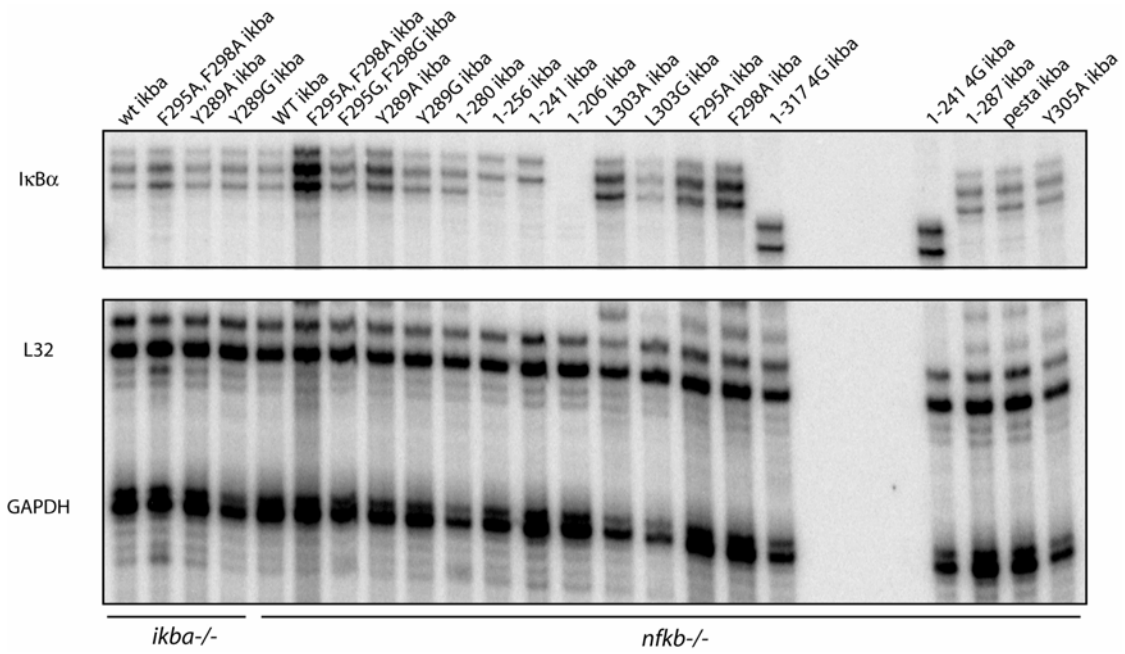

Figure 5-9. RNase Protection Assay for steady state levels of IκBα mRNA
Total mRNA from *ikba*$^{-/-}$ or *nfkb*$^{-/-}$ cells expressing various mutants of IκBα were compared using an RNase Protection Assay. L32 and GAPDH are used as loading controls. 1-206 IκBα is not detected with this probe, and the 4G mutation alters the migration of RNA.

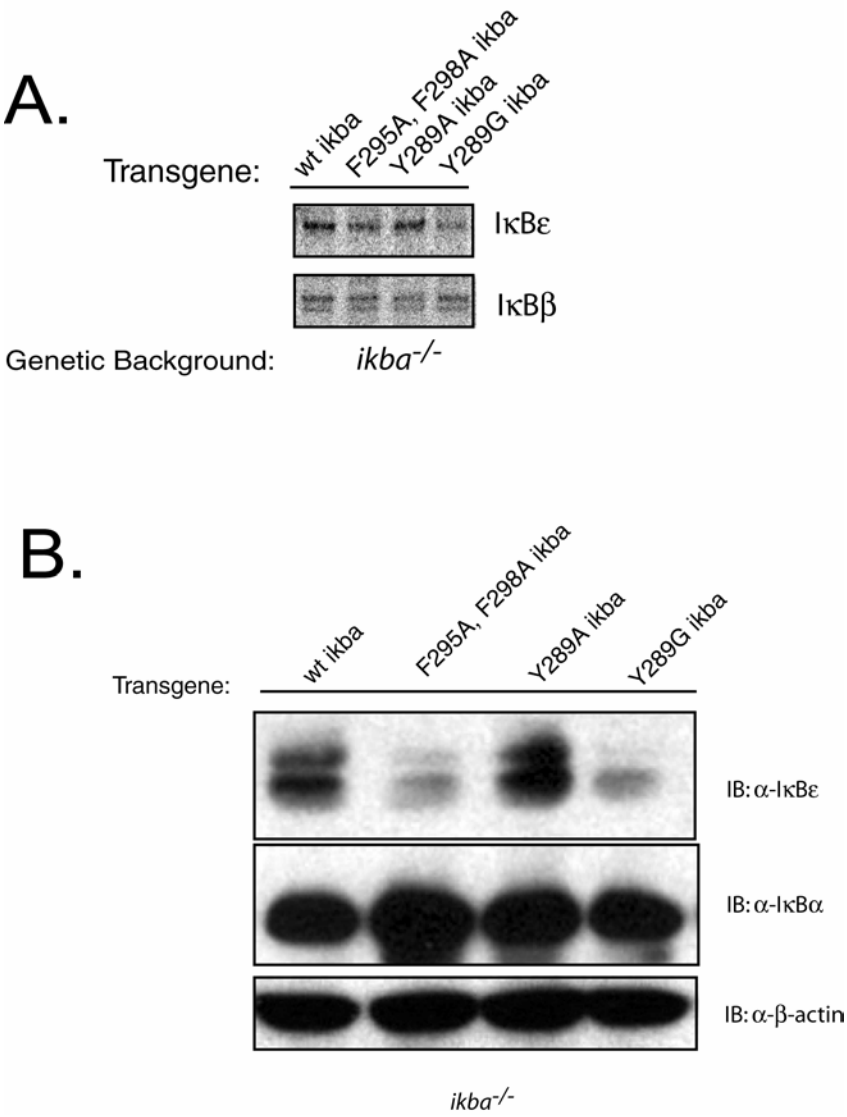

Figure 5-10. IκBε mRNA and protein levels are reduced in F295A, F298A and Y289G IκBα expressing cells. (A). mRNA levels of IκBε and IκBβ in various mutant cell lines. (B) Western blot against IκBε, IκBα, and β-actin. At both the mRNA level and protein level, the expression of IκBε is lower in both Y289G and F295A, F298A expressing cells.

C. Discussion

1. Proteasomal Recognition and Thermodynamic Stability

For efficient proteasomal degradation, a protein must have a flexible region to begin proteolysis (Prakash et al., 2004). This may be achieved by unfolding of a protein by ATPases which are part of the 26S proteasome, or is an inherent property of the protein. IκBα is not a globular folded protein, and has several flexible regions, such as the PEST domain as well as the 5th and 6th ankyrin repeats. Thorough biophysical studies have shown that the 5th and 6th ankyrin repeats are very flexible and exchange with solvent rapidly (Truhlar et al., 2006), and that upon binding to NF-κB, these regions become much more structured. It has also been shown that altering the flexibility of these regions leads to slower proteasomal degradation (Truhlar et al., 2008). In this study, we have shown that the removal of the entire PEST domain actually increases the degradation rate of free IκBα as compared to the IκBαΔC288 truncation. This may be explained by the folding back of the Cα backbone as seen in the crystal structure of IκBα (Figure 5-1A) containing residues 285-288 (Huxford et al., 1998). These residues may have a propensity to form a cap and prevent rapid degradation, in addition to the removal of residues C-terminal to 287. In the IκBαΔC281 truncation, this 'cap' is removed, which could increase the flexibility, and therefore, the degradation. The IκBαΔC242 and IκBαΔC257 truncations also end in established flexible regions and their degradation rates are increased significantly, similar to WT IκBα . These proteins are recognized by the proteasome, and only

when IκBα is truncated to the end of the less flexible 4th ankyrin repeat does free IκBα degradation slow down once again. Therefore, a degradation signal exists within the 5th ankyrin repeat that leads to rapid degradation. This is in contrast to a previous study in which the construct IκBαΔC257 was used for *in vitro* 20S proteasome degradation studies (Kroll et al., 1997). This discrepancy may be explained by the propensity of IκBαΔC257 to aggregate (Ferreiro et al., 2007). This aggregation may therefore prevent proteasomal degradation, since it cannot fit through the axial channel leading to the catalytic sites of the proteasome.

The correlation between hydrophobic residues and proteasomal recognition coincides with several reports which support this hypothesis (Lucchiari-Hartz et al., 2003); (Giulivi et al., 1994); (Bogusz et al., 2006);(Chandra et al., 2008). In this study, we observed the dramatic effect of the 4G mutation in the IκBαΔC242 background. This means that the proteasomal signal in the 5th ankyrin repeat is dependent on hydrophobic residues. However, since we only see slight slowing of degradation of the 4G mutation in the full-length background, the degradation signal in the 5th ankyrin repeat is not accessed by the proteasome when the PEST domain is present. This suggests that degradation of free IκBα occurs in a C to N-terminal manner, and/or the 5th ankyrin region is partly folded in context of the full length protein. This degradation signal does give some insight as to what is required for intracellular protein degradation - both a flexible region and hydrophobic residues.

2. Hydrophobic residues within the PEST domain

The PEST domain is often associated with proteins that have a rapid turnover rate (Rogers et al., 1986). Interestingly, PEST domains are often found in unstructured regions as well (Singh et al., 2006). In the case of unbound IκBα, the C-terminal region which contains a PEST domain is also flexible (Croy et al., 2004). Phosphorylation by CK2 within the PEST region of IκBα has been implicated in increasing the rate of proteasomal degradation; however, other residues which contribute to this degradation have not been explored. In this study, we determine the influence of mutating hydrophobic residues in this region and measuring the effect on free IκBα degradation. We find that mutation of all hydrophobic residues within the PEST region affect free IκBα degradation, with various stabilities of the mutant proteins. However, when L303, F295 and F298 are mutated to glycine, this stabilization effect is gone. This suggests that flexibility plays a significant role in degradation, since secondary structure prediction showed helical propensity in the F295A, F298A mutant which is absent in the F295G, F298G mutant. Meanwhile, mutating Y289 to both alanine and glycine had similar stabilization effects, suggesting that this tyrosine is specific to free IκBα degradation. It is possible that this tyrosine is phosphorylated as predicted by NetPhos 2.0, and several kinases were predicted by GPS, but none have been tested or identified previously. However, this is an attractive model for regulating free IκBα degradation, and worth investigating. The identification of Y289 as a possible regulator of free IκBα degradation certainly opens the door for more investigation into PEST regulated degradation.

3. Stabilization of free IκBα and the consequence on NF-κB activation

Although Y289 does interact with NF-κB, we explored the effect of altering this residue on NF-κB activation. Interestingly, we observed a differential effect between Y289A and Y289G, which was unexpected due to the similar degradation rates in *nfkb*$^{-/-}$ cells and mRNA levels in transgenic *ikba*$^{-/-}$ cells. Mutation of Y289 to alanine increases the amount of 'free' IκBα and dampens NF-κB activation, while mutation to glycine does not accumulate IκBα and nor dampens NF-κB activation. These mutations could affect NF-κB binding, where Y289A has decreased binding to NF-κB and mutation of Y289 to glycine could increase the binding affinity to NF-κB compared to WT IκBα, enough to decrease the amount of basal NF-κB and explain the low IκBε protein level. However, this may not be the case, since it is not clear whether truncations of IκBα ending at 287 and 317 have similar or different affinities to NF-κB (Bergqvist et al., 2006; Phelps et al., 2000) . Nonetheless, we do see an effect of this excess IκBα on NF-κB activation in the Y289A expressing cells.

We also explored the influence of the F295A, F298A double mutation on NF-κB activation, although slowed degradation rate in *nfkb*$^{-/-}$ cells may be due to an indirect effect. Slowing of free IκBα degradation as well as increasing the overall protein level through higher mRNA levels increased the amount of free IκBα; this affected both NF-κB activation and gene expression. It is still unclear the exact mechanisms of ubiquitin independent IκBα degradation, but we have revealed insights previously unknown as to the influence of both a flexible region and hydrophobic residues towards the degradation of an ubiquitin-independent substrate.

This chapter includes text and figures from the publication in preparation: Mathes E**,** Ghosh G. "Hydrophobic residues within flexible regions of IkappaBalpha contribute to ubiquitin-independent degradation" with permission. The dissertation author was the primary investigator and author of this material.

VI. Discussion

A. The switch between ubiquitin-independent and ubiquitin dependent degradation

In order for a protein to alter between two degradation pathways, there must be a molecular switch that determines which path of destruction it will go through. As we clearly shown in this study, the switch that determines the pathway of IκBα degradation is the C-terminus. When IκBα is bound to NF-κB, most of the C-terminus is in contact with NF-κB. However, when it is not bound, this region is extremely flexible, and available for recognition by the proteasome. This masking and exposure of the degradation signal may be similar in other ubiquitin-independent substrate systems. For instance, monomeric ODC can be degraded through the 20S proteasome and is regulated by the NAD(P)H quinone oxidase 1, NQO1. However, ODC as a dimer is resistant to 20S proteasomal degradation suggesting that its degradation signal is masked (Asher et al., 2006). Part of the elegance of the IκB:NF-κB system is this simple switch from ubiquitin-independent degradation of IκBα to ubiquitin dependent as directed by exposure of the C-terminus of IκBα.

B. Two Degrons within IκBα

As mentioned above, the switch for determining IκBα degradation pathway is located in the C-terminus which is protected when bound to NF-κB subunits. This suggests that structural elements are important for degradation. Consistent with this hypothesis, we have uncovered two degradation signals within IκBα; one, from 287-317, as well as another that resides in the flexible AR 5. Once the 5th repeat is

removed, degradation is slowed significantly. The reason for two degrons could be to promote the complete degradation of IκBα. It is possible that the C-terminal PEST motif could initiate degradation, while the AR5 repeat degron could promote continuous degradation through the rest of the ankyrin repeats. In this way, IκBα has been designed to be completely degraded. Fragments of IκBα remaining would be detrimental because they would not be able to fully inhibit NF-κB, and allow for constitutive NF-κB in the nucleus. This has been the case in Hodgkin's lymphoma, where it has been found that C-terminal truncations of IκBα exist which cannot fully inhibit NF-κB (Emmerich et al., 1999; Jungnickel et al., 2000).

C. The Common Thread that Links Ubiquitin-independent Substrates

While many proteins have now been shown to be degraded in an ubiquitin-independent manner, many have their own degradation pathway and mechanism, and none have a consensus primary sequence targeting them for degradation. For instance, while p21 and SRC-3 are regulated by the REGγ proteasome regulator, the substrates ODC, p53 and p73α have been shown to be inhibited by the NAD(P)H quinone oxidase 1, NQO1 (Asher et al., 2006). None of these proteins have strong sequence similarity with each other, or with IκBα. The common thread that connects them all, however, is flexible regions which promote degradation. Since it is known that IκBα is a dynamic protein, it is plausible that other IκB proteins are also flexible. However, the correlation between degradation and flexibility for the other IκB proteins has not yet been shown. IκBβ has been shown to form higher order oligomers when purified

in vitro, suggesting that IκBβ is even more flexible than IκBα, which can be purified as a monomer (Huxford et al., 2000). It is very possible that the other IκBs are also susceptible to ubiquitin-independent degradation pathways, and that these also correlate to structural flexibility. However, as of yet, there have not been thorough biophysical studies on other IκB molecules. Pairing of biophysical methods with cellular techniques is very powerful in understanding ubiquitin independent degradation pathways, as flexibility is the one common requirement for all substrates.

D. Fine Tuning Flexibility Affects Protein Degradation

It is well established that a common feature of ubiquitin-independent degradation of proteins is the lack of secondary structure to initiate degradation. This was also demonstrated in IκBα where alteration of this secondary structure affected degradation rates. This was achieved either through consensus mutation of AR6, or by inducing helical propensity within the PEST domain, although this remains to be determined experimentally. Interestingly, although mutation of all CK2 phosphorylation sites in IκBα to alanine (PESTA) slows free IκBα degradation, these mutations are predicted to induce a helical structure. It is possible that slowed degradation of the PESTA IκBα is due to increased structural propensity, rather than direct recognition of serine/threonine phosphorylation by the proteasome. This is supported by a study which showed that a PEST motif become more unstructured with phosphorylation, which correlates with a faster degradation rate (Garcia-Alai et al.,

2006). Further analysis is required to prove this hypothesis, although overall results establish that degradation of IκBα is regulated by structural transitions.

E. IκBα degradation is dependent on Y289

Although much of IκBα degradation is dependent on structural motifs, the mutation of Y289 to either glycine or alanine slowed unbound IκBα degradation significantly. Phosphorylation is a typical modification of tyrosines, performed by tyrosine kinases. Predictions show that it is possible that this tyrosine is phosphorylated by several kinases, although there is no experimental evidence to support this claim.

Interestingly, we observe differences in NF-κB activation when Y289 is mutated to either alanine or glycine. When Y289A expressing cells are stimulated with TNF-α, NF-κB translocation is dampened slightly. However, Y289G expressing cells have a NF-κB activation profile similar to WT IκBα, although we have slowed the free IκBα degradation pathway. Y289 is observed in close proximity to NF-κB in the crystal structure, which suggests that Y289 may be important for binding. It is possible that the binding affinity of these mutants to NF-κB differ. One observation that supports the slightly differing binding affinities is the fact that the NF-κB dependent gene, IκBε, has lower protein and mRNA levels in Y289G expressing cells, but not in Y289A expressing cells. If Y289G IκBα binds slightly better to NF-κB, the amount of basal NF-κB would decrease. A decrease in basal NF-κB would lead to a decrease in IκBε and perhaps other NF-κB dependent genes, or other inhibitory

molecules which restrict NF-κB translocation. However, it is still unclear exactly how these mutations have altered the NF-κB signaling system. The decrease in basal NF-κB could have long-range effects, since the decreased basal NF-κB dependent expression of PKC-δ augments apoptosis through the JNK pathway (Liu et al., 2006b).

F. The proteasome

Through this study, we have gained a much better understanding of IκB regulation, however, all we know is that IκBα is a proteasome substrate, but could not recapitulate our cell based studies *in vitro* with either the 20S proteasome or the 26S proteasome. It is possible that proteasome gate opening is regulated by another regulator, such as NQO1, or AZ1, or other chaperones such as Hsp90 (Jariel-Encontre et al., 2008). Studies aimed at finding interacting partners of unbound IκBα will shed insight into what other molecules may be involved.

References:

Alvarez-Castelao, B. and Castano, J.G. (2005) Mechanism of direct degradation of IkappaBalpha by 20S proteasome. *FEBS Lett*, **579**, 4797-4802.

Asher, G., Bercovich, Z., Tsvetkov, P., Shaul, Y. and Kahana, C. (2005) 20S proteasomal degradation of ornithine decarboxylase is regulated by NQO1. *Mol Cell*, **17**, 645-655.

Asher, G., Reuven, N. and Shaul, Y. (2006) 20S proteasomes and protein degradation "by default". *Bioessays*, **28**, 844-849.

Baeuerle, P.A. and Baltimore, D. (1988) Activation of DNA-binding activity in an apparently cytoplasmic precursor of the NF-[kappa]B transcription factor. *Cell*, **53**, 211.

Baghdiguian, S., Martin, M., Richard, I., Pons, F., Astier, C., Bourg, N., Hay, R.T., Chemaly, R., Halaby, G., Loiselet, J., Anderson, L.V., Lopez de Munain, A., Fardeau, M., Mangeat, P., Beckmann, J.S. and Lefranc, G. (1999) Calpain 3 deficiency is associated with myonuclear apoptosis and profound perturbation of the IkappaB alpha/NF-kappaB pathway in limb-girdle muscular dystrophy type 2A. *Nat Med*, **5**, 503-511.

Bajorek, M. and Glickman, M.H. (2004) Keepers at the final gates: regulatory complexes and gating of the proteasome channel. *Cell Mol Life Sci*, **61**, 1579-1588.

Baldwin, A.S., Jr. (1996) The NF-kappa B and I kappa B proteins: new discoveries and insights. *Annu Rev Immunol*, **14**, 649-683.

Barken, D., Werner, S.L., Cheng, C. and Hoffmann, A. (2007) A temporal code for inflammatory signaling. *in preparation*.

Barkett, M., Xue, D., Horvitz, H.R. and Gilmore, T.D. (1997) Phosphorylation of Ikappa B-alpha Inhibits Its Cleavage by Caspase CPP32 in Vitro. *J. Biol. Chem.*, **272**, 29419-29422.

Barrick, D., Ferreiro, D.U. and Komives, E.A. (2008) Folding landscapes of ankyrin repeat proteins: experiments meet theory. *Current Opinion in Structural Biology*, **18**, 27.

Baugh, J.M., Viktorova, E.G. and Pilipenko, E.V. (2009) Proteasomes can degrade a significant proportion of cellular proteins independent of ubiquitination. *J Mol Biol*, **386**, 814-827.

Bergqvist, S., Croy, C.H., Kjaergaard, M., Huxford, T., Ghosh, G. and Komives, E.A. (2006) Thermodynamics reveal that helix four in the NLS of NF-kappaB p65 anchors IkappaBalpha, forming a very stable complex. *J Mol Biol*, **360**, 421-434.

Blom, N., Gammeltoft, S. and Brunak, S. (1999) Sequence and structure-based prediction of eukaryotic protein phosphorylation sites. *J Mol Biol*, **294**, 1351-1362.

Bloom, J., Amador, V., Bartolini, F., DeMartino, G. and Pagano, M. (2003) Proteasome-mediated degradation of p21 via N-terminal ubiquitinylation. *Cell*, **115**, 71-82.

Bochtler, M., Ditzel, L., Groll, M., Hartmann, C. and Huber, R. (1999) The proteasome. *Annu Rev Biophys Biomol Struct*, **28**, 295-317.

Bogusz, A.M., Brickley, D.R., Pew, T. and Conzen, S.D. (2006) A novel N-terminal hydrophobic motif mediates constitutive degradation of serum- and glucocorticoid-induced kinase-1 by the ubiquitin-proteasome pathway. *Febs J*, **273**, 2913-2928.

Chandra, S., Shao, J., Li, J.X., Li, M., Longo, F.M. and Diamond, M.I. (2008) A common motif targets huntingtin and the androgen receptor to the proteasome. *J Biol Chem*, **283**, 23950-23955.

Chen, X., Chi, Y., Bloecher, A., Aebersold, R., Clurman, B.E. and Roberts, J.M. (2004) N-acetylation and ubiquitin-independent proteasomal degradation of p21(Cip1). *Mol Cell*, **16**, 839-847.

Cheong, R., Bergmann, A., Werner, S.L., Regal, J., Hoffmann, A. and Levchenko, A. (2006) Transient IkappaB kinase activity mediates temporal NF-kappaB dynamics in response to a wide range of tumor necrosis factor-alpha doses. *J Biol Chem*, **281**, 2945-2950.

Coulombe, P., Rodier, G., Bonneil, E., Thibault, P. and Meloche, S. (2004) N-Terminal ubiquitination of extracellular signal-regulated kinase 3 and p21 directs their degradation by the proteasome. *Mol Cell Biol*, **24**, 6140-6150.

Courtois, G. and Gilmore, T.D. (2006) Mutations in the NF-kappaB signaling pathway: implications for human disease. *Oncogene*, **25**, 6831-6843.

Croy, C.H., Bergqvist, S., Huxford, T., Ghosh, G. and Komives, E.A. (2004) Biophysical characterization of the free IkappaBalpha ankyrin repeat domain in solution. *Protein Sci*, **13**, 1767-1777.

Davies, K.J. (2001) Degradation of oxidized proteins by the 20S proteasome. *Biochimie*, **83**, 301-310.

Dobrzanski, P., Ryseck, R.P. and Bravo, R. (1993) Both N- and C-terminal domains of RelB are required for full transactivation: role of the N-terminal leucine zipper-like motif. *Mol Cell Biol*, **13**, 1572-1582.

Emmerich, F., Meiser, M., Hummel, M., Demel, G., Foss, H.D., Jundt, F., Mathas, S., Krappmann, D., Scheidereit, C., Stein, H. and Dorken, B. (1999) Overexpression of I kappa B alpha without inhibition of NF-kappaB activity and mutations in the I kappa B alpha gene in Reed-Sternberg cells. *Blood*, **94**, 3129-3134.

Ferreiro, D.U., Cervantes, C.F., Truhlar, S.M., Cho, S.S., Wolynes, P.G. and Komives, E.A. (2007) Stabilizing IkappaBalpha by "consensus" design. *J Mol Biol*, **365**, 1201-1216.

Ferreiro, D.U., Cho, S.S., Komives, E.A. and Wolynes, P.G. (2005) The energy landscape of modular repeat proteins: topology determines folding mechanism in the ankyrin family. *J Mol Biol*, **354**, 679-692.

Frankenberger, M., Pforte, A., Sternsdorf, T., Passlick, B., Baeuerle, P.A. and Ziegler-Heitbrock, H.W. (1994) Constitutive nuclear NF-kappa B in cells of the monocyte lineage. *Biochem J*, **304 (Pt 1)**, 87-94.

Gao, X. and Hu, H. (2008) Quality control of the proteins associated with neurodegenerative diseases. *Acta Biochim Biophys Sin (Shanghai)*, **40**, 612-618.

Garcia-Alai, M.M., Gallo, M., Salame, M., Wetzler, D.E., McBride, A.A., Paci, M., Cicero, D.O. and de Prat-Gay, G. (2006) Molecular basis for phosphorylation-dependent, PEST-mediated protein turnover. *Structure*, **14**, 309-319.

Gerondakis, S., Grumont, R., Gugasyan, R., Wong, L., Isomura, I., Ho, W. and Banerjee, A. (2006) Unravelling the complexities of the NF-kappaB signalling pathway using mouse knockout and transgenic models. *Oncogene*, **25**, 6781-6799.

Ghosh, S. and Karin, M. (2002) Missing pieces in the NF-kappaB puzzle. *Cell*, **109 Suppl**, S81-96.

Ghosh, S., May, M.J. and Kopp, E.B. (1998) NF-kappa B and Rel proteins: evolutionarily conserved mediators of immune responses. *Annu Rev Immunol*, **16**, 225-260.

Gilmore, T.D. (2006) Introduction to NF-kappaB: players, pathways, perspectives. *Oncogene*, **25**, 6680-6684.

Giulivi, C., Pacifici, R.E. and Davies, K.J. (1994) Exposure of hydrophobic moieties promotes the selective degradation of hydrogen peroxide-modified hemoglobin by the multicatalytic proteinase complex, proteasome. *Arch Biochem Biophys*, **311**, 329-341.

Groll, M. and Clausen, T. (2003) Molecular shredders: how proteasomes fulfill their role. *Curr Opin Struct Biol*, **13**, 665-673.

Hoffmann, A., Leung, T.H. and Baltimore, D. (2003) Genetic analysis of NF-kappaB/Rel transcription factors defines functional specificities. *Embo J*, **22**, 5530-5539.

Hoffmann, A., Levchenko, A., Scott, M.L. and Baltimore, D. (2002a) The Ikappa B-NF-kappa B Signaling Module: Temporal Control and Selective Gene Activation. *Science*, **298**, 1241-1245.

Hoffmann, A., Levchenko, A., Scott, M.L. and Baltimore, D. (2002b) The IkappaB-NF-kappaB signaling module: temporal control and selective gene activation. *Science*, **298**, 1241-1245.

Hoffmann, A., Natoli, G. and Ghosh, G. (2006) Transcriptional regulation via the NF-kappaB signaling module. *Oncogene*, **25**, 6706-6716.

Huang, T.T., Kudo, N., Yoshida, M. and Miyamoto, S. (2000) A nuclear export signal in the N-terminal regulatory domain of IkappaBalpha controls cytoplasmic localization of inactive NF-kappaB/IkappaBalpha complexes. *Proc Natl Acad Sci U S A*, **97**, 1014-1019.

Huxford, T., Huang, D.B., Malek, S. and Ghosh, G. (1998) The crystal structure of the IkappaBalpha/NF-kappaB complex reveals mechanisms of NF-kappaB inactivation. *Cell*, **95**, 759-770.

Huxford, T., Malek, S. and Ghosh, G. (2000) Preparation and crystallization of dynamic NF-kappa B.Ikappa B complexes. *J Biol Chem*, **275**, 32800-32806.

Jacobs, M.D. and Harrison, S.C. (1998) Structure of an IkappaBalpha/NF-kappaB complex. *Cell*, **95**, 749-758.

Jariel-Encontre, I., Bossis, G. and Piechaczyk, M. (2008) Ubiquitin-independent degradation of proteins by the proteasome. *Biochim Biophys Acta*, **1786**, 153-177.

Johnson, C., Van Antwerp, D. and Hope, T.J. (1999) An N-terminal nuclear export signal is required for the nucleocytoplasmic shuttling of IkappaBalpha. *Embo J*, **18**, 6682-6693.

Johnson, P.R., Swanson, R., Rakhilina, L. and Hochstrasser, M. (1998) Degradation signal masking by heterodimerization of MATalpha2 and MATa1 blocks their mutual destruction by the ubiquitin-proteasome pathway. *Cell*, **94**, 217-227.

Jungnickel, B., Staratschek-Jox, A., Brauninger, A., Spieker, T., Wolf, J., Diehl, V., Hansmann, M.L., Rajewsky, K. and Kuppers, R. (2000) Clonal deleterious mutations in the IkappaBalpha gene in the malignant cells in Hodgkin's lymphoma. *J Exp Med*, **191**, 395-402.

Kahana, C., Asher, G. and Shaul, Y. (2005) Mechanisms of protein degradation: an odyssey with ODC. *Cell Cycle*, **4**, 1461-1464.

Karin, M. and Ben-Neriah, Y. (2000) Phosphorylation meets ubiquitination: the control of NF-[kappa]B activity. *Annu Rev Immunol*, **18**, 621-663.

Kato, T., Jr., Delhase, M., Hoffmann, A. and Karin, M. (2003) CK2 Is a C-Terminal IkappaB Kinase Responsible for NF-kappaB Activation during the UV Response. *Mol Cell*, **12**, 829-839.

Kawai, H., Nie, L. and Yuan, Z.M. (2002) Inactivation of NF-kappaB-dependent cell survival, a novel mechanism for the proapoptotic function of c-Abl. *Mol Cell Biol*, **22**, 6079-6088.

Kearns, J.D., Basak, S., Werner, S.L., Huang, C.S. and Hoffmann, A. (2006) IkappaBepsilon provides negative feedback to control NF-kappaB oscillations, signaling dynamics, and inflammatory gene expression. *J Cell Biol*, **173**, 659-664.

Kisselev, A.F., Kaganovich, D. and Goldberg, A.L. (2002) Binding of hydrophobic peptides to several non-catalytic sites promotes peptide hydrolysis by all active sites of 20 S proteasomes. Evidence for peptide-induced channel opening in the alpha-rings. *J Biol Chem*, **277**, 22260-22270.

Krappmann, D. and Scheidereit, C. (1997) Regulation of NF-kappa B activity by I kappa B alpha and I kappa B beta stability. *Immunobiology*, **198**, 3-13.

Krappmann, D., Wulczyn, F.G. and Scheidereit, C. (1996) Different mechanisms control signal-induced degradation and basal turnover of the NF-kappaB inhibitor IkappaB alpha in vivo. *Embo J*, **15**, 6716-6726.

Kroll, M., Conconi, M., Desterro, M.J., Marin, A., Thomas, D., Friguet, B., Hay, R.T., Virelizier, J.L., Arenzana-Seisdedos, F. and Rodriguez, M.S. (1997) The carboxy-terminus of I kappaB alpha determines susceptibility to degradation by the catalytic core of the proteasome. *Oncogene*, **15**, 1841-1850.

Li, J., Mahajan, A. and Tsai, M.-D. (2006a) Ankyrin Repeat:A Unique Motif Mediating Protein Protein Interactions. *Biochemistry*, **45**, 15168-15178.

Li, X., Lonard, D.M., Jung, S.Y., Malovannaya, A., Feng, Q., Qin, J., Tsai, S.Y., Tsai, M.J. and O'Malley, B.W. (2006b) The SRC-3/AIB1 coactivator is degraded in a ubiquitin- and ATP-independent manner by the REGgamma proteasome. *Cell*, **124**, 381-392.

Lin, R., Beauparlant, P., Makris, C., Meloche, S. and Hiscott, J. (1996) Phosphorylation of IkappaBalpha in the C-terminal PEST domain by casein kinase II affects intrinsic protein stability. *Mol Cell Biol*, **16**, 1401-1409.

Liu, C.W., Corboy, M.J., DeMartino, G.N. and Thomas, P.J. (2003) Endoproteolytic activity of the proteasome. *Science*, **299**, 408-411.

Liu, C.W., Li, X., Thompson, D., Wooding, K., Chang, T.L., Tang, Z., Yu, H., Thomas, P.J. and DeMartino, G.N. (2006a) ATP binding and ATP hydrolysis play distinct roles in the function of 26S proteasome. *Mol Cell*, **24**, 39-50.

Liu, J., Yang, D., Minemoto, Y., Leitges, M., Rosner, M.R. and Lin, A. (2006b) NF-kappaB is required for UV-induced JNK activation via induction of PKCdelta. *Mol Cell*, **21**, 467-480.

Lucchiari-Hartz, M., Lindo, V., Hitziger, N., Gaedicke, S., Saveanu, L., van Endert, P.M., Greer, F., Eichmann, K. and Niedermann, G. (2003) Differential proteasomal processing of hydrophobic and hydrophilic protein regions: contribution to cytotoxic T lymphocyte epitope clustering in HIV-1-Nef. *Proc Natl Acad Sci U S A*, **100**, 7755-7760.

Malek, S., Huang, D.B., Huxford, T., Ghosh, S. and Ghosh, G. (2003) X-ray crystal structure of an IkappaBbeta x NF-kappaB p65 homodimer complex. *J Biol Chem*, **278**, 23094-23100.

Mathes, E., O'Dea, E.L., Hoffmann, A. and Ghosh, G. (2008) NF-kappaB dictates the degradation pathway of IkappaBalpha. *Embo J*, **27**, 1357-1367.

McElhinny, J.A., Trushin, S.A., Bren, G.D., Chester, N. and Paya, C.V. (1996) Casein kinase II phosphorylates I kappa B alpha at S-283, S-289, S-293, and T-291 and is required for its degradation. *Mol Cell Biol*, **16**, 899-906.

Miyamoto, S., Chiao, P.J. and Verma, I.M. (1994) Enhanced I kappa B alpha degradation is responsible for constitutive NF-kappa B activity in mature murine B-cell lines. *Mol Cell Biol*, **14**, 3276-3282.

Mosavi, L.K., Cammett, T.J., Desrosiers, D.C. and Peng, Z.Y. (2004) The ankyrin repeat as molecular architecture for protein recognition. *Protein Sci*, **13**, 1435-1448.

Murakami, Y., Matsufuji, S., Hayashi, S., Tanahashi, N. and Tanaka, K. (2000) Degradation of ornithine decarboxylase by the 26S proteasome. *Biochem Biophys Res Commun*, **267**, 1-6.

O'Connor, S., Shumway, S.D., Amanna, I.J., Hayes, C.E. and Miyamoto, S. (2004) Regulation of constitutive p50/c-Rel activity via proteasome inhibitor-resistant IkappaBalpha degradation in B cells. *Mol Cell Biol*, **24**, 4895-4908.

O'Dea, E.L., Barken, D., Peralta, R.Q., Tran, K.T., Werner, S.L., Kearns, J.D., Levchenko, A. and Hoffmann, A. (2007) A homeostatic model of I[kappa]B metabolism to control constitutive NF-[kappa]B activity. *Mol Syst Biol*, **3**.

Orlowski, M. and Wilk, S. (2003) Ubiquitin-independent proteolytic functions of the proteasome. *Arch Biochem Biophys*, **415**, 1-5.

Pando, M.P. and Verma, I.M. (2000) Signal-dependent and -independent degradation of free and NF-kappa B-bound IkappaBalpha. *J Biol Chem*, **275**, 21278-21286.

Phelps, C.B., Sengchanthalangsy, L.L., Huxford, T. and Ghosh, G. (2000) Mechanism of I kappa B alpha binding to NF-kappa B dimers. *J Biol Chem*, **275**, 29840-29846.

Pickart, C.M. and Cohen, R.E. (2004) Proteasomes and their kin: proteases in the machine age. *Nat Rev Mol Cell Biol*, **5**, 177-187.

Prakash, S., Tian, L., Ratliff, K.S., Lehotzky, R.E. and Matouschek, A. (2004) An unstructured initiation site is required for efficient proteasome-mediated degradation. *Nat Struct Mol Biol*, **11**, 830-837.

Rechsteiner, M., Realini, C. and Ustrell, V. (2000) The proteasome activator 11 S REG (PA28) and class I antigen presentation. *Biochem J*, **345 Pt 1**, 1-15.

Rice, N.R. and Ernst, M.K. (1993) In vivo control of NF-kappa B activation by I kappa B alpha. *Embo J*, **12**, 4685-4695.

Rogers, S., Wells, R. and Rechsteiner, M. (1986) Amino acid sequences common to rapidly degraded proteins: the PEST hypothesis. *Science*, **234**, 364-368.

Savinova, O., Hoffmann, A. and Ghosh, G. (2009) The nfkb1 and nfkb2 proteins p105 and p100 function as the core of heterogeneous NF-kBsomes. *Mol Cell, in review*.

Scherer, D.C., Brockman, J.A., Chen, Z., Maniatis, T. and Ballard, D.W. (1995) Signal-Induced Degradation of I{kappa}B{alpha} Requires Site-Specific Ubiquitination. *PNAS*, **92**, 11259-11263.

Schwarz, E.M., Van Antwerp, D. and Verma, I.M. (1996) Constitutive phosphorylation of IkappaBalpha by casein kinase II occurs preferentially at serine 293: requirement for degradation of free IkappaBalpha. *Mol Cell Biol*, **16**, 3554-3559.

Scott, M.L., Fujita, T., Liou, H.C., Nolan, G.P. and Baltimore, D. (1993) The p65 subunit of NF-kappa B regulates I kappa B by two distinct mechanisms. *Genes Dev*, **7**, 1266-1276.

Sedgwick, S.G. and Smerdon, S.J. (1999) The ankyrin repeat: a diversity of interactions on a common structural framework. *Trends Biochem Sci*, **24**, 311-316.

Sen, R. and Baltimore, D. (1986) Inducibility of kappa immunoglobulin enhancer-binding protein Nf-kappa B by a posttranslational mechanism. *Cell*, **47**, 921-928.

Sheaff, R.J., Singer, J.D., Swanger, J., Smitherman, M., Roberts, J.M. and Clurman, B.E. (2000) Proteasomal turnover of p21Cip1 does not require p21Cip1 ubiquitination. *Mol Cell*, **5**, 403-410.

Shen, J., Channavajhala, P., Seldin, D.C. and Sonenshein, G.E. (2001) Phosphorylation by the protein kinase CK2 promotes calpain-mediated degradation of IkappaBalpha. *J Immunol*, **167**, 4919-4925.

Shringarpure, R. and Davies, K.J. (2002) Protein turnover by the proteasome in aging and disease. *Free Radic Biol Med*, **32**, 1084-1089.

Shumway, S.D., Maki, M. and Miyamoto, S. (1999) The PEST domain of IkappaBalpha is necessary and sufficient for in vitro degradation by mu-calpain. *J Biol Chem*, **274**, 30874-30881.

Singh, G.P., Ganapathi, M., Sandhu, K.S. and Dash, D. (2006) Intrinsic unstructuredness and abundance of PEST motifs in eukaryotic proteomes. *Proteins*, **62**, 309-315.

Singh, H., Sen, R., Baltimore, D. and Sharp, P.A. (1986) A nuclear factor that binds to a conserved sequence motif in transcriptional control elements of immunoglobulin genes. *Nature*, **319**, 154-158.

Sue, S.C., Cervantes, C., Komives, E.A. and Dyson, H.J. (2008) Transfer of flexibility between ankyrin repeats in IkappaBalpha upon formation of the NF-kappaB complex. *J Mol Biol*, **380**, 917-931.

Sullivan, J.C., Kalaitzidis, D., Gilmore, T.D. and Finnerty, J.R. (2007) Rel homology domain-containing transcription factors in the cnidarian Nematostella vectensis. *Dev Genes Evol*, **217**, 63-72.

Sun, S., Elwood, J. and Greene, W.C. (1996) Both amino- and carboxyl-terminal sequences within I kappa B alpha regulate its inducible degradation. *Mol Cell Biol*, **16**, 1058-1065.

Sun, S.C. and Ley, S.C. (2008) New insights into NF-kappaB regulation and function. *Trends Immunol*, **29**, 469-478.

Takada, Y., Mukhopadhyay, A., Kundu, G.C., Mahabeleshwar, G.H., Singh, S. and Aggarwal, B.B. (2003) Hydrogen Peroxide Activates NF-{kappa}B through Tyrosine Phosphorylation of I{kappa}B{alpha} and Serine Phosphorylation of p65: EVIDENCE FOR THE INVOLVEMENT OF I{kappa}B{alpha} KINASE AND Syk PROTEIN-TYROSINE KINASE. *J. Biol. Chem.*, **278**, 24233-24241.

Takeuchi, J., Chen, H. and Coffino, P. (2007) Proteasome substrate degradation requires association plus extended peptide. *Embo J*, **26**, 123-131.

Tergaonkar, V., Bottero, V., Ikawa, M., Li, Q. and Verma, I.M. (2003) I{kappa}B Kinase-Independent I{kappa}B{alpha} Degradation Pathway: Functional NF-{kappa}B Activity and Implications for Cancer Therapy. *Mol. Cell. Biol.*, **23**, 8070-8083.

Thompson, J.D., Higgins, Desmond G., Gibson, Toby J. San Diego Supercomputer Biology Workbench, p. CLUSTALW: A multiple sequence alignment tool.

Tofaris, G.K., Layfield, R. and Spillantini, M.G. (2001) alpha-synuclein metabolism and aggregation is linked to ubiquitin-independent degradation by the proteasome. *FEBS Lett*, **509**, 22-26.

Touitou, R., Richardson, J., Bose, S., Nakanishi, M., Rivett, J. and Allday, M.J. (2001) A degradation signal located in the C-terminus of p21WAF1/CIP1 is a binding site for the C8 alpha-subunit of the 20S proteasome. *Embo J*, **20**, 2367-2375.

Truhlar, S.M., Mathes, E., Cervantes, C.F., Ghosh, G. and Komives, E.A. (2008) Pre-folding IkappaBalpha alters control of NF-kappaB signaling. *J Mol Biol*, **380**, 67-82.

Truhlar, S.M., Torpey, J.W. and Komives, E.A. (2006) Regions of IkappaBalpha that are critical for its inhibition of NF-kappaB.DNA interaction fold upon binding to NF-kappaB. *Proc Natl Acad Sci U S A*, **103**, 18951-18956.

Ustrell, V., Hoffman, L., Pratt, G. and Rechsteiner, M. (2002) PA200, a nuclear proteasome activator involved in DNA repair. *Embo J*, **21**, 3516-3525.

Van Antwerp, D.J. and Verma, I.M. (1996) Signal-induced degradation of I(kappa)B(alpha): association with NF-kappaB and the PEST sequence in I(kappa)B(alpha) are not required. *Mol Cell Biol*, **16**, 6037-6045.

Werner, S.L., Barken, D. and Hoffmann, A. (2005) Stimulus specificity of gene expression programs determined by temporal control of IKK activity. *Science*, **309**, 1857-1861.

Whitby, F.G., Masters, E.I., Kramer, L., Knowlton, J.R., Yao, Y., Wang, C.C. and Hill, C.P. (2000) Structural basis for the activation of 20S proteasomes by 11S regulators. *Nature*, **408**, 115.

Xue, Y., Zhou, F., Zhu, M., Ahmed, K., Chen, G. and Yao, X. (2005) GPS: a comprehensive www server for phosphorylation sites prediction. *Nucl. Acids Res.*, **33**, W184-187.

Yamamoto, M. and Takeda, K. (2008) Role of nuclear IkappaB proteins in the regulation of host immune responses. *J Infect Chemother*, **14**, 265-269.

Zandi, E., Chen, Y. and Karin, M. (1998) Direct phosphorylation of IkappaB by IKKalpha and IKKbeta: discrimination between free and NF-kappaB-bound substrate. *Science*, **281**, 1360-1363.